

PDF hosted at the Radboud Repository of the Radboud University Nijmegen

The following full text is a publisher's version.

For additional information about this publication click this link.

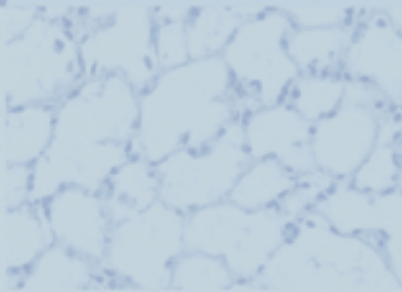
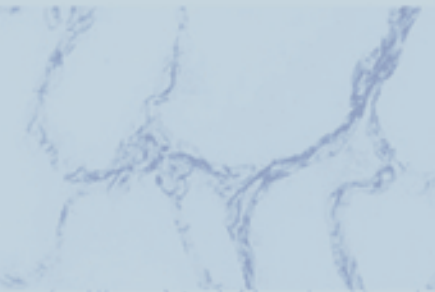
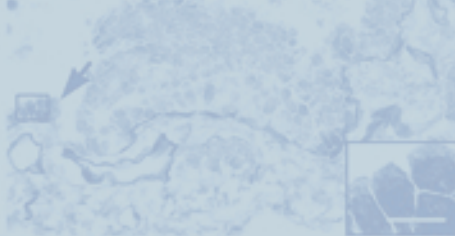
<http://hdl.handle.net/2066/74426>

Please be advised that this information was generated on 2017-12-06 and may be subject to change.

Heparan Sulfates in Human Lung

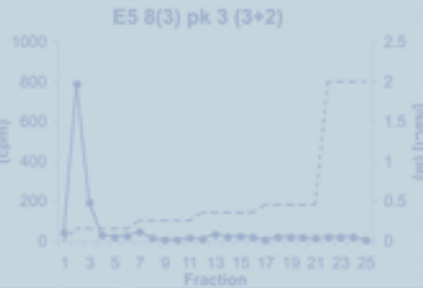
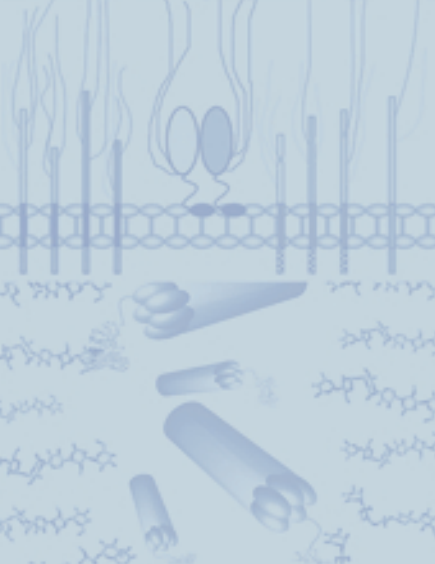
development of tools
and
relation with emphysema

Human lung



already in an advance
Morphological analysis of
lesions. This especially ho
parenchymal destruction
DI is a more sensitive para
parameter for airspace
analysis of emphysema.

Phage Display



Heparan Sulfat
Nicole C. Smits



Heparan Sulfates in Human Lung

development of tools and relation with emphysema

Nicole Christianne Smits

Smits, Nicole Christianne

Heparan Sulfates in Human Lung

development of tools and relation with emphysema

Thesis, Radboud University Nijmegen, Medical Centre

ISBN 978-90-9024488-4

©2009, by Nicole C. Smits

Cover illustration and lay-out: Nicole C. Smits

Printed by: Ipskamp Drukkers Enschede

All rights reserved. No parts of this publication may be reproduced, stored in a retrieval system, or transmitted in any form or by any means, without prior written permission of the holder of the copyright.



Heparan Sulfates in Human Lung

development of tools and relation with emphysema

Een wetenschappelijke proeve op het gebied van de
Medische Wetenschappen

Proefschrift

ter verkrijging van de graad van doctor
aan de Radboud Universiteit Nijmegen
op gezag van de rector magnificus prof. mr. S.C.J.J. Kortmann,
volgens besluit van het college van decanen
in het openbaar te verdedigen op maandag 21 september
om 13.30 uur precies
door

Nicole Christianne Smits

Geboren op 8 januari 1976
te Ulf

Promotores

Prof. dr. J.J.H.H.M. De Pont

Prof. dr. P.N.R. Dekhuijzen

Copromotor

Dr. T.H. van Kuppevelt

Manuscriptcommissie

Prof. dr. J. Schalkwijk (voorzitter)

Prof. dr. J.H.M. Berden

Prof. dr. E.F.M Wouters (Maastricht Universitair Medisch Centrum)

The studies presented in this thesis were performed at the Department of Biochemistry, Radboud University Nijmegen, Medical Centre, Nijmegen Centre for Molecular Life Sciences (NCMLS), Nijmegen, The Netherlands, and were financially supported by the Radboud University Nijmegen, Medical Centre.

In loving memory of Mike

Table of contents

9	Chapter 1 General introduction: Heparan sulfates in the lung; structure, diversity, and role in pulmonary emphysema. <i>The Anatomical Record</i> 2009, <i>In Press</i>
29	Chapter 2 Phage display-derived human antibodies against specific glycosaminoglycan epitopes. <i>Methods in Enzymology</i> 2006, 416 :61-87
51	Chapter 3 Heterogeneity of heparan sulfates in human lung. <i>American Journal of Respiratory Cell and Molecular Biology</i> 2004, 30 :166-173
69	Chapter 4 A rare, highly sulfated heparan sulfate sequence (GlcNS6S-IdoA2S) ₃ has a strict topography and is involved in cell behavior. <i>Submitted</i>
87	Chapter 5 Overexpression of heparanase and loss of heparan sulfate: initiating events in pulmonary emphysema. <i>Submitted</i>
103	Chapter 6 Aberrant fibrillin-1 expression in early emphysematous human lung: a proposed predisposition for emphysema. <i>Modern Pathology</i> 2008, 21 (3):297-307
121	Chapter 7 Summary / Samenvatting Future perspectives / Toekomstvisie 122 Summary 124 Future Perspectives 125 Samenvatting 127 Toekomstvisie
129	Chapter 8 Author information 130 Curriculum Vitae 131 Curriculum Vitae (English) 132 List of publications 133 Dankwoord
137	Color figures

Abbreviations used in this thesis

AQP	aquaporin
BSA	bovine serum albumin
CDR3	complementarity determining region 3
CHO	chinese hamster ovary
COPD	chronic obstructive pulmonary disease
CS	chondroitin sulfate
DAB	3, 3'-diaminobenzidine
DI	destructive index
DS	dermatan sulfate
ECM	extracellular matrix
ELISA	enzyme linked immunosorbent assay
FCS	fetal calf serum
FEV₁	forced expiratory volume in 1 second
FGF	fibroblast growth factor
GAG	glycosaminoglycan
Gal	D-galactose
GalNAc	<i>N</i> -acetyl-D-galactosamine
GlcA	D-glucuronic acid
GlcNAc	<i>N</i> -acetyl-D-glucosamine
GOLD	global initiative for chronic obstructive lung disease
HA	hyaluronic acid
HS	heparan sulfate
HS2ST	heparan sulfate 2- <i>O</i> -sulfotransferase
HS3ST	heparan sulfate 3- <i>O</i> -sulfotransferase
HS6ST	heparan sulfate 6- <i>O</i> -sulfotransferase
HSPG	heparan sulfate proteoglycan
IdoA	L-iduronic acid
IPTG	isopropyl- β -D-thiogalactosidase
K_{co}	diffusion capacity for carbon monoxide corrected for alveolar volume
KS	keratan sulfate
MLI	mean linear intercept
NDST	<i>N</i> -deacetylase/ <i>N</i> -sulfotransferase
PBS	phosphate buffered saline
PG	panel grading
% pred	percentage of the predicted value
RV	residual volume
scFv	single chain variable fragment
SD	standard deviation
TLC	total lung capacity
TRITC	tetramethylrhodamine isothiocyanate
TUNEL	terminal deoxynucleotidyl transferase dUTP nick end labeling
VC	vital capacity
VEGF	vascular endothelial growth factor



Chapter 1

The Anatomical Record 2009, In Press
Invited Review

General introduction
&
Aim and outline of this thesis

Heparan sulfates in the lung: structure, diversity and role in pulmonary emphysema

Nicole C. Smits •, ••

Nicholas W. Shworak ••

Richard P.N. Dekhuijzen •••

Toin H. van Kuppevelt •

- *Department of Biochemistry, Radboud University Nijmegen Medical Centre, NCMLS, Nijmegen, The Netherlands*
- *Department of Medicine, Dartmouth Medical School, Hanover, New Hampshire, USA*
- *Department of Pulmonary Diseases, Radboud University Nijmegen Medical Centre, Nijmegen, The Netherlands*

There is an emerging interest in the extracellular matrix (ECM) of the lung, especially in the role it plays in development and disease. There is a rapid change from the classical view of the ECM as a supporting structure towards a view of the ECM as a regulatory entity with profound effects on proliferation, migration and differentiation of pulmonary cells. In the ECM a variety of molecules is present in a highly organized pattern. Next to the abundant fiber-forming molecules such as collagens and elastin, a large number of less abundant molecules are part of the ECM, including proteoglycans. In this review, we will focus on one class of proteoglycans, the heparan sulfate proteoglycans. We will particularly address the structure, biosynthesis, and function of their saccharide moiety, the heparan sulfates, including their role in development and (patho)physiology.

The lung is a highly dynamic organ which during life undergoes a constant change in volume. This puts special demands on the pulmonary connective tissue, particularly lung alveoli, where the actual gas exchange process takes place. For efficient functioning of the lung, alveolar walls have to be thin to obtain proper gas exchange, firm to prevent collapse of the alveolus, and flexible to cope with volume changes during breathing.

Extracellular matrix

The extracellular matrix (ECM) maintains the functions of the lung by supporting its structure and by interactions with a large number of regulatory components. Providing structural and mechanical properties has been considered the prime role of the ECM for a long time. It is now becoming increasingly clear that the ECM has many other physiological roles, mediated through the regulation of a variety of cellular processes¹. Proper functioning of the ECM can only be attained when components are fine-tuned with respect to each other. The constant change in volume during breathing puts high demands on the ECM, and even minor disturbances in the ECM can be expected to have an impact on the lungs' functioning.

The most prominent structural (fibrillar) components of the lungs' ECM are collagen and elastin. Collagens are known to endow pulmonary tissue with structural integrity, whereas elastin plays a role in the elastic characteristics of the lung². Less abundantly present, but functionally very important, are a large number of glycoproteins, including fibronectin, laminins, entactin, fibrillins, and a variety of proteoglycans.

The group of proteoglycans, with their characteristic glycosaminoglycan (GAG) chains, seems to play a particular role in the lung, due to their capacity to bind and modulate a myriad of proteins -including many effector molecules-, their strategic location on cell surfaces and in basement membranes, and their huge variability. Current research is increasingly focused on non-fibrillar components like proteoglycans. In an official statement of the *American Thoracic Society* on future research on pulmonary emphysema, it was stated that: 'Future directions should explore the specific role of pulmonary parenchymal GAGs in maintaining alveolar integrity'³.

Although little is known about the exact roles proteoglycans and GAGs play in the lung, their distribution over various components, their strategic ultrastructural

location ⁴, and their involvement during developmental stages ⁵ suggest their crucial importance for the architecture and functioning of the lung. In this review we will focus on heparan sulfate proteoglycans (HSPGs), especially on their sugar moiety, the heparan sulfates.

Heparan sulfate proteoglycans

Proteoglycans constitute a large family of glycoproteins, consisting of a core protein with highly variable GAG moieties attached to it. GAGs are long unbranched polysaccharides consisting of alternating hexosamine and hexuronic acid residues (Table 1). Keratan sulfate (KS) is an exception since it lacks hexuronic acids. Hyaluronic acid (hyaluronan) is the only GAG that is not attached to a core protein. Depending on the nature of their backbone, the following classes of GAGs can be discerned (see Table 1): heparan sulfate (HS)/heparin, chondroitin/dermatan sulfate (CS/DS), KS and hyaluronan. Heparin is structurally similar to HS, but has a higher degree of *N*-, and *O*-sulfation. The majority of proteoglycans in lung tissue carry HS, DS or CS side chains. The amount of each type of proteoglycan, however, differs in the different compartments of the lung. For example, in the tracheobronchial tree

the major species is a large cartilaginous CS/KS proteoglycan; the pleural lining of the lung contains mainly small DS proteoglycans (DSPGs), whereas heparin, the GAG component of the proteoglycan serglycin, is abundantly present in mast cells. In (alveolar) basement membranes and on cell surfaces HSPGs are the major class. The differences in amount, type, and distribution reflect the different roles of proteoglycans in distinct lung compartments (Figure 1). Basically, three major classes of HSPGs can be discerned: one class primarily confined to basement membranes, one class bound to the cell membrane by a GPI-anchor (*the glypicans*), and one class consisting of transmembrane proteoglycans (*the syndecans*).

Perlecan, agrin, and type XVIII collagen are basement membrane-associated HSPGs (Figure 2). Perlecan has a large, multi-domain core protein of about 467 kDa in humans. The major sites for GAG attachment reside in the extreme amino terminal domain of the perlecan core protein ⁶. These three sites are usually occupied by HS, though CS substitution has also been described. Its complex core protein structure provides the potential to interact with numerous proteins. HS degradation of perlecan

Table 1: Various types of glycosaminoglycans

Glycosaminoglycan	Disaccharide composition	Possible modifications
Chondroitin sulfate	GlcA(β1,3)-GalNAc(β1,4)	2-, 4- and 6-O sulfation
Dermatan sulfate	IdoA(α1,3)/GlcA(β1,3)-GalNAc(β1,4)	2-, 4-, and 6-O sulfation, C5 epimerization
Heparan sulfate/ Heparin	GlcA(β1,4)/IdoA(α1,4)-GlcNAc(α1,4)	<i>N</i> -deacetylation/ <i>N</i> -sulfation C5 epimerization, 2-, 3-, and 6-O sulfation
Keratan sulfate	Gal(β1,4)-GlcNAc(β1,3)	6-O-sulfation
Hyaluronic acid	GlcA(β1,3)-GlcNAc(β1,4)	-

Gal, D-galactose; GalNAc, *N*-acetyl-D-galactosamine; GlcA, glucuronic acid; GlcNAc, *N*-acetyl-D-glucosamine; IdoA, L-iduronic acid.

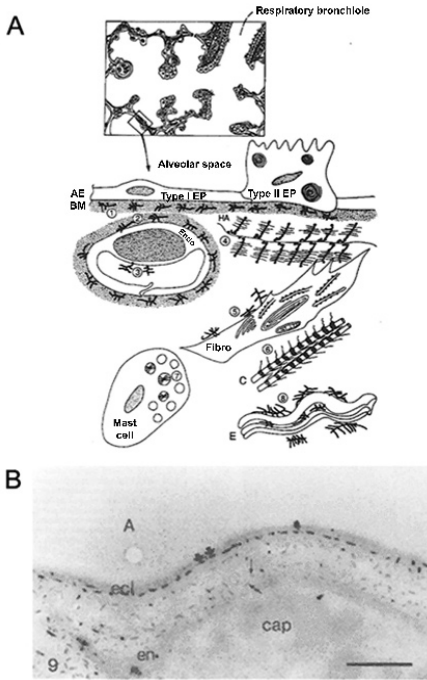


Figure 1. Location of various proteoglycans in lung parenchyma. A. Schematic representation of various proteoglycans present in the alveolar septum. 1) Heparan sulfate (HS) proteoglycan associated with epithelial cell basement membrane; 2) HS proteoglycan associated with endothelial cell basement membrane; 3) HS proteoglycan associated with endothelial cell surface; 4) fibroblast chondroitin sulfate (CS) proteoglycan aggregates with hyaluronan; 5) fibroblast cell surface HS proteoglycan and CS proteoglycan; 6) collagen fibril-associated dermatan sulfate proteoglycan; 7) heparin proteoglycan-containing granules in mast cells; 8) elastin-associated CS proteoglycan. AE, alveolar epithelium; BM, basement membrane; Type I Ep, type I alveolar epithelial cell; Type II Ep, type II alveolar epithelial cell; Endo, endothelial cell; Fibro, fibroblast; C, collagen; E, elastin (adapted from Juul et al, *Proteoglycans. In: The Lung, Scientific Foundations, Vol I, Crystal RC, West JB, Raven Press, NY. 1991;413-420*)¹²⁴. B. Location of heparan sulfate proteoglycans in the blood-air barrier of human alveoli. To visualize

proteoglycans, cuprolinic blue was used according to the critical electrolyte concentration method¹²⁴. Each electron dense filament (arrows) represents a proteoglycan.

Highly sulfated HS-proteoglycans are located in the basement membrane of type I alveolar epithelial cells, where they appear to be located in one plane. In the capillary basement membrane HS-proteoglycans are less sulfated and distributed in a more random fashion.

A, alveolar airspace; cap, capillary; ecl, type I alveolar epithelial cell; en, endothelial cell. Bar, 0.5 μm (Reproduced and adapted with permission from van Kuppevelt et al, 1985).

by the action of HS-degrading enzymes (e.g., heparanases) has been associated with the ability of some metastatic cancer cells to penetrate basement membranes⁷. In the lung, perlecan is associated with basement membrane-producing cells and is also found in all vascularized and some connective tissues (e.g., cartilage).

Perlecan is able to interact with growth factors such as basic fibroblast growth factor (FGF-2) via its HS chains, a property shared with other HSPGs. It can regulate interaction of FGF-2 with its receptor and thereby modulate tissue metabolism. In the lung, FGF-2 is largely bound by HS (Figure 3)^{8, 9}. The multiple functions of perlecan are evident from the tissue disruption that occurs in both perlecan-null mice^{10, 11}, and in humans with mutations in the perlecan gene where disturbances occur in organ development owing to basement membrane perturbation¹¹. Perlecan plays a major role in maintaining the integrity of basement membranes and the cartilage matrix, but has no apparently critical function in (alveolar) basement membrane assembly. Despite the ability of perlecan to interact with several

components of the basement membrane, basement membranes assemble in the absence of perlecan and appear morphologically normal. A likely explanation for this finding is that other HSPGs substitute for the loss of perlecan. A possible candidate could be agrin, which is present in most (if not all) basement membranes and which is also able to bind growth factors.

Agrin induces clustering of acetylcholine receptors and acetylcholine esterases at the postsynaptic membrane of neuromuscular junctions. It has been shown to be distributed in basement membranes of numerous cells. The 220-250 kDa agrin core protein contains two GAG attachment sites. In addition to its

HS chains, agrin also contains *O*-linked glycans in its mucin region and *N*-linked glycans, which bind to other proteins including collagen type IV, several isoforms of laminin, and tenascin. Agrin may interact with carbohydrates, which may affect its activity. In the lung, agrin has been found in alveolar basement membranes¹².

Collagen XVIII is a basement membrane component with the structural properties of both a collagen and a proteoglycan. It is in fact the only currently known collagen that carries HS chains¹³. Proteolytic cleavage within the C-terminal domain releases a fragment, endostatin, which has been reported to have anti-angiogenesis effects¹⁴.

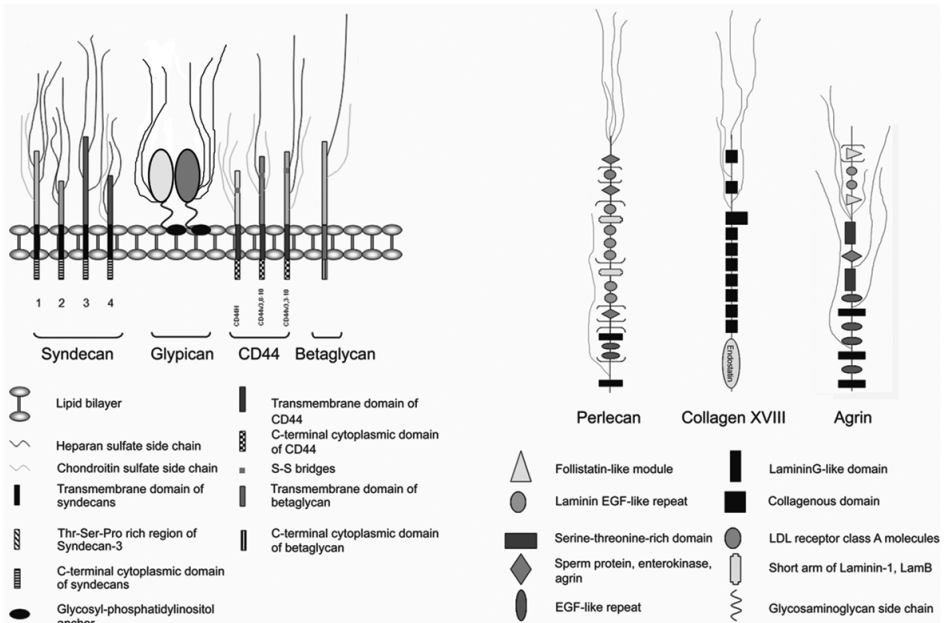


Figure 2. Highly schematic representation of HSPG core proteins, containing HS and/or CS side chains. Shown are the four isoforms of syndecan, two (out of six) isoforms of glypican, three isoforms of CD44 and betaglycan. The three major basement membrane-associated HSPGs, viz: perlecan, collagen XVIII and agrin are also shown.

Collagen XVIII is generally present in epithelia and endothelia, including the basement membranes of the lung, retina, epidermis, pia, cardiac and striated muscle, kidney, and blood vessels^{15, 16}.

Two main types of cell surface-bound proteoglycan core proteins have been identified: the glycosylphosphatidylinositol-linked *glypicans* and secondly the transmembrane *syndecans* (Figure 2). In the lung both glypicans and syndecans are more densely arranged along the alveolar than the capillary surface¹⁷.

Whereas glypicans are linked to the cell surface, the syndecans are a family of highly conserved type I transmembrane HSPGs that are expressed in a developmental and cell type-specific pattern. Syndecans comprise a family of molecules consisting of four members¹⁸⁻²². They are highly expressed at basolateral surfaces of vascular endothelial cells²³, are variably expressed by smooth muscle cells, and can also be found in all layers of the the intima, the media and the adventitia²⁴⁻²⁷. The majority of GAGs added to syndecan core proteins are of the HS type, but syndecan-1 and syndecan-4 may also contain CS²⁸. Biological activity, however, depends largely on the HS moiety²⁹. Syndecan isoforms are expressed in distinct cell-, tissue- and development-specific patterns. Syndecan-1 expression has been reported to be high in lung airway epithelia and skin^{30, 31}. In the lung, matrilysin-mediated shedding of syndecan-1 is involved in directing neutrophil influx to sites of injury³².

CD44 is, like syndecans, a widely distributed type I transmembrane glycoprotein^{33, 34} (Figure 2). It can carry either CS and/or HS side chains and is

upregulated on many activated/diseased cells. *CD44* is also known as a 'part time' proteoglycan, as its glycanation sites are not always occupied with GAG chains. Splicing may result in isoforms that lack transmembrane and cytoplasmic domains, thus yielding secreted, soluble *CD44*³⁵. In the lung, *CD44* is present on parenchymal cells like fibroblasts and epithelial cells. A role for *CD44* in lung pathology has also been demonstrated. In patients with diffuse panbronchiolitis (DPB), a disease characterized by chronic inflammation of respiratory bronchioles, alveolar macrophage dysfunction may result from abnormalities of *CD44* expression which could contribute to the pathogenesis of DPB³⁶. In addition, an impressive role for *CD44* was reported in allergic eosinophilic airway inflammation (experimental asthma)³⁷.

Betaglycan, a transmembrane CS/HSPG, is a major TGF- β binding molecule on most cell types³⁸ (Figure 2). The GAG chains of betaglycan are not necessary for expression at the cell surface, or for the binding of TGF- β ³⁹. Binding of betaglycan with FGF increases the affinity of FGF's to cell receptors, and protects FGFs from proteolysis⁴⁰.

Heparan sulfate biosynthesis

HS has important functions in a variety of developmental, morphogenetic, and pathogenetic processes. The specificities of the interactions between HS and its protein ligands are thought to be due, at least in part, to the fine structure of HS characterized by the specific sulfation patterns and the hexuronic acid isoform residues (Figure 4)⁴¹⁻⁴⁴. The divergent fine structures of HS are generated in the Golgi apparatus through the coordinate actions of HS modification enzymes.

Biosynthesis of HS begins with the addition of xylose to selected serine residues in proteoglycan core proteins. Subsequently, two Gal units and a GlcA residue are added by three distinct glycosyltransferases^{41, 42}. This linkage region is common to HS/heparin but also to CS chains, and in part explains why many HSPGs can also carry CS chains. After the formation of the linkage region, the HS backbone is synthesized by a set of glycosyltransferases belonging to the *EXT* gene family (exostosin proteins EXT1, EXT2, EXTL1, EXTL2 and EXTL3). The backbone is then modified by a semi-ordered series of reactions, which generate distinct HS motifs. During polymerization of the HS chain, HS *N*-deacetylase/*N*-sulfotransferase (NDST) deacetylates and *N*-sulfates subsets of *N*-acetylglucosamine residues of the growing polymer^{45, 46}, Figure 4. Four NDST isoforms have been identified^{43, 47, 48}. *NDST-1* and the less abundant *NDST-2* are widely expressed in a variety of tissues^{45, 46, 49, 50}, whereas *NDST-3* and *NDST-4* are restrictively expressed. The subsequent modification step is C-5 epimerization of GlcA to IdoA by the enzyme D-glucuronyl C5-epimerase^{50, 51}. No isoforms of this enzyme are known. Next, *O*-sulfation occurs at various positions (C-2, C-3, and C-6) by different sulfotransferases. For 3-*O*-sulfation, the rarest modification in HS biosynthesis, at least seven related sulfotransferases exist^{52, 53}. For 6-*O*-sulfation, three isoenzymes are known, whereas 2-*O*-sulfation is mediated by only one enzyme.

The HS modification reactions are generally incomplete, resulting in HS molecules displaying a domain-type arrangement of highly modified saccharide sequences alternating with re-

gions having a low density of modification (Figure 4). Information about HS domain structures in the lung is sparse. HS is very diverse with respect to sulfation⁵⁴⁻⁵⁶, indicating a large heterogeneity with respect to domain and motif structure. The alveolar basement membrane beneath type I cells is highly sulfated compared to those beneath type II cells^{57, 58}. This difference is

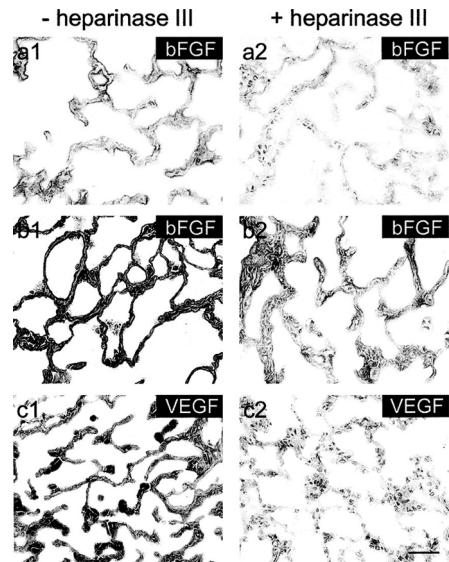


Figure 3. Heparan sulfate binds FGF-2 and VEGF in human lung tissue. Non-treated (a1–c1) and heparinase III-treated (a2–c2) cryosections of human lung parenchyma were incubated with an antibody to FGF-2 (bFGF) (a, b) or VEGF (c). Heparinase III removes HS from the sections. Sections b and c were pretreated with 20 µg/ml recombinant FGF-2 and VEGF respectively, before incubation with an antibody to FGF-2 or VEGF. Heparinase III treatment removed endogenous FGF-2 (a2), and reduced binding of recombinant FGF-2 and recombinant VEGF to sections (b2, c2). Scale bar: 50 µm (Reproduced and adapted with permission from Smits et al. 2004).

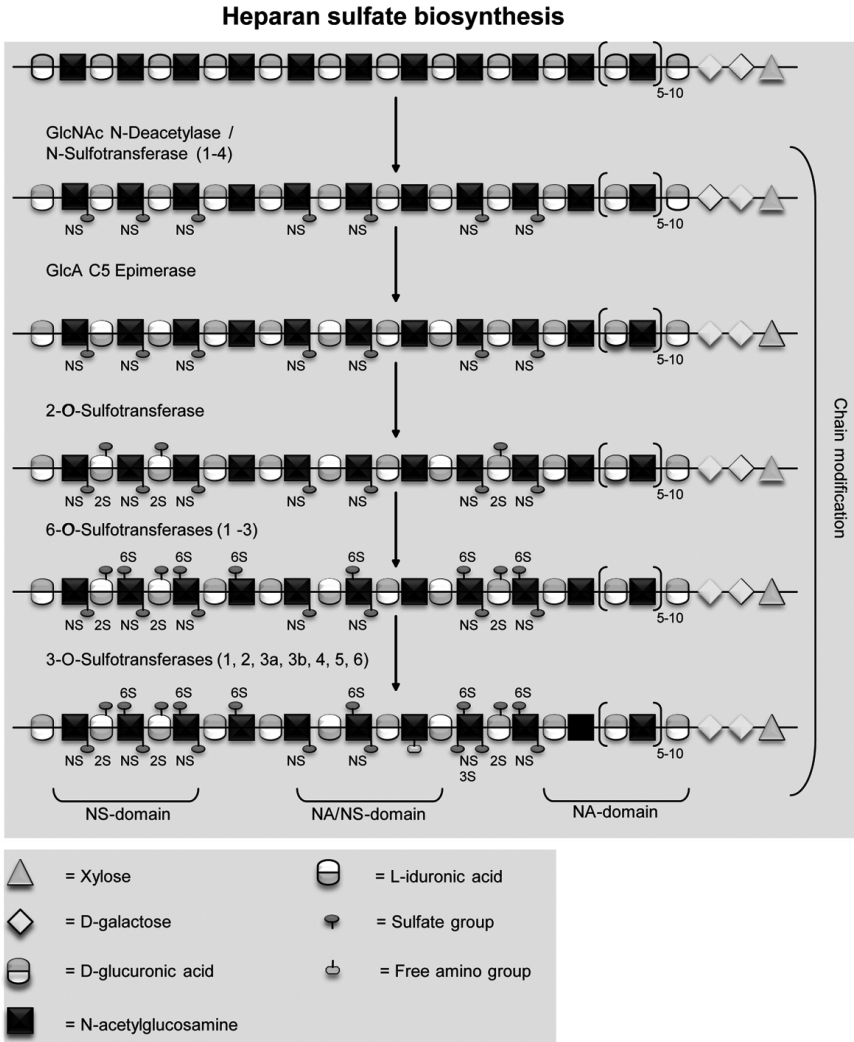


Figure 4. Biosynthesis of heparan sulfate. In heparan sulfate (HS) biosynthesis *N*-deacetylase/*N*-sulfotransferase (NDST) enzymes are responsible for the first modification step. *N*-deacetylation and *N*-sulfation of GlcNAc, has an important function, since the remaining *N*-acetylated regions will largely escape subsequent modifications. The *N*-sulfated regions are subject to additional modification steps at various positions, including C-5 epimerization of glucuronic acid (GlcA) to IdoA (by C5-epimerase), and *O*-sulfation. The various *O*-sulfotransferases include: 2-*O*-sulfotransferase (2-*O*-sulfation of iduronic acid (IdoA) and GlcA); 6-*O*-sulfotransferase (6-*O*-sulfation of *N*-acetyl/sulfo-glucosamine), and 3-*O*-sulfotransferase (3-*O*-sulfation of *N*-unsubstituted/sulfo-glucosamine). The formation of the *N*-unsubstituted glucosamine is possibly due to an incomplete *N*-deacetylation/*N*-sulfation reaction (Reprinted with permission from Esko JD, Selleck JB, 2002).

mainly due to the presence of HSPGs as shown histochemically by differential enzymatic digestions^{57, 58}. Using phage display-derived antibodies against lung HS, the location of structurally different HS chains has been demonstrated (Figure 5)⁸. Substrata containing CS and heparin with different degrees of sulfation modulate the response of alveolar type II cells *in vitro* to growth factors including FGF-1, -2 and -7, and (highly sulfated) heparin seems to reduce responsiveness to FGF's^{59, 60}. Highly sulfated proteoglycans modified by NDSTs are responsible for the spreading of cells during transdifferentiation of type II cells to mature type I cells⁶¹.

Heparan sulfate and lung development/pathology

The generation of knockout mice for various proteoglycan core proteins and proteins involved in the biosynthesis of HS has added significantly to our understanding of the physiological role of HS⁶². Due to their capacity to bind a diverse set of proteins (Table 2), HS/heparin present in the ECM and on cell surfaces has been implicated in many cellular processes such as angiogenesis, cell proliferation and differentiation, cell adhesion, metastasis, tumor growth, tissue repair, and protein expression.

Specific HS modifications have been linked to binding/modulation of ligands. For example, FGF-2 requires *N*- and 2-*O*-sulfates for binding. The 6-*O*-sulfate group is not essential for binding of FGF-2, but is critical for activation of the FGF-receptor. Activation of antithrombin by HS/heparin is mediated by a specific pentasaccharide in which an internal 3-*O*-sulfate and an adjacent 6-*O*-sulfate group are crucial²³. The necessity for the correct

complement of enzymes to generate these specific HS domains at various stages of development is becoming apparent from studies of biosynthetic enzyme mutants.

Interestingly, mice deficient in one of the enzymes involved in HS biosynthesis have abnormal phenotypes. Despite the fact that the defects observed are characteristic of the missing/mutated enzyme, significant overlapping lung phenotypes have been observed for some HS mutants (Table 3). Mouse embryos carrying a homozygous deletion of the gene *Ext1* lack an organized mesoderm and extra embryonic tissues, and die at the gastrulation stage⁶³. Inactivation of *Ext1* abolishes the production of HS, illustrating the importance of *Ext* genes in HS synthesis. Loss of *Ext2* results in early embryonic lethality⁶⁴. The lack of *Ext2* leads to a gastrulation defect and abnormalities in the formation of extra-embryonic structures.

NDST-1 deficient mice have under-sulfated HS in which *N*-sulfation and 2-*O*-sulfation are reduced, but in which 6-*O*-sulfation seems normal⁶⁵. Null mice experience severe respiratory difficulties as judged from their gasping breath and skin color. They die shortly after birth due to respiratory failure caused by immaturity of type II pneumocytes, which results in insufficient production of surfactant^{65, 66}.

The lack of NDST-2 in mice does not affect normal life span and fertility, but NDST-2 deficient mice display severe mast cell defects, caused by a complete lack of heparin. Surprisingly, they show no obvious HS defects^{67, 68}. The lack of HS defects in NDST-2 deficient mice indicates that other isoforms of NDSTs are more important in HS biosynthesis or that these isoforms are able to compensate

Table 2: Glycosaminoglycan-binding proteins (partial list)

- Chemokines	- Nuclear proteins
CXC chemokines, CC chemokines	Histones, transcription factors
- Enzymes	- Morphogens
Elastase	Activin
Lipoprotein lipase	Bone morphogenetic proteins
Superoxide dismutase	Sonic hedgehog
Thrombin	Sprouty peptides
- Enzyme inhibitors	Wnts
Antithrombin	- Cell adhesion molecules
Heparin cofactor II	Selectins, integrins, neural cell adhesion molecules
Protein C inhibitor	
- Growth factors	- Lipoproteins
Epidermal growth factors	Low and very low density lipoproteins
Fibroblast growth factors	Apolipoproteins
Hepatocyte growth factors	- Other proteins
Platelet-derived growth factors	Prion proteins
Transforming growth factors	Amyloid proteins
Vascular endothelial growth factors	Fibrin
- Growth factor-binding proteins	Ion channels
Follistatin	- Extracellular matrix proteins
IGF binding proteins	Collagens, fibrillins
TGF β binding proteins	Fibronectin, laminin
FGF receptor	Thrombospondin, vitronectin

Reprinted with permission from Esko JD, and Selleck JB, 2002

for the lack of NDST-2.

Mice deficient in NDST-3 are fertile and show subtle changes in their behavior and in some hematological parameters⁶⁹. In the adult brain, a region-specific activity of NDST-3 could be detected leading to changes in HS sulfation. However, no significant overall changes in HS sulfation and no obvious lung defects could be detected. In addition, mice that are deficient in both NDST-

1 and NDST-3 have a complete lack of disulfated disaccharide products⁶⁹.

Targeted disruption of D-glucuronyl C5-epimerase gene results in mouse embryos with GlcA but no IdoA residues and a highly distorted sulfation pattern, including a strong reduction of 2-O-sulfation⁷⁰. Lungs of mutant mice are immature and poorly inflated with thickened, cell-rich interalveolar septa. Not surprising, the corresponding phenotype is

lethal.

Mice homozygous for a gene trap mutation that disrupts the gene encoding HS 2-*O*-sulfotransferase (*HS2ST*) exhibit bilateral renal agenesis, resulting from a failure of ureteric bud branching and mesenchymal condensation. They show defects of the eye and skeleton⁷¹, but no obvious lung defects.

HS6ST-1 (HS 6-*O*-sulfotransferase-1) deficient mice exhibit increased neonatal lethality, decreased growth and show aberrant lung morphology⁷². In another study⁷³, morphological and marker analysis of lungs of null mice at birth reveal no obvious changes in cellular profile, architecture, or expression of differentiation markers. However, adult mice show enlargement of the airspaces suggesting that 6-*O*-sulfation of HS is essential for homeostasis of alveoli. Airspace enlargement was associated with fragmented and irregularly deposited elastin in alveoli, a feature suggestive of pulmonary emphysema. The formation of lung alveoli is known to be regulated by *Wnt5a*, *FGF-10*, and *BMP4*, which bind to HS/heparin. *HS6ST-1* is expressed strongly at the tips of branching tubules in the developing lung⁷⁴ and *FGF-10* is preferentially bound to 6-*O*-sulfate residues rather than 2-*O*-sulfate residues in HS. A deficiency in *HS6ST-1* is potentially relevant to impaired lung development. Decreased 6-*O*-sulfation may affect the signaling of growth factors and ECM proteins in the lung which impact alveolarization.

Mice deficient in HS 3-*O*-sulfotransferase-1 (*HS3ST-1*) are seemingly healthy, but develop several unanticipated abnormalities. These include spontaneous eye degeneration, aberrant cardiovascular response to anesthesia, reduced male and

female fertility, postnatal lethality and intrauterine growth retardation⁷⁵.

Recently, a novel family of glucosamine-6-sulfatases has been identified⁷⁶⁻⁷⁹. *Sulf1* and *Sulf2* are members of (extracellular) 6-*O*-endosulfatases and remove 6-*O*-sulfates from HS⁷⁶. Homozygous mice with a gene trap disruption of the *Sulf2* gene display strain-specific defects in viability, growth and lung development. A number of the *Sulf2* homozygotes display lung-related defects as can be judged from their breathing difficulties and enlarged airspaces⁸⁰. It

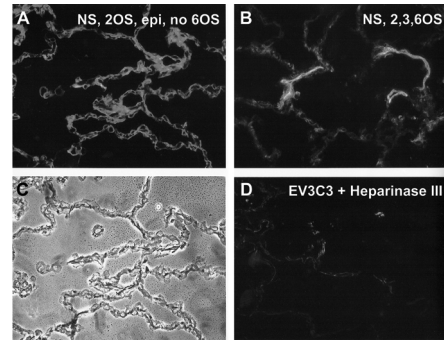
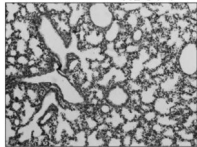
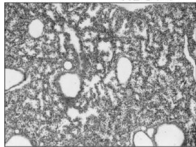
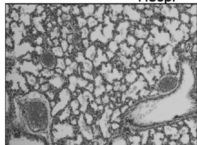
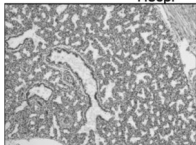
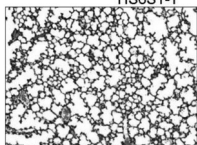
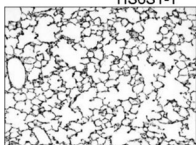
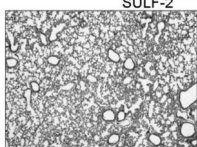


Figure 5. Immunostaining for different heparan sulfate domains in human lung parenchyma using phage display-derived single chain antibodies. A: staining with single chain antibody EV3C3, which recognizes heparan sulfate domains characterized by *N*- and 2-*O*-sulfation, C-5 epimerization, but which is inhibited by 6-*O*-sulfation. B: Phase contrast image of section used in a. C: staining with single chain antibody HS4C3, which shows high affinity for *N*-, 2-, 3-, and 6-*O*-sulfated heparan sulfate domains. D: antibody staining of section after pre-treatment with heparinase III which removes heparan sulfates. Note that the two antibodies stain different areas in human lung parenchyma, EV3C3 primarily reacting with basement membranes in the alveolus, HS4C3 primarily reacting with small blood vessels.

Table 3: Pulmonary phenotypes in mice lacking a specific HS biosynthetic enzyme

Enzyme	Pulmonary phenotype		
NDST-1	Respiratory failure due to immature type II pneumocytes resulting in insufficient production of surfactant, and atelectasis ⁶⁶		
Hsepi	Poorly inflated, immature lungs ⁷⁰		
HS6ST-1	Impaired lung development. Airspace enlargement during postnatal period associated with abnormal elastin deposition ⁷²		
SULF-2	Incompletely penetrant lung phenotype, including enlarged air spaces ⁸⁰		

Given are HS mutants with an obvious lung phenotype. It should be noted that other HS mutants exist, but no obvious lung phenotype has been reported. Reproduced with permission.

should be noted here, that lung phenotypes observed in mice defective in HS biosynthetic enzymes are likely the result of a disturbed lung development and that the airspace enlargements observed may be due to defects in (secondary) septation that gives rise to formation of alveoli.

Mutations in the core proteins themselves can also lead to lung defects. For example, glypican-3 deficient mice exhibit developmental overgrowth, cystic and dysplastic kidneys, and defective

lung development ⁸¹. They often develop respiratory infections with high frequency. Interestingly, lungs from null mice were found to be disproportionately heavy at time of birth, weighing about 28% more than their normal littermates. This disproportionate overgrowth is only evident in newborn mice and might be due to the accumulation of debris observed in the lungs after birth.

Although many knock out models, deficient in enzymes involved in HS biosynthesis, have been developed, the

lungs are generally overlooked and not studied at great length. A more detailed analysis of mouse models will very likely reveal more subtle phenotypes, some of which may be related to lung pathology. The construction of conditionally and lung-specific knock out models will allow for a better understanding of the complex *in vivo* roles of HS in lung pathology.

Heparan sulfate and pulmonary emphysema

HS binds and modulates various classes of proteins which are involved in the pathogenesis of emphysema. These include proteases and protease inhibitors (protease anti-protease hypothesis^{82, 83}), enzymes involved in neutralizing reactive oxygen species like superoxide dismutase⁸⁴ and xanthine oxidase^{85, 86}, chemokines (emphysema as a immunological disorder hypothesis⁸⁷), and growth factors/cytokines (aberrant tissue repair hypothesis⁸⁸).

HS forms fulfill many functions that may relate them to the pathogenesis of emphysema. They:

- a) are involved in the fibrillogenesis of collagen and elastin⁸⁹⁻⁹²
- b) offer protection against proteolysis of collagen and elastin^{93, 94}
- c) posses anti-protease activity (e.g., anti-elastase, anti-cathepsin)⁹⁵⁻⁹⁸
- d) bind and modulate growth factors/ cytokines
- e) have a high water-binding capacity providing resilience to the alveolar wall⁹⁹
- f) are able to inhibit neutrophil function

Alterations in proteoglycan/GAG structure and/or content have been observed in lung tissue derived from both patients with emphysema and animal models,

although results tend to be contradictory¹⁰⁰⁻¹⁰⁴. In urine samples of emphysematous patients a decrease of a specific HS epitope has been noticed¹⁰⁵, and in lung tissue from patients with severe emphysema a diminished staining for HSPG as well as for the interstitial proteoglycans decorin and biglycan has been reported¹⁰⁶. HS is prone to depolymerization by reactive oxygen and nitrogen species like hydroxyl radicals¹⁰⁷, and nitric oxide¹⁰⁸, and the level of HS/GAG is compromised by toxic levels of oxygen¹⁰⁹.

HSPGs have also been implicated in the pathogenesis of emphysema in mammalian models. Specific inhibition of proteoglycan synthesis induces emphysematous lesions in rats¹¹⁰. In elastase-induced emphysema in rats, HS is readily removed from the lungs by degradation of the protein core of HSPGs¹¹¹. As a consequence the protective protease (elastase) inhibiting capacity of HS may be lost^{96, 97}. For elastase-induced emphysema in rats, the only long-term disturbance was a decrease in the HS/collagen ratio and the HS/elastin ratio¹¹².

Taken together, data indicate that HS plays a crucial role in the homeostasis of the lung, especially in the parenchymal tissue. HS is compromised in emphysema, and (given the multiple functions ascribed to this GAG) may lead to a major disturbance in the coordination of effector molecules ranging from growth factors and morphogens to proteases and matrix molecules, thus compromising orderly tissue repair and regeneration, cumulating in the development of emphysematous lesions. Studies on HS in the lung pathology, however, are scarce, and primarily due to a lack of appropriate

tools to study them. New tools are now entering the field, including antibodies defining specific HS domains^{8, 113-116}, sequencing techniques to establish the monosaccharide sequence of HS^{117, 118}, and new ways to chemically synthesize defined HS oligosaccharides¹¹⁹. This new armamentarium may spark new avenues of research into the role of GAGs in general, and HS in particular, in the lung. Future discoveries may be especially rewarding with respect to the development of new therapeutics to fight emphysema. The therapeutic potential of GAGs and HS was already indicated at the end of last century when it was shown that heparin (= highly sulfated HS) and sulfated polysaccharides could prevent elastase-induced emphysema in mice and hamsters^{96, 120-122}. Recently, the protective role of aerosolized hyaluronan against elastase-induced or smoke-induced lung damage including airspace enlargement has been reported¹²³. Clearly, the exploration of the intriguing field of lung glycobiology has only just begun.

Aim and outline of this thesis

In the research towards the ECM of the lung and its involvement in the pathogenesis of emphysema, proteoglycans have been studied. However, these studies primarily focused on the protein core, largely ignoring the GAG moiety of the proteoglycans. Investigating the role of GAGs has long been hampered by the lack of appropriate tools, e.g.,

antibodies. The aim underlying the study described in this thesis was to isolate HS from human lung, to generate highly specific antibodies against human lung HS by means of phage display technology, as well as to investigate the distribution of these HS epitopes in human lung. In addition, the involvement of HS in the pathogenesis of emphysema has been addressed. An overview of the present knowledge concerning GAGs in the lung is given in **Chapter 1**. In **Chapter 2** a description is given of the use of phage display technology to generate and select antibodies against human GAG epitopes. Phage display technology was used to select 7 unique antibodies against human lung HS, as described in **Chapter 3**. These novel antibodies were used to evaluate the expression of distinct HS epitopes in human lung tissue. **Chapter 4** deals with the unraveling of the monosaccharide sequence recognized by phage display-derived antibody, NS4F5. Special attention is given to the characterization of the HS sequence which was (GlcNS-6S-IdoA2S)₃. In **Chapter 5**, lung tissue from subjects with microscopical emphysema was used to demonstrate that heparanase expression and loss of HS in the lung are early events in the development of emphysema. In **Chapter 6**, focus is on fibrillin-1, a major component of the microfibrillar part of elastic fibers, another important player in the onset of pulmonary emphysema. **Chapter 7** concludes this thesis with a summary as well as indications for future research.

References

1. Frevert, C. W. & Sannes, P. L. Matrix proteoglycans as effector molecules for epithelial cell function. *Eur Respir Rev* 14, 137-144 (2005).
2. Nakamura, T. et al. Fibulin-5/DANCE is essential for elastogenesis in vivo. *Nature* 415, 171-5 (2002).
3. Update: future directions for research on diseases of the lung. The American Thoracic Society. *Am J Respir Crit Care Med* 158, 320-34 (1998).
4. van Kuppevelt, T. H. et al. Ultrastructural localization and characterization of proteoglycans in human lung alveoli. *Eur J Cell Biol* 36, 74-80. (1985).
5. Wang, Y., Sakamoto, K., Khosla, J. & Sannes, P. L. Detection of chondroitin sulfates and decorin in developing fetal and neonatal rat lung. *Am J Physiol Lung Cell Mol Physiol* 282, L484-90 (2002).
6. Costell, M., Mann, K., Yamada, Y. & Timpl, R. Characterization of recombinant perlecan domain I and its substitution by glycosaminoglycans and oligosaccharides. *Eur J Biochem* 243, 115-21 (1997).
7. Dempsey, L. A., Brunn, G. J. & Platt, J. L. Heparanase, a potential regulator of cell-matrix interactions. *Trends Biochem Sci* 25, 349-51 (2000).
8. Smits, N. C. et al. Heterogeneity of heparan sulfates in human lung. *Am J Respir Cell Mol Biol* 30, 166-73 (2004).
9. Sannes, P. L., Burch, K. K. & Khosla, J. Immunohistochemical localization of epidermal growth factor and acidic and basic fibroblast growth factors in postnatal developing and adult rat lungs. *Am J Respir Cell Mol Biol* 7, 230-7 (1992).
10. Costell, M. et al. Perlecan maintains the integrity of cartilage and some basement membranes. *J Cell Biol* 147, 1109-22 (1999).
11. Nicole, S. et al. Perlecan, the major proteoglycan of basement membranes, is altered in patients with Schwartz-Jampel syndrome (chondrodystrophic myotonia). *Nat Genet* 26, 480-3 (2000).
12. Groffen, A. J. et al. Primary structure and high expression of human agrin in basement membranes of adult lung and kidney. *Eur J Biochem* 254, 123-8 (1998).
13. Halfter, W., Dong, S., Schurer, B. & Cole, G. J. Collagen XVIII is a basement membrane heparan sulfate proteoglycan. *J Biol Chem* 273, 25404-12 (1998).
14. Marneros, A. G. & Olsen, B. R. Physiological role of collagen XVIII and endostatin. *Faseb J* 19, 716-28 (2005).
15. Dong, S., Cole, G. J. & Halfter, W. Expression of collagen XVIII and localization of its glycosaminoglycan attachment sites. *J Biol Chem* 278, 1700-7 (2003).
16. Li, Q. & Olsen, B. R. Increased angiogenic response in aortic explants of collagen XVIII/endostatin-null mice. *Am J Pathol* 165, 415-24 (2004).
17. Negrini, D., Passi, A. and De Luca, G. in *Lung Biology in Health and Disease* (Marcel Dekker, inc, New York, 2003).
18. Carey, D. J. Syndecans: multifunctional cell-surface co-receptors. *Biochem J* 327 (Pt 1), 1-16 (1997).
19. David, G. Integral membrane heparan sulfate proteoglycans. *Faseb J* 7, 1023-30 (1993).
20. Couchman, J. R. & Woods, A. Syndecans, signaling, and cell adhesion. *J Cell Biochem* 61, 578-84 (1996).
21. Bernfield, M. et al. Biology of the syndecans: a family of transmembrane heparan sulfate proteoglycans. *Annu Rev Cell Biol* 8, 365-93 (1992).
22. Rapraeger, A. C. & Ott, V. L. Molecular interactions of the syndecan core proteins. *Curr Opin Cell Biol* 10, 620-8 (1998).
23. Rosenberg, R. D., Shworak, N. W., Liu, J., Schwartz, J. J. & Zhang, L. Heparan sulfate proteoglycans

- of the cardiovascular system. Specific structures emerge but how is synthesis regulated? *J Clin Invest* 99, 2062-70 (1997).
24. Kojima, T. Molecular biology of ryudocan, an endothelial heparan sulfate proteoglycan. *Semin Thromb Hemost* 26, 67-73 (2000).
 25. Cizmeci-Smith, G., Stahl, R. C., Showalter, L. J. & Carey, D. J. Differential expression of transmembrane proteoglycans in vascular smooth muscle cells. *J Biol Chem* 268, 18740-7 (1993).
 26. Cizmeci-Smith, G., Langan, E., Youkey, J., Showalter, L. J. & Carey, D. J. Syndecan-4 is a primary-response gene induced by basic fibroblast growth factor and arterial injury in vascular smooth muscle cells. *Arterioscler Thromb Vasc Biol* 17, 172-80 (1997).
 27. Rosenberg, R. D., Shworak, N. W., Liu, J., Schwartz, J. J. & Zhang, L. Heparan sulfate proteoglycans of the cardiovascular system. Specific structures emerge but how is synthesis regulated? *J Clin Invest* 100, S67-75 (1997).
 28. Deepa, S. S., Yamada, S., Zako, M., Goldberger, O. & Sugahara, K. Chondroitin sulfate chains on syndecan-1 and syndecan-4 from normal murine mammary gland epithelial cells are structurally and functionally distinct and cooperate with heparan sulfate chains to bind growth factors. A novel function to control binding of midkine, pleiotrophin, and basic fibroblast growth factor. *J Biol Chem* 279, 37368-76 (2004).
 29. Langford, J. K., Stanley, M. J., Cao, D. & Sanderson, R. D. Multiple heparan sulfate chains are required for optimal syndecan-1 function. *J Biol Chem* 273, 29965-71 (1998).
 30. Shah, L. et al. Expression of syndecan-1 and expression of epidermal growth factor receptor are associated with survival in patients with nonsmall cell lung carcinoma. *Cancer* 101, 1632-8 (2004).
 31. Elenius, V., Gotte, M., Reizes, O., Elenius, K. & Bernfield, M. Inhibition by the soluble syndecan-1 ectodomains delays wound repair in mice overexpressing syndecan-1. *J Biol Chem* 279, 41928-35 (2004).
 32. Li, Q., Park, P. W., Wilson, C. L. & Parks, W. C. Matrilysin shedding of syndecan-1 regulates chemokine mobilization and transepithelial efflux of neutrophils in acute lung injury. *Cell* 111, 635-46 (2002).
 33. Pall, T. et al. Recombinant CD44-HABD is a novel and potent direct angiogenesis inhibitor enforcing endothelial cell-specific growth inhibition independently of hyaluronic acid binding. *Oncogene* 23, 7874-81 (2004).
 34. Teriete, P. et al. Structure of the regulatory hyaluronan binding domain in the inflammatory leukocyte homing receptor CD44. *Mol Cell* 13, 483-96 (2004).
 35. Yu, Q. & Toole, B. P. A new alternatively spliced exon between v9 and v10 provides a molecular basis for synthesis of soluble CD44. *J Biol Chem* 271, 20603-7 (1996).
 36. Katoh, S. et al. Characterization of CD44 expressed on alveolar macrophages in patients with diffuse panbronchiolitis. *Clin Exp Immunol* 126, 545-50 (2001).
 37. Katoh, S. et al. A role for CD44 in an antigen-induced murine model of pulmonary eosinophilia. *J Clin Invest* 111, 1563-70 (2003).
 38. Lopez-Casillas, F. et al. Betaglycan expression is transcriptionally up-regulated during skeletal muscle differentiation. Cloning of murine betaglycan gene promoter and its modulation by MyoD, retinoic acid, and transforming growth factor-beta. *J Biol Chem* 278, 382-90 (2003).
 39. Lopez-Casillas, F., Wrana, J. L. & Massague, J. Betaglycan presents ligand to the TGF beta signaling receptor. *Cell* 73, 1435-44 (1993).
 40. Roberts, C. R., Wight, T. N. & Gascall, V. C. in *The Lung: Scientific Foundations Second Edition* (eds. Crystal, R. G. & West, J. B.) 757-767 (Lippincott - Raven Publishers, Philadelphia, Philadelphia, 1997).
 41. Esko, J. D. & Selleck, S. B. Order out of chaos: assembly of ligand binding sites in heparan sulfate. *Annu Rev Biochem* 71, 435-71 (2002).
 42. Sugahara, K. & Kitagawa, H. Recent advances in the study of the biosynthesis and functions of

- sulfated glycosaminoglycans. *Curr Opin Struct Biol* 10, 518-27 (2000).
43. Eriksson, I., Sandback, D., Ek, B., Lindahl, U. & Kjellen, L. cDNA cloning and sequencing of mouse mastocytoma glucosaminyl N-deacetylase/N-sulfotransferase, an enzyme involved in the biosynthesis of heparin. *J Biol Chem* 269, 10438-43 (1994).
 44. Hashimoto, Y., Orellana, A., Gil, G. & Hirschberg, C. B. Molecular cloning and expression of rat liver N-heparan sulfate sulfotransferase. *J Biol Chem* 267, 15744-50 (1992).
 45. Humphries, D. E., Sullivan, B. M., Aleixo, M. D. & Stow, J. L. Localization of human heparan glucosaminyl N-deacetylase/N-sulphotransferase to the trans-Golgi network. *Biochem J* 325 (Pt 2), 351-7 (1997).
 46. Kusche-Gullberg, M., Eriksson, I., Pikas, D. S. & Kjellen, L. Identification and expression in mouse of two heparan sulfate glucosaminyl N-deacetylase/N-sulfotransferase genes. *J Biol Chem* 273, 11902-7 (1998).
 47. Orellana, A., Hirschberg, C. B., Wei, Z., Swiedler, S. J. & Ishihara, M. Molecular cloning and expression of a glycosaminoglycan N-acetylglucosaminyl N-deacetylase/N-sulfotransferase from a heparin-producing cell line. *J Biol Chem* 269, 2270-6 (1994).
 48. Aikawa, J. & Esko, J. D. Molecular cloning and expression of a third member of the heparan sulfate/heparin GlcNAc N-deacetylase/ N-sulfotransferase family. *J Biol Chem* 274, 2690-5 (1999).
 49. Aikawa, J., Grobe, K., Tsujimoto, M. & Esko, J. D. Multiple isozymes of heparan sulfate/heparin GlcNAc N-deacetylase/GlcN N-sulfotransferase. Structure and activity of the fourth member, NDST4. *J Biol Chem* 276, 5876-82 (2001).
 50. Crawford, B. E., Olson, S. K., Esko, J. D. & Pinhal, M. A. Cloning, Golgi localization, and enzyme activity of the full-length heparin/heparan sulfate-glucuronic acid C5-epimerase. *J Biol Chem* 276, 21538-43 (2001).
 51. Li, J. P., Gong, F., El Darwish, K., Jalkanen, M. & Lindahl, U. Characterization of the D-glucuronyl C5-epimerase involved in the biosynthesis of heparin and heparan sulfate. *J Biol Chem* 276, 20069-77 (2001).
 52. Mochizuki, H. et al. Characterization of a heparan sulfate 3-O-sulfotransferase-5, an enzyme synthesizing a tetrasulfated disaccharide. *J Biol Chem* 278, 26780-7 (2003).
 53. Shworak, N. W. et al. Multiple isoforms of heparan sulfate D-glucosaminyl 3-O-sulfotransferase. Isolation, characterization, and expression of human cdnas and identification of distinct genomic loci. *J Biol Chem* 274, 5170-84 (1999).
 54. Linker, A. & Hovingh, P. The heparitin sulfates (heparan sulfates). *Carbohydr Res* 29, 41-62 (1973).
 55. Radhakrishnamurthy, B., Jeansonne, N. E. & Berenson, G. S. Heterogeneity of heparan sulfate chains in a proteoglycan from bovine lung. *Biochim Biophys Acta* 802, 314-20 (1984).
 56. Linker, A. & Hovingh, P. Structural studies of heparitin sulfates. *Biochim Biophys Acta* 385, 324-33 (1975).
 57. Sannes, P. L. Differences in basement membrane-associated microdomains of type I and type II pneumocytes in the rat and rabbit lung. *J Histochem Cytochem* 32, 827-33 (1984).
 58. van Kuppevelt, T. H., Cremers, F. P., Domen, J. G. & Kuyper, C. M. Staining of proteoglycans in mouse lung alveoli. II. Characterization of the Cuproinic blue-positive, anionic sites. *Histochem J* 16, 671-86 (1984).
 59. Sannes, P. L., Khosla, J. & Cheng, P. W. Sulfation of extracellular matrices modifies responses of alveolar type II cells to fibroblast growth factors. *Am J Physiol* 271, L688-97 (1996).
 60. Sannes, P. L., Khosla, J., Li, C. M. & Pagan, I. Sulfation of extracellular matrices modifies growth factor effects on type II cells on laminin substrata. *Am J Physiol* 275, L701-8 (1998).
 61. Li, Z. Y., Hirayoshi, K. & Suzuki, Y. Expression of N-deacetylase/sulfotransferase and 3-O-sulfotransferase in rat alveolar type II cells. *Am J Physiol Lung Cell Mol Physiol* 279, L292-301 (2000).

62. Forsberg, E. & Kjellen, L. Heparan sulfate: lessons from knockout mice. *J Clin Invest* 108, 175-80 (2001).
63. Lin, X. et al. Disruption of gastrulation and heparan sulfate biosynthesis in EXT1-deficient mice. *Dev Biol* 224, 299-311 (2000).
64. Stickens, D., Zak, B. M., Rougier, N., Esko, J. D. & Werb, Z. Mice deficient in *Ext2* lack heparan sulfate and develop exostoses. *Development* 132, 5055-68 (2005).
65. Ringvall, M. et al. Defective heparan sulfate biosynthesis and neonatal lethality in mice lacking N-deacetylase/N-sulfotransferase-1. *J Biol Chem* 275, 25926-30. (2000).
66. Fan, G. et al. Targeted disruption of NDST-1 gene leads to pulmonary hypoplasia and neonatal respiratory distress in mice. *FEBS Lett* 467, 7-11 (2000).
67. Forsberg, E. et al. Abnormal mast cells in mice deficient in a heparin-synthesizing enzyme. *Nature* 400, 773-6 (1999).
68. Humphries, D. E. et al. Heparin is essential for the storage of specific granule proteases in mast cells. *Nature* 400, 769-72 (1999).
69. Pallerla, S. R. et al. Altered heparan sulfate structure in mice with deleted NDST3 gene function. *J Biol Chem* (2008).
70. Li, J. P. et al. Targeted disruption of a murine glucuronyl C5-epimerase gene results in heparan sulfate lacking L-iduronic acid and in neonatal lethality. *J Biol Chem* 278, 28363-6 (2003).
71. Bullock, S. L., Fletcher, J. M., Beddington, R. S. & Wilson, V. A. Renal agenesis in mice homozygous for a gene trap mutation in the gene encoding heparan sulfate 2-sulfotransferase. *Genes Dev* 12, 1894-906 (1998).
72. Habuchi, H. et al. Mice deficient in heparan sulfate 6-O-sulfotransferase-1 exhibit defective heparan sulfate biosynthesis, abnormal placentation and late embryonic lethality. *J Biol Chem* (2007).
73. Izvolsky, K. I., Lu, J., Martin, G., Albrecht, K. H. & Cardoso, W. V. Systemic inactivation of *Hs6st1* in mice is associated with late postnatal mortality without major defects in organogenesis. *Genesis* 46, 8-18 (2008).
74. Izvolsky, K. I. et al. Heparan sulfate-FGF10 interactions during lung morphogenesis. *Dev Biol* 258, 185-200 (2003).
75. Shworak, N. W., HajMohammadi, S., de Agostini, A. I. & Rosenberg, R. D. Mice deficient in heparan sulfate 3-O-sulfotransferase-1: normal hemostasis with unexpected perinatal phenotypes. *Glycoconj J* 19, 355-61 (2002).
76. Dhoot, G. K. et al. Regulation of Wnt signaling and embryo patterning by an extracellular sulfatase. *Science* 293, 1663-6 (2001).
77. Morimoto-Tomita, M., Uchimura, K., Werb, Z., Hemmerich, S. & Rosen, S. D. Cloning and characterization of two extracellular heparin-degrading endosulfatases in mice and humans. *J Biol Chem* 277, 49175-85 (2002).
78. Nagamine, S., Koike, S., Keino-Masu, K. & Masu, M. Expression of a heparan sulfate remodeling enzyme, heparan sulfate 6-O-endosulfatase sulfatase FP2, in the rat nervous system. *Brain Res Dev Brain Res* 159, 135-43 (2005).
79. Ohto, T. et al. Identification of a novel nonlysosomal sulphatase expressed in the floor plate, choroid plexus and cartilage. *Genes Cells* 7, 173-85 (2002).
80. Lum, D. H., Tan, J., Rosen, S. D. & Werb, Z. Gene trap disruption of the mouse heparan sulfate 6-O-endosulfatase gene, *Sulf2*. *Mol Cell Biol* 27, 678-88 (2007).
81. Cano-Gauci, D. F. et al. Glypican-3-deficient mice exhibit developmental overgrowth and some of the abnormalities typical of Simpson-Golabi-Behmel syndrome. *J Cell Biol* 146, 255-64 (1999).
82. Snider, G. L. Emphysema: the first two centuries--and beyond. A historical overview, with suggestions for future research: Part 2. *Am Rev Respir Dis* 146, 1615-22 (1992).
83. Gadek, J. E. & Pacht, E. R. The protease-antiprotease balance within the human lung: implications

- for the pathogenesis of emphysema. *Lung* 168 Suppl, 552-64 (1990).
84. Tibell, L. A., Sethson, I. & Buevich, A. V. Characterization of the heparin-binding domain of human extracellular superoxide dismutase. *Biochim Biophys Acta* 1340, 21-32 (1997).
 85. Adachi, T., Fukushima, T., Usami, Y. & Hirano, K. Binding of human xanthine oxidase to sulphated glycosaminoglycans on the endothelial-cell surface. *Biochem J* 289 (Pt 2), 523-7 (1993).
 86. Repine, J. E., Bast, A. & Lankhorst, I. Oxidative stress in chronic obstructive pulmonary disease. Oxidative Stress Study Group. *Am J Respir Crit Care Med* 156, 341-57. (1997).
 87. Finkelstein, R., Fraser, R. S., Ghezzi, H. & Cosio, M. G. Alveolar inflammation and its relation to emphysema in smokers. *Am J Respir Crit Care Med* 152, 1666-72. (1995).
 88. Timens, W., Coers, W., Van Straaten, J.F.M., Postma, D.S. Extracellular matrix and inflammation: a role for fibroblast-mediated defective tissue repair in the pathogenesis of emphysema? *Eur Respir Rev* 7, 119-123 (1997).
 89. Danielsen, C. C. Mechanical properties of reconstituted collagen fibrils. Influence of a glycosaminoglycan: dermatan sulfate. *Connect Tissue Res* 9, 219-25 (1982).
 90. Vogel, K. G., Paulsson, M. & Heinegard, D. Specific inhibition of type I and type II collagen fibrillogenesis by the small proteoglycan of tendon. *Biochem J* 223, 587-97 (1984).
 91. Hinek, A., Mecham, R. P., Keeley, F. & Rabinovitch, M. Impaired elastin fiber assembly related to reduced 67-kD elastin-binding protein in fetal lamb ductus arteriosus and in cultured aortic smooth muscle cells treated with chondroitin sulfate. *J Clin Invest* 88, 2083-94 (1991).
 92. McGowan, S. E., Liu, R. & Harvey, C. S. Effects of heparin and other glycosaminoglycans on elastin production by cultured neonatal rat lung fibroblasts. *Arch Biochem Biophys* 302, 322-31 (1993).
 93. Werb, Z., Banda, M. J. & Jones, P. A. Degradation of connective tissue matrices by macrophages. I. Proteolysis of elastin, glycoproteins, and collagen by proteinases isolated from macrophages. *J Exp Med* 152, 1340-57 (1980).
 94. Stone, P. J., McMahon, M. P., Morris, S. M., Calore, J. D. & Franzblau, C. Elastin in a neonatal rat smooth muscle cell culture has greatly decreased susceptibility to proteolysis by human neutrophil elastase. An in vitro model of elastolytic injury. *In Vitro Cell Dev Biol* 23, 663-76 (1987).
 95. Redini, F., Lafuma, C., Hornebeck, W., Choay, J. & Robert, L. Influence of heparin fragments on the biological activities of elastase(s) and alpha 1 proteinase inhibitor. *Biochem Pharmacol* 37, 4257-61 (1988).
 96. Rao, N. V., Kennedy, T. P., Rao, G., Ky, N. & Hoidal, J. R. Sulfated polysaccharides prevent human leukocyte elastase-induced acute lung injury and emphysema in hamsters. *Am Rev Respir Dis* 142, 407-12 (1990).
 97. Walsh, R. L., Dillon, T. J., Scicchitano, R. & McLennan, G. Heparin and heparan sulphate are inhibitors of human leucocyte elastase. *Clin Sci (Lond)* 81, 341-6 (1991).
 98. Webb, L. M., Ehrenguber, M. U., Clark-Lewis, I., Baggiolini, M. & Rot, A. Binding to heparan sulfate or heparin enhances neutrophil responses to interleukin 8. *Proc Natl Acad Sci U S A* 90, 7158-62 (1993).
 99. Al Jamal, R., Roughley, P. J. & Ludwig, M. S. Effect of glycosaminoglycan degradation on lung tissue viscoelasticity. *Am J Physiol Lung Cell Mol Physiol* 280, L306-15. (2001).
 100. Karlinsky, J. B. Glycosaminoglycans in emphysematous and fibrotic hamster lungs. *Am Rev Respir Dis* 125, 85-8 (1982).
 101. Konno, K. et al. A biochemical study on glycosaminoglycans (mucopolysaccharides) in emphysematous and in aged lungs. *Am Rev Respir Dis* 126, 797-801 (1982).
 102. Lafuma, C., Moczar, M., Lange, F. & Robert, L. Biosynthesis of hyaluronic acid, heparan sulfate and structural glycoproteins in hamster lung explants during elastase induced emphysema. *Connect Tissue Res* 13, 169-79 (1985).
 103. Radhakrishnamurthy, B., Jeansonne, N. E., Smart, F. W. & Berenson, G. S. Proteoglycans from lungs

- of rabbits treated with pronase and cadmium chloride. *Am Rev Respir Dis* 131, 855-61 (1985).
104. Laros, C. D., Kuyper, C. M. & Janssen, H. M. The chemical composition of fresh human lung parenchyma. An approach to the pathogenesis of lung emphysema. *Respiration* 29, 458-67 (1972).
 105. van de Lest, C. H. et al. Altered composition of urinary heparan sulfate in patients with COPD. *Am J Respir Crit Care Med* 154, 952-8. (1996).
 106. van Straaten, J. F. et al. Proteoglycan changes in the extracellular matrix of lung tissue from patients with pulmonary emphysema. *Mod Pathol* 12, 697-705. (1999).
 107. Raats, C. J., Bakker, M. A., van den Born, J. & Berden, J. H. Hydroxyl radicals depolymerize glomerular heparan sulfate in vitro and in experimental nephrotic syndrome. *J Biol Chem* 272, 26734-41 (1997).
 108. Vilar, R. E. et al. Nitric oxide degradation of heparin and heparan sulphate. *Biochem J* 324 (Pt 2), 473-9 (1997).
 109. Ferrara, T. B. & Fox, R. B. Effects of oxygen toxicity on cuproinic blue-stained proteoglycans in alveolar basement membranes. *Am J Respir Cell Mol Biol* 6, 219-24 (1992).
 110. van Kuppevelt, T. H., van de Lest, C. H., Versteeg, E. M., Dekhuijzen, P. N. & Veerkamp, J. H. Induction of emphysematous lesions in rat lung by beta-D-xyloside, an inhibitor of proteoglycan synthesis. *Am J Respir Cell Mol Biol* 16, 75-84. (1997).
 111. van de Lest, C. H., Versteeg, E. M., Veerkamp, J. H. & van Kuppevelt, T. H. Digestion of proteoglycans in porcine pancreatic elastase-induced emphysema in rats. *Eur Respir J* 8, 238-45. (1995).
 112. Karlinsky, J. et al. The balance of lung connective tissue elements in elastase-induced emphysema. *J Lab Clin Med* 102, 151-62 (1983).
 113. Smits, N. C. et al. Phage display-derived human antibodies against specific glycosaminoglycan epitopes. *Methods Enzymol* 416 (2006).
 114. van De Westerlo, E. M. et al. Human single chain antibodies against heparin: selection, characterization, and effect on coagulation. *Blood* 99, 2427-33 (2002).
 115. Lensen, J. F. et al. Selection and characterization of a unique phage display-derived antibody against dermatan sulfate. *Matrix Biol* 25, 457-61 (2006).
 116. Smetsers, T. F. et al. Human single-chain antibodies reactive with native chondroitin sulfate detect chondroitin sulfate alterations in melanoma and psoriasis. *J Invest Dermatol* 122, 707-16 (2004).
 117. Turnbull, J. E., Hopwood, J. J. & Gallagher, J. T. A strategy for rapid sequencing of heparan sulfate and heparin saccharides. *Proc Natl Acad Sci U S A* 96, 2698-703. (1999).
 118. Shriver, Z. et al. Sequencing of 3-O sulfate containing heparin decasaccharides with a partial antithrombin III binding site. *Proc Natl Acad Sci U S A* 97, 10359-64 (2000).
 119. Petitou, M. & van Boeckel, C. A. A synthetic antithrombin III binding pentasaccharide is now a drug! What comes next? *Angew Chem Int Ed Engl* 43, 3118-33 (2004).
 120. Lafuma, C., Frisdal, E., Harf, A., Robert, L. & Hornebeck, W. Prevention of leucocyte elastase-induced emphysema in mice by heparin fragments. *Eur Respir J* 4, 1004-9 (1991).
 121. Eriksson, S. The potential role of elastase inhibitors in emphysema treatment. *Eur Respir J* 4, 1041-3 (1991).
 122. Kreuger, J., Spillmann, D., Li, J. P. & Lindahl, U. Interactions between heparan sulfate and proteins: the concept of specificity. *J Cell Biol* 174, 323-7 (2006).
 123. Cantor, J. O. & Turino, G. M. Can exogenously administered hyaluronan improve respiratory function in patients with pulmonary emphysema? *Chest* 125, 288-92 (2004).
 124. Juul S.E., Wight T.N., Hascall V.C. Proteoglycans. In: Crystal R.C., West J.B., editors. *The lung, scientific foundations*. Vol I. NY: Raven Press. 413-420. (1991).
 125. van Kuppevelt, T. H. & Veerkamp, J. H. Application of cationic probes for the ultrastructural localization of proteoglycans in basement membranes. *Microsc Res Tech* 28, 125-40 (1994).



Chapter 2

Methods in Enzymology 2006, 416:61-87

Phage display-derived human antibodies against specific glycosaminoglycan epitopes

Nicole C. Smits •
Joost F.M. Lensen •
Tessa J.M. Wijnhoven •

Gerdy B. ten Dam •
Guido J. Jenniskens •
Toin H. van Kuppevelt •

Glycosaminoglycans (GAGs) are long unbranched polysaccharides, most of which are linked to a core protein to form proteoglycans. Depending on the nature of their backbone, one can discern galactosaminoglycans (chondroitin sulfate (CS), and dermatan sulfate (DS)) and glucosaminoglycans (heparan sulfate (HS), heparin, hyaluronic acid, and keratan sulfate). Modification of the backbone by sulfation, deacetylation, and epimerization results in unique sequences within GAG molecules which are instrumental in the binding of a large number of proteins. Investigating the exact roles of GAGs has long been hampered by the lack of appropriate tools. In recent years, we have successfully implemented phage display technology to generate a large panel of antibodies against CS, DS, HS, and heparin epitopes. These antibodies provide unique and highly versatile tools to study the topography, structure and function of specific GAG domains. In this chapter, we describe the selection, characterization, and application of antibodies against specific GAG epitopes.

Antibodies are widely used in the research on proteoglycans. They have been applied to evaluate proteoglycan expression patterns in a variety of tissues in health and disease, and have also been used as (immuno) precipitating agents. Most of the antibodies available to date are directed against the core protein of proteoglycans. Only a few antibodies that are reactive with the glycosaminoglycan (GAG) moiety have been described¹⁻⁵. However, these were all generated using proteoglycans rather than isolated GAGs.

As stated earlier, investigating the biological role of GAGs has long been hampered by the lack of appropriate tools. Using phage display technology we have generated a large panel of epitope-specific antibodies against heparan sulfate (HS), heparin, chondroitin sulfate (CS), and dermatan sulfate (DS)⁶⁻¹⁰ (Table 1). Characterization of the GAGs bound by the antibodies revealed that specific modification patterns are recognized^{10,11}. For instance, one specific antibody against HS requires 3-*O*-sulfates and recognizes an epitope that resembles the antithrombin-III binding pentasaccharide

sequence¹. A variety of anti-GAG antibodies was used to study the distribution of GAG epitopes in spleen², lung³, kidney¹⁵, and skeletal muscle⁴. GAG-specific antibodies were also used to study changes in expression pattern in diseased versus healthy tissue, especially melanoma and psoriasis^{8,17}. Next to immunohistochemical evaluation, antibodies were applied to analyze the biological function of GAGs e.g., growth factor binding. The endogenous expression of anti-HS antibodies resulted in the functional knockout of specific HS epitopes, which was shown to interfere with ion housekeeping in skeletal muscle cells⁵. Our panel of antibodies thus provides a unique and highly versatile tool to study the topography, structure, and function of GAGs. Here, we describe the selection, and evaluation of single-chain variable fragment (scFv) antibodies against specific GAG epitopes.

Phage display

One of the most successful applications of phage display has been the selection of specific antibodies from phage display libraries¹⁹⁻²¹. DNA's encoding antibodies

are cloned into a suitable vector as a fusion to the gene encoding one of the phage coat proteins (pIII, pVI, or pVIII). Upon assembly in bacteria, the antibody-coat protein fusion will be part of the surface of the phage, thus ‘displaying’ the antibody. A phage display library is a large collection of phages, each displaying an individual antibody. Phage display allows for generation of antibodies against ‘self antigens’, which is favorable because GAGs are largely nonimmunogenic.

The phage display system is illustrated in Figure 1. First, the phage display library is incubated with the ‘antigen’ (GAGs) immobilized onto a tube. Phages that display antibodies that are specific for the antigen will bind, nonadherent phages will be washed away. Phages expressing a specific anti-GAG antibody can then be recovered from the tube (e.g., by altering the pH), and multiplied by infection into bacteria. This biopanning procedure is repeated several times. Se-

lected phages are then analyzed for anti-GAG antibodies by ELISA and immunohistochemistry (IHC).

In principle, any phage display library can be used. In the protocol described here, a human semisynthetic library [Library no.1, ⁶] was used, consisting of $> 10^8$ different clones, each expressing a unique antibody. The semisynthetic Library no.1 contains 50 different V_H genes combined with a single light chain gene (DPL16). In the library, variable parts of the heavy and light chains are joined to each other by a linker sequence to form so-called scFv. All antibodies contain a *c-Myc* tag for identification. Due to the use of an amber codon combined with a suppressor *Escherichia coli* (*E. coli*) strain, one can easily produce soluble scFv antibodies from selected phage clones.

To rescue and amplify phages following selection, a helper phage is required to allow for phage assembly. VCS-M13 is a commonly used helper

Table 1: Characteristics of different scFv antibodies

scFv	V_H	DP Gene	V_H CDR3	Class of GAG	Reference
RB4EA12	3	32	RRYALDY	HS	(Jenniskens et al., 2000)
HS4C3	3	38	GRRLKD	HS	(van Kuppevelt et al., 1998)
EV3C3	3	42	GYRPRF	HS	(Smits et al., 2004)
HS4E4	3	38	HAPLRNTRTNT	HS	(Dennissen et al., 2002)
AO4B08	3	47	SLRMNGWRAHQ	HS	(Jenniskens et al., 2000)
IO3H10	1	7	AKRLDW	CS	(Smetsers et al., 2004)
LKN1	1	25	GIKL	DS	(Lensen et al., 2005)
MPB49	3	38	WRNDRQ	-(control)	-

Given are the scFv antibody code, V_H germ line gene family, DP gene segment number, amino acid sequence of the V_H complementarity determining region 3 (CDR3), and the class of GAG with which the antibody reacts. Selection of the antibodies is described in the indicated reference. GAG, glycosaminoglycan; HS, heparan sulfate; CS, chondroitin sulfate; DS, dermatan sulfate. All scFv antibodies recognize specific epitopes as based on different staining patterns, and different reactivities toward various HS/CS/DS preparations.

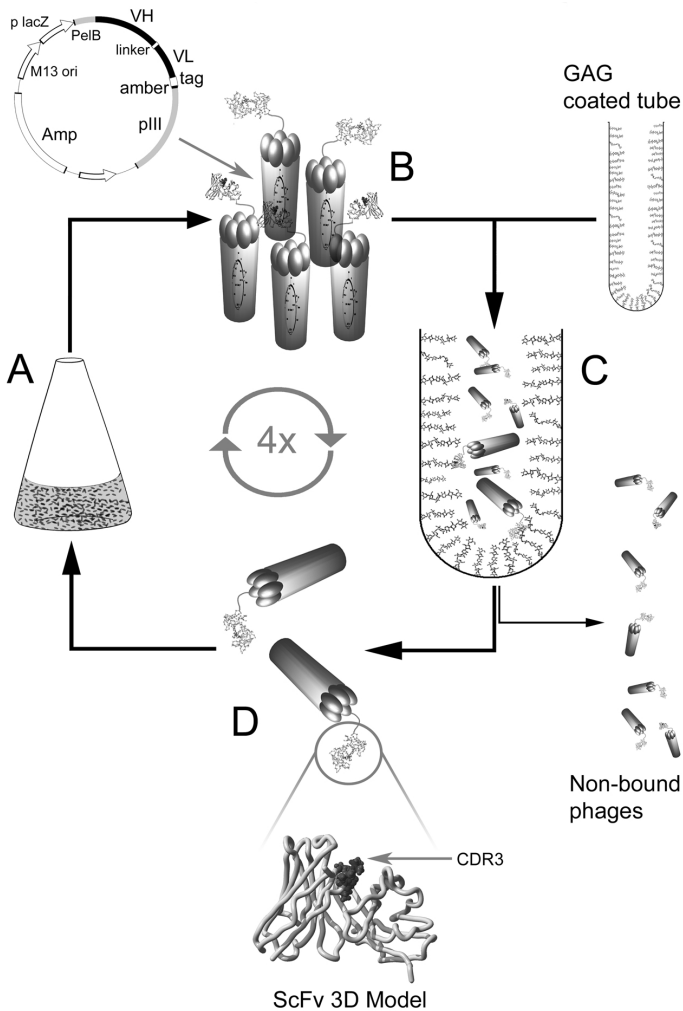


Figure 1. Schematic outline of the phage display technique. A library of phage-infected bacteria is grown and induced to produce phages expressing ('displaying') scFv antibody fragments on their surface (A). Phages are isolated (B) and used for selection ('panning'; C) against glycosaminoglycans (GAGs), which are immobilized onto the surface of a selection tube. Non-binding phages are washed away, whereas phages displaying antibodies that are reactive with GAGs stay bound to the tube. Thus, the library becomes enriched for phages displaying GAG-reactive antibodies. Selected phages are harvested (D), allowed to infect a fresh *Escherichia coli* culture, and used for another round of panning (A-D). Individual clones can be isolated after four rounds of panning.

Insert top left: schematic representation of the phagemid encoding antibody-expressing phages. At the bottom a three-dimensional model of a scFv antibody showing the light and heavy chain (ribbon) and the CDR3 region is depicted (space filling). CDR3, complementarity determining region 3.

phage that bears the kanamycin-resistance gene, which, along with the ampicillin-resistance gene carried by compatible phagemids, enables the selection of cells that contain both the helper phage and the phagemid. Helper phages usually have a defective origin of replication⁷, which allows the preferential packaging of the phagemid DNA over the helper phage DNA and results in a greater output of phagemid phage over helper phage. This is especially important during selection, because only the phagemid contains the DNA encoding the antibody of interest.

Preparation of helper phage VCS-M13

Materials

Bacterial strain: *E. coli* TG1 suppressor strain (K12, *supE*, *hsdΔ5*, *thi*, Δ [*lac-proAB*], F'*[traD36, proAB+, lacIq, lac-ZΔM15]*)¹

Solutions

Ampicillin (100 mg/ml)

H-top agar: 10 g/l peptone, 8 g/l NaCl, 8 g/l Bacto-Agar in H₂O; dissolve, bring the volume to 1 l with H₂O. Autoclave and store at 4°C. Melt in a microwave before use.

H-bottomplates: 10 g/l peptone, 8 g/l NaCl, 15 g/l Bacto-Agar in H₂O; dissolve, bring the volume to 1 l with H₂O and autoclave. Mix gently and pour into Petri dishes. (Plates are stored at 4°C).

Kanamycin (25 mg/ml)

Minimal media agar plates: 15 g/l Bacto-Agar, 10.5 g/l K₂HPO₄, 4.5 g/l KH₂PO₄, 1 g/l (NH₄)₂SO₄, 0.5 g/l sodium citrate

in 985 ml H₂O; dissolve and autoclave. Cool the solution to 60°C and add 500 μl of 20% MgSO₄, 0.5 ml of 1% B1 (thiamine HCl, filter-sterilized 0.2 μm) and 5 ml 40% glucose (filter-sterilized 0.2 μm). Mix gently and pour into Petri dishes. (Plates are stored at 4°C).

0.1M NaOH/1% (w/v) sodium dodecyl-sulfate (SDS).

Phosphate-buffered saline (PBS)

20% (w/v) polyethylene glycol 6000 (PEG)/2.5M NaCl

Tris/EDTA (TE) buffer: 10mM Tris-HCl, pH 8.0 and 1mM EDTA, pH 8.0

1M Tris-HCl, pH 7.4

2 × TY medium

2 × TY medium containing 100 μg/ml ampicillin and 1% glucose

TYE plates: 10 g/l peptone, 5 g/l Bacto-yeast extract, 8 g/l NaCl, 15 g/l Bacto-Agar in H₂O; dissolve, bring the volume to 1 l, and autoclave. Cool the solution to 60°C and add 1 ml of 100 mg/ml ampicillin and 25 ml of 40% glucose to achieve final concentrations of 100 μg/ml ampicillin and 1% glucose. Mix gently and pour into Petri dishes. (Plates are stored at 4°C).

Methods

Day 1

1. Streak *E. coli* TG1 cells from a glycerol stock on a minimal media agar plate and incubate o/n at 37°C. Do not use antibiotics; *E. coli* TG1 has no antibiotic resistance genes.

Day 2

¹ *E. coli* TG1 is a T-phage-resistant strain that harbors a mutated tRNA gene. The mutated tRNA will suppress the UAG amber (stop codon). To allow expression of scFv-pIII fusion protein on the phage tip, the amber codon will be substituted by a glutamine.

1. Inoculate 5 ml $2 \times$ TY medium containing 1% glucose with a single colony of *E. coli* TG1 cells from the minimal media agar plate and incubate o/n at 37°C.

Day 3

1. Inoculate 50 ml $2 \times$ TY medium containing 1% glucose with 500 μ l of the o/n culture. Grow the culture, while shaking, at 37°C until an absorbance at 600 nm of 0.4-0.5 is reached.
2. Prepare 10^{-6} , 10^{-7} , and 10^{-8} dilutions of the commercially obtained VCS-M13 preparation (usually in the range of 1×10^{11} plaque-forming units [pfu]/ml in $2 \times$ TY medium containing 1% glucose. Add 10 μ l of these dilutions to 200 μ l *E. coli* TG1 cultures (Day 3; step 1).
3. Incubate for 30 min at 37°C, without shaking, to allow for infection of *E. coli* cells with helper phage.
4. Add 3 ml of liquefied H-top agar (not warmer than 50°C) to the infected culture, mix gently, and pour onto H-bottom plates that have been prewarmed to 37°C. Incubate o/n at 37°C. The aim is to obtain a plate from which single VCS-M13 plaques can be picked easily (i.e., *E. coli* colonies that are growing slower because of infection with VCS-M13).
5. Determine the titer of the VCS-M13 phages from the number of plaques.
6. Separately, inoculate 5 ml $2 \times$ TY medium containing 1% glucose with a single colony of *E. coli* TG1 cells from the minimal media agar plate (Day 1; step 1) and grow o/n at 37°C.

Day 4

1. Inoculate 50 ml $2 \times$ TY medium containing 1% glucose with 500 μ l

of the o/n culture (Day 3; step 5). Grow the culture, while shaking, at 37°C until an absorbance at 600 nm of 0.4-0.5 is reached. (When necessary, the *E. coli* culture can be kept on ice before infection for a moment. However, do not exceed 30 min because of the loss of F-pili).

2. Transfer a single VCS-M13 plaque from the H-bottom plate (Day 3; step 4) to 4 ml of the *E. coli* culture (step 1) and incubate, while shaking, for 2 h at 37°C (phage infection).
3. Transfer the infected 4 ml culture to a 2-liter Erlenmeyer flask containing 500 ml of prewarmed $2 \times$ TY medium and grow the culture, while shaking, for 1 h at 37°C.
4. Add 1.2 ml of 25 mg/ml kanamycin to a final concentration of 60 μ g/ml and grow, while shaking, o/n at 37°C.

Day 5

1. Cool the culture (Day 4; step 4) on ice for 20 min.
2. Collect the bacteria by centrifugation at 5,000g for 10 min at 4°C (after centrifugation phages are present in the supernatant!).
3. Add 100 ml of ice-cold PEG-NaCl to the phage supernatant, mix gently, and incubate on ice for 1 h. In this step, phages are precipitated.
4. Pellet the phages at 10,000g for 30 min at 4°C.
5. Resuspend the phage pellet in 40 ml H₂O. Transfer the solution to a 50-ml tube and add 8 ml of ice-cold PEG-NaCl. Mix well and incubate on ice for 20 min.
6. Centrifuge the phage solution at 10,000g for 30 min at 4°C. Decant the supernatant, centrifuge briefly, and remove residual PEG-NaCl with a

- capillary.
7. Resuspend the phage pellet in 2.5 ml TE buffer and centrifuge at 10,000g.
 8. Wet a 0.45 disposable filter with TE buffer and filter the phage solution to remove any remaining bacterial debris. Note that it can be difficult to filter the phage solution and that this step may result in the loss of phages that remain in the filter.
 9. Titrate the phages to 10-12 pfu/ml.
 10. Store the phage solution at 4°C (up to 5 days).

Panning methodology

Panning methodology (Figure 1, Table 2) involves the physical contact of the phage display library with the antigen (in this case GAGs), and can be regarded as an affinity selection system. In practice, a small volume containing the phage display library is incubated with the antigen immobilized to a tube. Panning consists of several rounds of binding phages to the immobilized GAGs, a defined number of washing steps, and elution of the bound phages by altering the pH. Eluted phages are subjected to another round of panning. During each round of panning specific binding clones are selected and amplified so they predominate after three to four rounds of panning. The input of each round should be in the range of 10^{12} phages.

Selection of phages displaying specific antibodies against GAGs using panning methodology

Materials

Bacterial strain: *E. coli* HB2151 non-

suppressor strain (K12, *ara*, *thi*, Δ [*lac-pro*], F' [*proAB*+, *lacIq*, $Z\Delta M15$])

Bacterial strain: *E. coli* TG1 suppressor strain (K12, *supE*, *hsd* Δ 5, *thi*, Δ (*lac-proAB*), F' (*traD36*, *proAB*+, *lacIq*, *lac-Z* Δ M15))

Glycerol stock of the (semi)-synthetic scFv Library no.1⁶ (Dr. G. Winter, MRC Centre for Protein Engineering, Cambridge, UK), stored at -80°C

VCS-M13 helper phages² used at a titer of 1×10^{12} pfu/ml (Stratagene) (for large amounts see preparation of helper phage VCS-M13)

Solutions

GAGs of interest: 10 mg/ml in H₂O

PBS containing 0.1% (v/v) Tween-20

PBS containing 2% (w/v) Marvel (prepare freshly)

PBS containing 4% (w/v) Marvel (prepare freshly)

100mM triethylamine (prepare freshly)

2 \times TY containing 100 μ g/ml ampicillin and 25 μ g/ml kanamycin

Methods

Several precautions need to be taken to avoid carryover of phages during the selections. The use of sterile solutions and disposable plastics is highly recommended. Nondisposable plastics should be soaked for 1 h in 2% (v/v) hypochlorite, followed by thorough washing and autoclaving. Glassware should be baked for at least 6 h at 180°C. Always use aerosol-resistant pipette tips (Molecular Bio-Products) when working with phages. It is recommended to work in a laminar-flow cabinet. Clean

² VCS-M13 phages provide phage coat proteins and enzymes that are crucial for rescue of the phages.

Table 2: Time schedule of experiments described in this chapter

Day	Activity	Sections	Notes
Selection of antibodies using panning methodology			
1	Growth of phage library	A.1.1-1.6	Inoculate original library or $n + 1$ generation (from section D.3.4); grow o/n at 37°C
	Coating of selection tubes	C.1.1	
	Inoculation of <i>E. coli</i> TG1	A.1.7	
2	Isolation of phages	B.1.1-1.8	Phages are used for selection (see section C.2.2-2.11)
	Preparation selection tube	C.2.1	To be used for selection (see section C.2.2-2.9)
	Round of panning	C.2.2-2.11	
3	Calculate titers	C.3.1	Store plates; individual clones can be used to inoculate master plate (see section E.3.1)
	Harvest phagemids	D.3.2-3.5	Phagemids can be stored at -80°C or used for a next round of selection (see section A.1.1-1.6)
	Inoculation of master plate	E.3.1	Stored as back up and used to inoculate induction plate (E.4.1-4.3)
Screening for antibody-expressing clones			
4	Preparation of induction plate	E.4.1-4.2	
	Storage of master plate	E.4.3	
	Coat ELISA plate	F.4.1	Coating of ELISA plates with the antigen that was used for selection
5	ELISA screening	F.5.1-5.10	Identification of active antibody-expressing clones
Characterization and large-scale production of antibodies			
6	Streak individual clones	G.6.1	Streak individual clones from master plate (see section E.4.3)
7	Inoculation of o/n cultures	G.7.1	
8	Production and isolation of antibodies	G.8.1-8.8	
	DNA isolation and sequencing	H.8.1-8.3	Identification and characterization of individual antibodies
9	Aliquot and store antibodies	G.9.1	Storage at 4°C (weeks) or at -20°C (months)
Miscellaneous analytical techniques			
	Immunofluorescence analysis	I	Characterization of epitope occurrence
	Direct ELISA analysis	J.1	Characterization of epitopes
	Competition ELISA analysis	J.2	Characterization of epitopes

³ M13 phages infect *F⁻ E. coli* via sex pili. For optimal infection, *E. coli* needs to be in the log phase (absorbance of 0.4-0.5 at 600 nm) at 37°C. When grown to a higher density, sex pili are lost very rapidly. A log phase culture can be held on ice for about 30 min.

the workplace (bench tops, etc.) with 0.1M NaOH/1% (w/v) SDS before and after each working day. Clean pipettes and other tools daily by wiping the outside with 0.1M NaOH/1% (w/v) SDS, followed by a rinse with water.

For a schematic representation of the following steps see Figure 1.

(A) *Growth of antibody phage display library*

- 1.1. Inoculate 50 ml of 2 × TY containing 100 µg/ml ampicillin and 1% glucose with 50 µl from a glycerol stock of the scFv Library no.1⁶.
- 1.2. Grow the culture, while shaking, at 37°C until an optical density at 600 nm of 0.5 is reached⁹. (This takes about 2-3 h).
- 1.3. Transfer 10 ml of the culture to a sterile 50-ml tube and add 50 µl VCS-M13 helper phages⁴. The ratio between bacteria and helper phages must be 1:20 (titer helper phages 10¹² pfu/ml).
- 1.4. Incubate at 37°C for 30 min without shaking (phage infection).
- 1.5. Centrifuge the infected culture at 4,000g for 10 min at room temperature. Decant the supernatant, and resuspend the pellet in 1 ml 2 × TY containing 100 µg/ml ampicillin and 25 µg/ml kanamycin.
- 1.6. Add the infected bacterial suspension to 300 ml of prewarmed (30°C) 2

× TY containing 100 µg/ml ampicillin and 25 µg/ml kanamycin (*no glucose*⁵). Incubate o/n, while shaking, at 30°C. This culture will be used in section 'B. Isolation of phages; step 1.1.'

Inoculate 10 ml of 2 × TY with a single colony of *E. coli* TG1 from a minimal medium plate (do not use antibiotics) and grow o/n, while shaking, at 37°C. This culture will be used in section 'C: Selection of phages binding to GAGs; Day 2, step 2.8.'

(B) *Isolation of phages*

- 1.1. Cool the culture from section 'A. Growth of antibody phage display library; step 1.6.' on ice for 10 min.
- 1.2. Centrifuge the culture at 5,000g for 15 min at 4°C. After centrifugation, the bacterial pellet can be discarded and the supernatant containing the phages transferred into a sterile bucket.
- 1.3. Add 60 ml of ice-cold PEG-NaCl to the supernatant to precipitate the phages⁶. Mix well by inverting, and leave the bucket on ice for 1 h.
- 1.4. Pellet the phages at 10,000g for 30 min at 4°C. Resuspend the pellet in 40 ml of ice-cold sterile H₂O. Transfer the phage suspension to a 50-ml tube and add 8 ml of ice-cold PEG-NaCl.

⁴ Take the remaining 40 ml of the culture, spin it down, and resuspend the pellet in 1 ml 2 ml 2 × TY. Spread it on TYE plates, and grow overnight at 37°C. Harvest the cells in 2 × 5 ml 2 × TY medium. Collect the cells in a 50-ml tube and centrifuge for 10 min at 10,000g. Resuspend the pellet in 500 µl of 2 × TY, add 500 µl of 60% glycerol to a final concentration of 30%, mix well, divide this stock in 50-µl aliquots, and store at -80°C as a back up for additional selections (this stock will be the n + 1 generation).

⁵ Glucose represses transcription of the scFv-pIII fusion protein through the Lac operon in the phagemid.

⁶ In this step, phages are precipitated and concentrated. Given that the TG1 suppression of the amber codon is never complete, this step is also necessary for removing any soluble antibodies present in the supernatant.

Mix well (as in the preceding step 1.3.) and leave on ice for 20 min.

- 1.5. Centrifuge the phage mixture at 10,000g for 30 min at 4°C. Decant the supernatant, centrifuge briefly, and remove residual PEG-NaCl with a capillary.
- 1.6. Resuspend the phage pellet in 2.5 ml PBS and centrifuge the phage solution at 10,000g for 5 min.
- 1.7. Wet a 0.45- μ m disposable filter with PBS and carefully filter the phage solution to remove any remaining bacterial debris. Note that it can be difficult to filter the phage solution.
- 1.8. This step may result in loss of phages that remain in the filter.
- 1.9. Store the phage solution at 4°C until use. Phages will be used in section 'C. Selection of phages binding to GAGs; Day 2, step 2.2.'.

(C) Selection of phages binding to GAGs

Day 1

- 1.1. Coat immunotubes with 3 ml of a 10 μ g/ml solution of GAG of interest and incubate o/n at room temperature, while rotating on an under-and-over turntable.

Day 2

- 2.1. Decant the GAG solution, wash the tube three times with PBS and block the tube with PBS containing 2% (w/v) Marvel to avoid nonspecific binding of phages to the surface of the tube. Fill the tube to the edge, cover it with Parafilm, and incubate for at least 2 h at room temperature on an under-and-over turntable. This step should be performed early in the day so the tube will be ready when the phages used for biopanning are obtained (section B. 'Isolation of

phages, step 1.8').

- 2.2. Empty the tube and add 2 ml of PBS containing 4% Marvel and 2 ml of phage supernatant from step 1.8 in section 'B: 'Isolation of phages'', cover the tube, and incubate for 1 h on an under-and-over turntable at room temperature, followed by standing for 1 h.
- 2.3. Discard the phage suspension and wash the tube 20 times with PBS containing 0.1% (v/v) Tween-20. After the last wash, fill the tube with PBS containing 0.1% (v/v) Tween-20 and rotate on an under-and-over turntable for 10 min at room temperature.
- 2.4. Empty the tube and wash the tube 20 times with PBS. Fill the tube with PBS and rotate on an over-and-under-table for 10 min at room temperature.
- 2.5. Empty the tube and add 1 ml of 100mM triethylamine solution. Cover the tube and rotate for 15 min on an under-and-over turntable at room temperature. In this step, bound phages are eluted.
- 2.6. Add the eluted phages to a 50-ml tube containing 0.5 ml of 1M Tris-HCl, pH 7.4 for neutralization. Additionally, add 200 μ l of 1M Tris-HCl, pH 7.4 to the remaining phages in the immunotube. At this point, phages can be stored at 4°C for a short period (up to 2 days) or used directly to infect *E. coli* TG1 cells. The latter is recommended.
- 2.7. Add the eluted phages (step 6) to 9 ml of exponentially growing *E. coli* TG1 cells in a 50-ml tube. Add 4 ml TG1 culture to the remaining phages in the immunotube (step 6). Incubate both cultures for 30 min at 37°C, without shaking, to allow in-

fection.

- 2.8. Exponentially growing TG1 culture is prepared as follows: Inoculate 50 ml of $2 \times$ TY with 0.5 ml of the o/n culture from section 'A. *Growth of antibody phage display library; step 1.7.*'. Grow the culture, while shaking, at 37°C until an absorbance at 600 nm of 0.4-0.5 is reached (this takes about 90 min). It is recommended to inoculate an additional 50 ml of $2 \times$ TY with 0.5 ml of the overnight culture 30 and 60 min after the first inoculation and use the culture with an absorbance of 0.4-0.5 for infection.
- 2.9. Pool both infected *E. coli* TG1 cultures (9 ml and 4 ml from step 2.8.) and take 100 μ l of the pooled cultures to make serial dilutions (10^2 , 10^4 , 10^6 , 10^8) in $2 \times$ TY to calculate the titer. Plate 100 μ l of the dilutions on TYE plates and grow o/n at 37°C. Centrifuge the infected TG1 culture for 10 min at 10,000g at room temperature (do not refrigerate!). Resuspend the cells in 2 ml $2 \times$ TY, spread on TYE plates and incubate o/n at 37°C.

Day 4

- 3.1. Count colonies and calculate the titer from the dilutions. An increase in titer is expected after each selection round, indicating enrichment of binding clones. Store plates with separate colonies, since individual clones will be used in section 'E. *Production of master plate and induc-*

tion plate of phage infected clones; Day 3, step 3.1.'.

(D) *Harvesting of selected phagemids*

- 3.2. Add 5 ml $2 \times$ TY medium to the TYE plates and scrape the bacterial cells from the plate with a glass spreader. Collect the bacteria in a 50-ml tube and centrifuge at 5,000g for 10 min at room temperature.
- 3.3. Decant the supernatant and resuspend the bacterial pellet in 2 ml $2 \times$ TY medium.
- 3.4. For a next round of selection, take 50 μ l of the bacterial suspension and use it to inoculate 50 ml $2 \times$ TY containing 100 μ g/ml ampicillin and 1% (w/v) glucose as in section 'A. *Growth of antibody phage display library; step 1.1.*'. Repeat this selection procedure for another three selection rounds (all steps of this section).
- 3.5. Add 1 ml of ice-cold 60% glycerol to the remaining cells, aliquot in 50 μ l fractions, snap-freeze in liquid nitrogen, and store at -80°C⁷.

Screening for clones expressing anti-GAG antibodies

To assess whether the panning experiment was successful, individual clones need to be selected and analyzed. This section describes a procedure to identify antibody-expressing clones after panning. An easy and fast method to test the selected clones for production of antibodies directed against GAGs is ELISA. Antibody-containing supernatants obtained from isopropyl- β -D-thio-

⁷ Glycerol stocks are used as a backup. When a subsequent selection found fails, use the glycerol stock for a new round of selection.

galactosidase (IPTG)-induced cultures can be used for this purpose. Clones with desired specificity in ELISA can be further analyzed by DNA sequencing to identify different clones (e.g., with unique CDR3 sequences). Clones of interest can then be used for large-scale production and purification.

(E) Production of master plate and induction plate of phage-infected clones

Materials

Sterile 96-well flat-bottom assay plates with high-binding surface (ELISA plate, Greiner) round-bottom Cellstar plates (master block) (Greiner)
p-Nitrophenyl phosphate disodium salt, hexahydrate (MP Biomedicals)

Solutions

1M diethanolamine, pH 9.8. Store in the dark at room temperature.
 GAGs of interest 10 mg/ml in H₂O
 1mM IPTG in H₂O (prepare freshly)
 10mM IPTG in 2 × TY
 PBST: 0.05 ml/l Tween-20 in PBS
 Secondary antibody solution: Mouse anti-*c-Myc* antibody (9E10, hybridoma culture supernatant⁸) diluted 1:10 with PBST containing 2% (w/v) bovine serum albumin (BSA)
 Tertiary antibody solution: Alkaline phosphatase-conjugated rabbit anti-mouse IgG (DAKO) diluted 1:2,000 with PBST containing 2% (w/v)

BSA

Substrate solution: Add 1 mg PNPP/ml to 1M diethanolamine solution (prepare freshly).

Washing solution: PBS containing 0.1% (v/v) Tween-20

Methods

Day 3

3.1. Pick individual bacterial clones with sterile toothpicks from the serial dilution plates of the last two selection rounds (round 3 and 4) (section ‘*C. Selection of phages binding to GAGs; Day 3, step 3.1.*’), and inoculate individual wells of a 96-well master block, filled with 500 μl of 2 × TY containing 100 μg/ml ampicillin and 1% glucose. Repeat this for 94 individual clones. Include a negative control (medium without bacterial clones) and a positive control (a clone that reacts with the antigen). When no positive clone is available, leave the well empty and use a commercially available antibody for further analysis. Secure the lid with tape and grow o/n, while shaking, at 37°C.

Day 4

4.1. Transfer 10 μl bacterial culture (*Day 1, step 1*) to the corresponding wells of a secondary sterile master block containing 1 ml 2 × TY

⁸ The hybridoma cell line (9E10 [anti-*c-Myc*]) is available from the American Type Culture Collection (ATCC). Alternatively, polyclonal rabbit anti-*c-Myc* antibody (A14, Santa Cruz Biotechnology) or purified 9E10 (Sigma) can be used.

⁹ Glucose (0.1%) is added to suppress the expression of scFv antibodies until a sufficient number of bacteria is produced for large-scale production of the antibody. The total amount of glucose will be fully metabolized at an absorbance of 0.9 at 600 nm.

¹⁰ Grow the culture in the induction plate for 3 h at 37°C while shaking. Bacterial growth should be clearly visible before adding IPTG.

containing 100 $\mu\text{g/ml}$ ampicillin and 0.1% glucose⁹. This plate will be the *induction plate*. Secure the lid with

tape, and grow at 37°C, while shaking, for 3 h¹⁰. Do not exceed 200 rpm to prevent contamination.

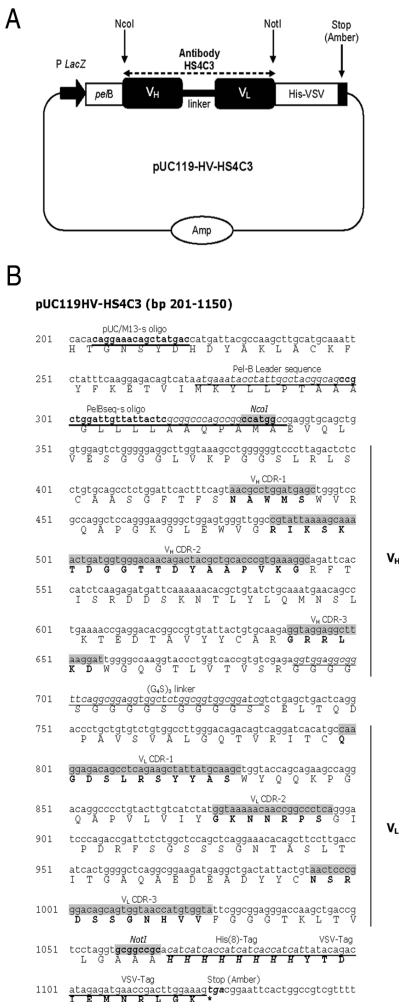


Figure 2. (A) Schematic representation of plasmid pUC119-HV, harboring the DNA encoding scFv antibody HS4C3 (pUC119-HV-HS4C3). (B) HS4C3-coding sequence cloned into plasmid pUC119-HV (*NcoI-NotI* cloning). Depicted are: Amp, ampicillin resistance-encoding gene; *P LacZ*, *LacZ* promoter; *peIB*, signal peptide of bacterial pectate lyase that targets antibodies to the periplasmic space; (G₄S)₃-linker, a 15 amino acid linker sequence connecting the V_H and V_L domains; His-tag, eight histidine residues used for protein purification; VSV-tag, peptide epitope used for immunodetection. Sequences encoding V_H and V_L complementarity determining regions (CDRs) are shaded. Also indicated are the nucleotide sequences of polymerase chain reaction (PCR) primers that can be used for sequencing (pUC/M13-s and PelBseq-s).

4.2. When bacterial growth is clearly visible in the induction plate, an absorbance at 600 nm of about 0.9 is reached. For induction, add 100 μl of 10mM IPTG in 2 \times TY to each well of the induction plate to reach a final concentration of 1mM IPTG. Incubate the plate, while gently shaking (do not exceed 200 rpm to prevent contamination) o/n at 30°C to induce the production of anti-GAG antibodies.

4.3. Fill a master block with 200 μl of the o/n culture and add 200 μl of ice-cold 60% glycerol to all wells to a final concentration of 30% (use a multichannel pipetter). Mix well, and store the plate immediately at -80°C. This plate will be the *master plate* and is used as a backup.

Day 5

5.1. Centrifuge the induction plate (*Day 2; step 2*) for 30 min at 5,000g to pellet bacteria. The supernatant containing antibodies will be used to screen for positive clones as described in the following section.

(F) ELISA screening for bacterial clones expressing anti-GAG antibodies

Methods

Day 4

- 4.1. Coat wells from an ELISA plate with 100 μl of a 10 $\mu\text{g}/\text{ml}$ GAG solution. Incubate o/n at 4°C. This step can be performed on Day 2 of the previous section.

Day 5

- 5.1. Discard the GAG solution and wash the plate six times with PBST.
- 5.2. Block the plate with 200 μl of 2% (w/v) BSA in PBST for 90 min at room temperature.
- 5.3. Empty the plate and add 100 μl culture supernatant from the induction plate (section 'E. Production of master plate and induction plate of phage-infected clones; Day 5, step 5.1.') containing soluble antibodies to the corresponding wells of the ELISA plate. Incubate for 2 h at room temperature¹¹.
- 5.4. Discard the culture supernatant and wash the plate six times with PBST.
- 5.5. Add 100 μl of the secondary antibody solution to each well and incubate for 1 h at room temperature.
- 5.6. Discard the secondary antibody solution and wash the plate six times with PBST.
- 5.7. Add 100 μl of the tertiary antibody solution to each well and incubate for 1 h at room temperature.
- 5.8. Discard the tertiary antibody solution and wash the plate six times with PBST. This step is followed by a single wash with 100 μl of 1M di-

ethanolamine solution to reduce background signals.

- 5.9. Add 100 μl of substrate solution to each well and incubate in the dark at room temperature until color development is clearly visible. Read the absorbance on an ELISA reader at 405 nm.

(G) Large scale production of periplasmic fractions containing soluble scFv antibodies

To obtain large amounts of soluble antibodies, periplasmic fractions of bacteria expressing the antibodies are used. Upon induction with IPTG, scFv chains are expressed with the *N*-terminal *pelB* bacterial leader sequence that targets the chains to the periplasm, where the *pelB* sequence is cleaved off by the enzyme signal peptidase. Within the periplasm, appropriate oxidizing conditions allow the antibody to fold and form functional scFv antibodies. Soluble scFv antibodies are obtained from the bacterial periplasm, through the addition of borate buffer, which selectively releases periplasmic proteins. Antibodies contained in this crude periplasmic fraction can be purified by various ways (e.g., by metal chelate chromatography using a His tag). However, the pHEN-1 vector into which the library is cloned (Figure 2) yields scFv antibodies with a *c-Myc* tag. To circumvent high background signals in IHC on, for example, tumor tissue (which express *c-Myc*), scFv antibodies are subcloned into pUC119-His-VSV (Figure 2; Raats, Department of Biochemistry [NWI], Nijmegen Centre for Molecular Life Sciences, Radboud

¹¹ Include negative controls (i.e., supernatant without scFv antibodies) and positive controls (if available).

University Nijmegen, Nijmegen, The Netherlands). This vector contains both a His- and VSV tag for purification and detection. Both the pHEN and the pUC119 vector contain β -lactamase (ampicillin selection) and a *LacZ* promoter upstream of the antibody gene of interest (IPTG induction of antibody expression).

Materials

EDTA-free protease inhibitor cocktail tablets (Roche Diagnostics)
Glycerol stock of bacteria producing anti-GAG antibody, stored at -80°C
Dialysis membrane (Medicell International, molecular weight cut-off < 20 kDa)

Solutions

Ampicillin (100 mg/ml)
0.5M Boric acid
Borate buffer: Adjust 0.5M boric acid to pH 8.0 with 0.5M sodium borate. Store at room temperature. Before use, add 1 EDTA-free protease inhibitor tablet, and 1.6 ml of 5M NaCl to 16 ml of the borate buffer, and adjust the volume to 40 ml with H_2O
LB medium
LB medium containing 1% glucose and 100 $\mu\text{g}/\text{ml}$ ampicillin
0.5M Sodium borate
TYE plates
2 \times TY containing 100 $\mu\text{g}/\text{ml}$ ampicillin and 0.1% glucose
2 \times TY containing 100 $\mu\text{g}/\text{ml}$ ampicillin and 1% glucose

Methods

Day 6

6.1. Streak individual clones that express GAG binding antibodies from a master plate on TYE plates and incu-

bate o/n at 37°C .

Day 7

7.1. Inoculate 20 ml 2 \times TY containing 100 $\mu\text{g}/\text{ml}$ ampicillin and 1% (w/v) glucose with a single colony from a fresh streak of an antibody-expressing clone. Incubate o/n, while shaking, at 37°C . Plates can be stored at 4°C for up to 1 month.

Day 8

8.1. Inoculate 1 l of 2 \times TY containing 100 $\mu\text{g}/\text{ml}$ ampicillin and 0.1% (w/v) glucose with 10 ml of the o/n bacterial culture and incubate, while shaking, at 37°C until an absorbance at 600 nm of 0.5-0.8 is reached. This takes about 2.5 to 3.0 h.
8.2. As a backup for additional antibody production, a glycerol stock is prepared. Add 500 μl of 60% glycerol to 500 μl of the o/n culture. Mix well, freeze in liquid nitrogen, and store at -80°C ; 1.5 ml of the remaining o/n culture is used for DNA Miniprep and sequencing as described in the section '*Sequence analysis of selected clones*'.
8.3. To the 1 l of induction culture add 1 ml of 1M IPTG to a final concentration of 1mM IPTG and incubate the culture, while shaking, for 3 h at 30°C .
8.4. Cool the culture on ice for 20 min.
8.5. Collect the bacteria by centrifugation at 5,000g for 10 min at 4°C . Decant the supernatant, and add 10 ml of ice-cold borate buffer to the bacterial pellet. Borate buffer dissolves the glycocalyx. scFv antibodies, which are present in the periplasmic space, become available and can be readily isolated.

- 8.6. Resuspend the pellet by vortexing and pipetting vigorously. Transfer the mixture to a 50-ml tube and centrifuge at 10,000g for 30 min at 4°C. The supernatant is the *periplasmic fraction* containing the soluble scFv antibodies.
- 8.7. Filter periplasmic fractions through a 0.45- μ m disposable filter.
- 8.8. Dialyze the periplasmic fraction o/n against PBS at 4°C.

Day 9

- 9.1. Divide the periplasmic fraction in aliquots (1 ml). Store at 4°C for direct use or freeze and store at -20°C to -80°C¹².

(H) Sequence analysis of selected clones

For DNA sequence analysis, purified phagemid DNA from an o/n culture of the selected clones is used, which can easily be isolated by a commercially available small-scale plasmid preparation kit. Sequence analysis of the antibody-producing clones is performed with one of the oligonucleotide primers given in the following subsection or any other suitable primer. The sequence can then be analyzed using the alignment program IgBLAST, which can be found on the Internet at <http://www.ncbi.nlm.nih.gov/igblast/>. V_H CDR3 sequences are especially useful to identify individual clones.

Materials

Plasmid DNA isolation kit (e.g., QIAprep Spin Miniprep Kit, QIAGEN)
 Sequencing kit (e.g., ABI Prism)
 Sequencing primers (see Figure 2 for details and location on vector)
 Forlinkseq: 5' -GCC ACC TCC GCC TGA ACC- 3' (sense)
 PelBseq: 5' -CCG CTG GAT TGT TAT TAC TC- 3' (anti-sense)

Solution

o/n culture of a selected bacterial clone grown at 37 °C.

Methods

- 8.1. Take 1.5 ml of the o/n culture (*large-scale production of periplasmic fractions containing soluble scFv antibodies; Day 8, step 8.1.*) and centrifuge 5 min at 5,000g.
- 8.2. Decant the supernatant and use the bacterial pellet for isolation of plasmid DNA according to the manufacturers' protocol.
- 8.3. Mix suitable amounts of Miniprep DNA and sequencing primer and submit for sequencing according to the manufacturers' protocol.

We have generated a large number of unique scFv antibodies that are specific for unique epitopes on GAG chains. Table 1 shows a selection of the scFv antibodies obtained. Note that all antibodies are

¹² The stability of scFv antibodies is highly variable. Whereas some antibodies can be stored at 4°C for weeks to months, others stay immunoreactive for only a couple of days. Most antibodies can be stored at -80°C for years. Bacterial supernatants containing scFv antibodies can be used for ELISA, but are often not suitable for immunohistochemistry. Periplasmic fractions, containing scFv antibodies, which are more concentrated, are suitable for both. For immunoprecipitation or addition to cell cultures, antibodies may be purified using Protein A (in case of antibodies belonging to the V_H3 family) or metal chelating column chromatography.

¹³ E.C. is the Enzyme Commission number.

different with respect to their CDR3.

(I) Evaluation of specificity of anti-GAG antibodies by immunofluorescence

To investigate GAG specificity of the scFv antibodies, cryosections can be incubated overnight with the glycosidases heparinase I (0.04 IU/ml in 50mM NaAc/50mM Ca(Ac)₂, pH 7.0 at 37°C) (E.C. 4.2.2.7)¹³, heparinase II (0.04 IU/ml in 50mM NaPO₄, pH 7.1 at 37°C), heparinase III (0.04 IU/ml in 50mM NaAc/50mM Ca(Ac)₂, pH 7.0 at 37°C) (E.C. 4.2.2.8), or a mix of these enzymes, to digest HS/heparin. CS and DS can be digested from cryosections by o/n incubation with the chondroitin lyases chondroitinase AC, which digests CS (1 IU/ml in 25mM Tris-HCl, pH 7.5 at 37°C), chondroitinase ABC, which digests both

CS and DS (1 IU/ml in 25mM Tris-HCl, pH 8.0 at 37°C), or chondroitinase B, which digests DS (1 IU/ml in 25mM Tris-HCl, pH 7.5 at 37°C). As a control, digestion buffer without the enzyme can be used. Digested cryosections are incubated with mouse anti-HS stub IgG antibody 3G10 to check for heparinase pretreatment or with mouse anti-CS/DS stub IgG antibody 2B6 to check for chondroitinase pretreatment.

Materials

Coverslips

2-5 μm tissue cryosections on glass slides

Solutions

Chondroitinase ABC, AC, B (Seikagaku)

Heparinase I, II, III (IBEX)

GAG digestion buffers:

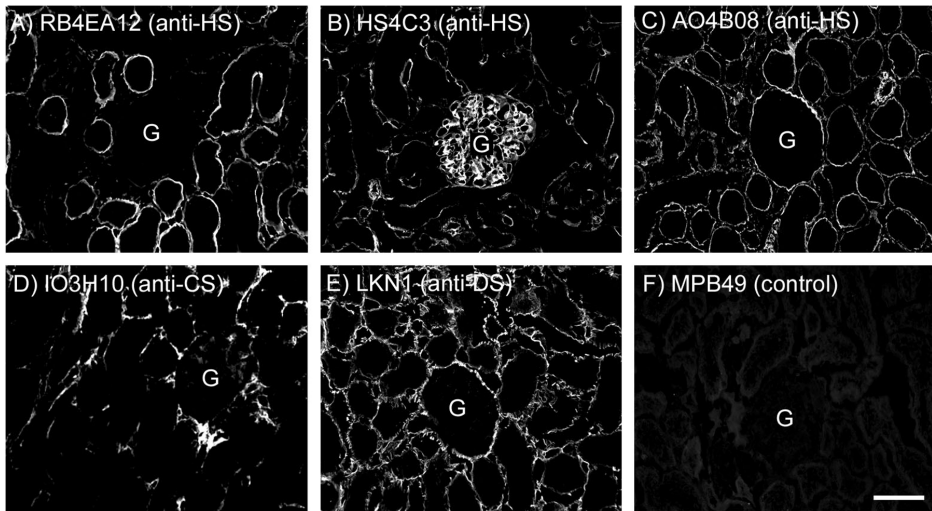


Figure 3. Immunostaining of normal rat kidney cryosections with six different scFv antibodies. Cryosections were incubated with anti-heparan sulfate (HS) antibodies RB4EA12 (A), HS4C3 (B), AO4B08 (C), anti-chondroitin sulfate (CS) antibody IO3H10 (D), anti-dermatan sulfate (DS) antibody LKN1 (E), and negative control antibody MPB49 (F). G, glomerulus. Note differential staining patterns. Scale bar, 50 μm.

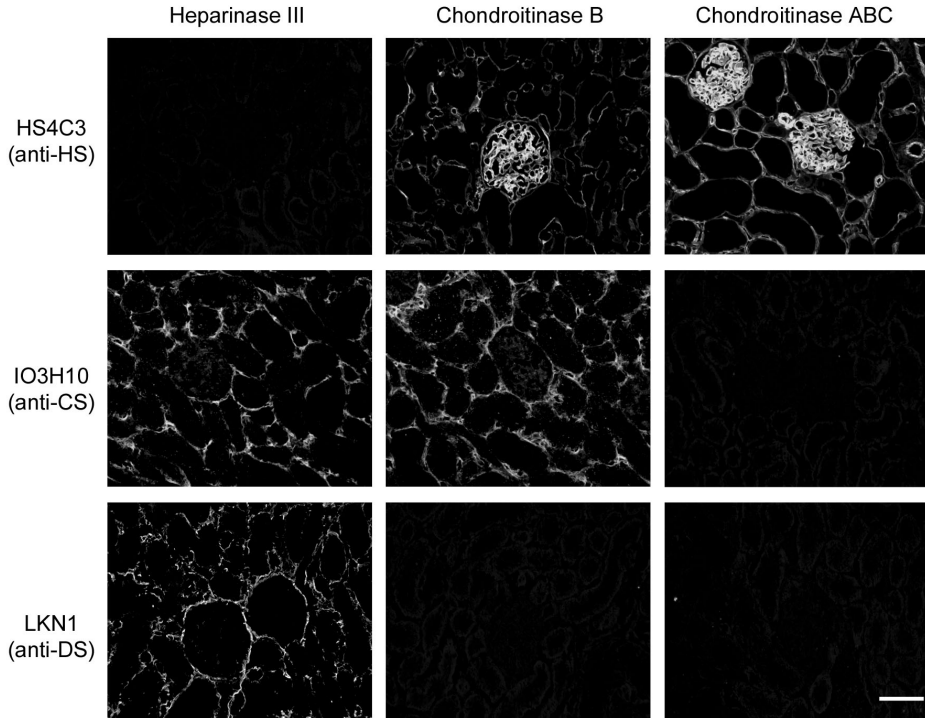


Figure 4. Specificity of anti-glycosaminoglycan antibodies. Normal rat kidney cryosections were treated with heparinase III, chondroitinase B, or chondroitinase ABC. Next, cryosections were stained using anti-heparan sulfate (HS) antibody HS4C3, anti-chondroitin sulfate (CS) antibody IO3H10, or anti-dermatan sulfate (DS) antibody LKN1. Scale bar, 50 μm .

- *Heparinase I, III digestion buffer*
50mM NaAc and 50mM $\text{Ca}(\text{Ac})_2$,
pH 7.0
 - *Heparinase II digestion buffer*
50mM NaPO_4 , pH 7.1
 - *Chondroitinase AC,B digestion buffer*
25mM Tris-HCl, pH 7.5
 - *Chondroitinase ABC digestion buffer*
25mM Tris-HCl, pH 8.0
- Mouse anti-HS stub IgG antibody 3G10
(Seikagaku)
- Mouse anti-CS/DS stub IgG antibody 2B6
(Seikagaku)
- Mowiol solution (Calbiochem): (10%
(w/v) in 0.1M Tris-HCl, pH 8.5/25%

- (v/v) glycerol/2.5% (w/v) NaN_3)
- Primary antibody solution: periplasmic
fraction diluted in PBST containing
2% (w/v) BSA, such that the antibody
gives maximal specific fluorescence
and minimal background staining.
- Secondary antibody solution: Mouse anti-
c-Myc antibody (9E10, hybridoma
culture supernatant [See footnote⁸])
or mouse anti-VSV antibody (P5D4,
hybridoma culture supernatant¹⁴) di-
luted 1:10 with 2% (w/v) BSA in
PBST.
- Tertiary antibody solution: Alexa-488-
conjugated anti-mouse IgG antibody

(Molecular Probes) diluted 1:250 with 2% (w/v) BSA in PBST.

Methods

1. Air-dry the cryosections for 30 min before use, to ensure attachment to microslide surface and to preserve the structure.
2. Rehydrate the cryosections with PBS for 5 min.
3. Block free binding sites with 2% (w/v) BSA in PBST for 20 min.
4. Incubate cryosections with the primary antibody solution for 45 min.
5. Remove the primary antibody solution and wash three times 5 min with PBST.
6. Incubate cryosections with secondary antibody solution for 30 min.
7. Remove secondary antibody solution and wash three times 5 min with PBST.
8. Incubate cryosections with tertiary antibody solution for 30 min.
9. Remove tertiary antibody solution and wash three times 5 min with PBST.
10. Fix cryosections in 96% ethanol for 10 seconds.
11. Air-dry the sections and use Mowiol solution for embedding; store at -20°C.
12. Analyze staining patterns by fluorescence microscopy¹⁵. Figure 3 is an example of staining pattern on renal cryosections using scFv antibodies.

To evaluate the specificity of the scFv antibodies, cryosections can be pre-incubated with the glycosidases in the desired buffer for 2 h at the optimal temperature (see earlier discussion). Cryosections are washed with PBST and blocked with 2% (w/v) BSA in PBST as in *step 4*. Proceed with the above procedure (begin at *step 5*). For staining patterns, see Figure 4.

(J) Characterization of scFv antibodies by ELISA

To analyze which chemical groups in HS/heparin or CS/DS are involved in antibody recognition, reactivity with a number of test molecules can be evaluated by additional ELISA experiments: (1) *direct* ELISA in which wells of microtiter plates are coated with the test molecules, or by (2) *competition* ELISA in which the scFv antibodies and test molecules are simultaneously incubated in wells of a microtiter plate coated with the molecule of interest.

(J1) Direct ELISA

Materials

See section 'F. ELISA screening of bacterial clones expressing anti-GAG antibodies'.

Methods

Day 1

1. Coat wells from an ELISA plate with 100 μ l of a 10 μ g/ml GAG solution. Incubate o/n at 4°C.

¹⁴ The hybridoma cell line (P5D4 [anti-VSV]) is available from the American Type Culture Collection (ATCC). Alternatively, polyclonal rabbit anti-VSV-G (Sigma) can be used.

¹⁵ Stained tissue sections can be kept for up to 3 years at 4°C. The fluorescent tag (Alexa-488) is very stable, and fading of the signal hardly occurs. Store stained sections at -20°C. Background staining can often be eliminated by additional blocking steps with BSA or with 1-5% (v/v) serum from the same species in which the tertiary antibody is raised.

Day 2

1. Discard the GAG solution and wash the plate six times with PBST.
2. Block the plate with 200 μ l of 2% (w/v) BSA in PBST for 90 min at room temperature.
3. Empty the plate and add 100 μ l of primary antibody solution (periplasmic fraction diluted 1:5 with 2% (w/v) BSA in PBST) to the plate. Incubate for 2 h at room temperature.
4. Proceed as in section '*F. ELISA screening for bacterial clones expressing anti-GAG antibodies; Day 5 step 5.4*'.
5. Analyze the absorbance values to determine apparent affinities/specificity towards various GAGs.

*(J2) Competition ELISA***Materials**

See section '*F. ELISA screening for bacterial clones expressing anti-GAG antibodies*'.

Methods*Day 1*

1. Coat wells from an ELISA plate with 100 μ l of a 10 μ g/ml GAG solution. Incubate o/n at 4°C.

Day 2

1. Discard the GAG solution and wash the plate six times with PBST.
2. Block the plate with 200 μ l of 2% (w/v) BSA in PBST for 90 min at room temperature.

3. Discard the 2% (w/v) BSA in PBST and add 100 μ l of primary antibody solution (periplasmic fraction diluted 1:5 with 2% (w/v) BSA in PBST) together with the test molecules (serially diluted) to the plate. Incubate for 2 h at room temperature.
4. Proceed as in the section '*ELISA screening for bacterial clones expressing anti-GAG antibodies; Day 2, step 4*'.
5. Analyze the absorbance values to determine apparent affinities/specificity towards various GAGs.

Acknowledgements

This work was financially supported by the Netherlands Organization for Scientific Research (NWO), grant 902-27-292 (to J.F.M.L., and T.J.M.W.), the Dutch Cancer Society (KWF), grant 2002-2762 (to G.B.t.D), and the International Human Frontier Science Program Organization (HFSP), grant RGP0062/2004-C101 (to G.J.J.). The authors express their gratitude to Dr. G. Winter (Cambridge University, Cambridge, UK) for providing the phage display library. They thank Dr. J.M.H. Raats (Department of Biochemistry, Faculty of Sciences, Nijmegen, The Netherlands) for providing the pUC119-His-VSV vector, and IBEX Technologies (Montreal, PQ, Canada) for providing recombinant heparinase III derived from *Flavobacterium heparinum*.

References

1. David, G., Bai, X. M., Van der Schueren, B., Cassiman, J. J. & Van den Berghe, H. Developmental changes in heparan sulfate expression: in situ detection with mAbs. *J Cell Biol* 119, 961-75 (1992).
2. Bao, X., Pavao, M. S., Dos Santos, J. C. & Sugahara, K. A functional dermatan sulfate epitope containing iduronate(2-O-sulfate)alpha1-3GalNAc(6-O-sulfate) disaccharide in the mouse brain: demonstration using a novel monoclonal antibody raised against dermatan sulfate of ascidian *Ascidia nigra*. *J Biol Chem* 280, 23184-93 (2005).
3. van den Born, J. et al. Presence of N-unsubstituted glucosamine units in native heparan sulfate revealed by a monoclonal antibody. *J Biol Chem* 270, 31303-9 (1995).
4. Caterson, B., Christner, J. E. & Baker, J. R. Identification of a monoclonal antibody that specifically recognizes corneal and skeletal keratan sulfate. Monoclonal antibodies to cartilage proteoglycan. *J Biol Chem* 258, 8848-54 (1983).
5. Sorrell, J. M., Mahmoodian, F., Schafer, I. A., Davis, B. & Caterson, B. Identification of monoclonal antibodies that recognize novel epitopes in native chondroitin/dermatan sulfate glycosaminoglycan chains: their use in mapping functionally distinct domains of human skin. *J Histochem Cytochem* 38, 393-402 (1990).
6. van Kuppevelt, T. H., Dennissen, M. A., van Venrooij, W. J., Hoet, R. M. & Veerkamp, J. H. Generation and application of type-specific anti-heparan sulfate antibodies using phage display technology. Further evidence for heparan sulfate heterogeneity in the kidney. *J Biol Chem* 273, 12960-6. (1998).
7. Jenniskens, G. J., Oosterhof, A., Brandwijk, R., Veerkamp, J. H. & van Kuppevelt, T. H. Heparan sulfate heterogeneity in skeletal muscle basal lamina: demonstration by phage display-derived antibodies. *J Neurosci* 20, 4099-111. (2000).
8. Smetsers, T. F. et al. Localization and characterization of melanoma-associated glycosaminoglycans: differential expression of chondroitin and heparan sulfate epitopes in melanoma. *Cancer Res* 63, 2965-70 (2003).
9. van De Westerlo, E. M. et al. Human single chain antibodies against heparin: selection, characterization, and effect on coagulation. *Blood* 99, 2427-33 (2002).
10. Dennissen, M. A. et al. Large, tissue-regulated domain diversity of heparan sulfates demonstrated by phage display antibodies. *J Biol Chem* 277, 10982-6 (2002).
11. ten Dam, G. B. et al. Detection of 2-O-sulfated iduronate and N-acetylglucosamine units in heparan sulfate by an antibody selected against acharan sulfate (IdoA2S-GlcNAc)n. *J Biol Chem* 279, 38346-52 (2004).
12. ten Dam, G. B. et al. 3-O-Sulfated oligosaccharide structures are recognized by anti-heparan sulfate antibody HS4C3. *J Biol Chem* (2005).
13. ten Dam, G. B., Hafmans, T., Veerkamp, J. H. & van Kuppevelt, T. H. Differential expression of heparan sulfate domains in rat spleen. *J Histochem Cytochem* 51, 727-39 (2003).
14. Smits, N. C. et al. Heterogeneity of heparan sulfates in human lung. *Am J Respir Cell Mol Biol* 30, 166-73 (2004).
15. Lensen, J. F. et al. Localization and functional characterization of glycosaminoglycan domains in the normal human kidney as revealed by phage display-derived single chain antibodies. *J Am Soc Nephrol* 16, 1279-88 (2005).
16. Jenniskens, G. J., Hafmans, T., Veerkamp, J. H. & Van Kuppevelt, T. H. Spatiotemporal distribution of heparan sulfate epitopes during myogenesis and synaptogenesis: A study in developing mouse intercostal muscle. *Dev Dyn* 225, 70-9 (2002).
17. Smetsers, T. F. et al. Human single-chain antibodies reactive with native chondroitin sulfate detect chondroitin sulfate alterations in melanoma and psoriasis. *J Invest Dermatol* 122, 707-16 (2004).

18. Jenniskens, G. J. et al. Disturbed Ca²⁺ kinetics in N-deacetylase/N-sulfotransferase-1 defective myotubes. *J Cell Sci* 116, 2187-93 (2003).
19. Hoogenboom, H. R. & Chames, P. Natural and designer binding sites made by phage display technology. *Immunol Today* 21, 371-8 (2000).
20. Winter, G., Griffiths, A. D., Hawkins, R. E. & Hoogenboom, H. R. Making antibodies by phage display technology. *Annu Rev Immunol* 12, 433-55 (1994).
21. Harrison, J. L., Williams, S. C., Winter, G. & Nissim, A. Screening of phage antibody libraries. *Methods Enzymol* 267, 83-109 (1996).
22. Nissim, A. et al. Antibody fragments from a 'single pot' phage display library as immunochemical reagents. *Embo J* 13, 692-8 (1994).
23. Vieira, J. & Messing, J. Production of single-stranded plasmid DNA. *Methods Enzymol* 153, 3-11 (1987).
24. Lensen, J. F. et al. Selection and characterization of a unique phage display-derived antibody against dermatan sulfate. *Matrix Biol* 25, 457-61 (2006).



Chapter 3

American Journal of Respiratory Cell and Molecular Biology 2004, 30:166-173

Heterogeneity of heparan sulfates in human lung

Nicole C. Smits •
Antoine A. Robbesom •
Elly M.M. Versteeg •

Els M.A. van de Westerlo •
Richard P.N. Dekhuijzen ••
Toin H. van Kuppevelt •

- *Department of Biochemistry, Radboud University Nijmegen Medical Centre, NCMLS, Nijmegen, The Netherlands*
- *Department of Pulmonary Diseases, Radboud University Nijmegen Medical Centre, Nijmegen, The Netherlands*

Heparan sulfates (HS), a class of glycosaminoglycans, are long linear complex polysaccharides covalently attached to a protein core. The HS molecules are made up of repeating disaccharides onto which modification patterns are superimposed. This results in a large structural heterogeneity and forms the basis of specific interactions of HS towards a vast array of proteins, including growth factors and proteases. To study HS heterogeneity in the lung, we used phage display technology to select seven antibodies against human lung HS. Antibodies reacted with HS/heparin, but not with other glycosaminoglycans or polyanions. Sulfate groups were essential for antibody binding. The amino acid sequence of the antibodies was established, the complementarity determining region 3 of the heavy chain containing basic amino acids. The antibodies defined HS epitopes with a characteristic tissue distribution. Antibody EV3A1 primarily stained macrophages. Other antibodies primarily stained basement membranes, but with different preference towards type of basement membrane. Antibody EV3C3 was the only antibody which clearly reacted with bronchiolar epithelial cells. In human lung parenchyma bFGF and VEGF were largely bound by HS. Some antibodies blocked a bFGF-binding site of HS, and one antibody blocked a VEGF-binding site of heparin. Taken together, these data suggest a specific role for HS epitopes in human lung. The antibodies obtained may be valuable tools to study HS in pulmonary diseases.

Introduction

Heparan sulfates (HS) are members of the glycosaminoglycan (GAG) family, consisting of repeating disaccharide units onto which modification patterns are superimposed. HS bind and modulate a myriad of molecules, including growth factors, cytokines, proteases, anti-proteases, matrix molecules and viral and bacterial proteins^{1,2}. This large number of interactions suggests an extensive structural variation within HS. The structural diversity of HS is brought about by specific chain modifications during the biosynthesis of HS, including deacetylation, sulfation and epimerisation. The addition of e.g., sulfate groups leads to generation of specific motifs that make HS highly versatile, protein-binding, cell regulators³⁻⁵. HS proteoglycans (HSPGs) are predominantly present on cell surfaces and in the extracellular matrix.

Little is known about the roles proteoglycans and GAGs play in the lung. However, their distribution over various

lung components⁶, their strategic ultra-structural location⁷, and their changes during developmental stages⁸ suggest that they are of crucial importance to the architecture and functioning of the lung. Due to their location in basement membranes and on cell surfaces, HSPGs deserve special attention.

The importance of specific HS modifications for lung functioning has been demonstrated in mice lacking *N*-deacetylase/*N*-sulfotransferase-1 (NDST-1), an enzyme involved in the deacetylation and sulfation of glucosamine residues in HS. *NDST-1*^{-/-} mice develop respiratory distress syndrome and die shortly after birth of respiratory failure^{9,10}. This effect has been attributed to immature type II pneumocytes, resulting in shortage of lung surfactant. Sulfation is a major determinant of the response of alveolar type II cells to growth factors¹¹. Growth factors like FGF's are retained by HS. Electron microscopical studies

using cationic probes indicate that HS in the basement membranes of alveolar type I and type II cells and of alveolar endothelial cells are differentially sulfated^{12, 13}. Sulfated proteoglycans play a central role in the modulation of the extracellular matrix of pulmonary fibroblasts, and HSPGs are involved in neutrophil trafficking to the alveolar space¹⁴.

Studies of HSPGs have mainly been focused on the protein core, whereas research on HS in the lung has been limited to the estimation of total HS content. Detailed structural analysis of HS domains have not been performed, simply because appropriate tools were lacking. Only a few antibodies that recognize HS epitopes have been generated, primarily because of the nonimmunogenic nature of HS. To circumvent this, we adapted the phage display technology to obtain specific antibodies against HS^{15, 16}.

In this study, we report on the isolation, characterization, and application of single chain antibodies selected against HS isolated from human lung. We provide evidence for the existence of several, differentially distributed HS epitopes in human lung, and show that binding of FGF-2 and VEGF to the alveolar matrix of human lung is mediated via HS. The antibodies may be very instrumental in elucidation of the role of HS domains in health and disease.

Experimental methods

Lung specimens were obtained from patients undergoing lobectomy or pneumonectomy for a localized malignant pulmonary process, at the University Lung Centre Nijmegen or the Rijnstate Hospital Arnhem, the Netherlands. A human semi-synthetic antibody phage

display library¹⁷, (now officially named synthetic scFv Library no.1) was generously provided by Dr. G. Winter, Cambridge University, Cambridge, United Kingdom). This library contains 50 different V_H genes with a synthetic random complementarity determining region 3 (CDR3) segments, which are 4-12 amino acid residues in length. The heavy chains are combined with a single light chain gene (DPL16). The library contains over 10⁸ different clones and all antibodies contain a c-*Myc* tag.

All chemicals used were purchased from Merck (Darmstadt, Germany) unless stated otherwise. Bacterial medium (2 × TY) was from Gibco BRL (Paisley, Scotland); chemically modified heparan sulfate kit, chemically modified heparin kit, anti-chondroitin sulfate (CS)/dermatan sulfate (DS) 'stub' antibody (2B6), anti-HS 'stub' antibody (3G10) and chondroitin 4, 6-disulfate from squid cartilage were from Seikagaku Kogyo (Tokyo, Japan). Heparin from porcine intestinal mucosa, HS from bovine kidney and from porcine intestinal mucosa, chondroitin 4-sulfate from whale cartilage, chondroitin 6-sulfate from shark cartilage, hyaluronate from human umbilical cord, DNA from calf thymus, dextran sulfate, sodium azide, bovine serum albumin (fraction V), chondroitinase ABC (*Flavobacterium heparinum*), and rabbit anti-rat FGF-2 were from Sigma (St Louis, MO); Microton 96-well microtiter plates were from Greiner (Frickenhausen, Germany); polystyrene Maxisorp Immunotubes were from Nunc (Roskilde, Denmark); mouse anti-c-*Myc* monoclonal IgG (clone 9E10) and mouse anti-VSV monoclonal IgG (clone P5D4) were from Boehringer Mannheim (Mannheim, Germany); rab-

bit anti-c-*Myc* polyclonal IgG (A-14) was from Santa Cruz Biotechnology (Santa Cruz, CA); alkaline phosphatase-conjugated rabbit anti-mouse IgG, mouse anti-human mast cell tryptase (clone AA1), and mouse anti-human CD68 (clone KP1), were from Dakopatts (Glostrup, Denmark); Alexa 488-conjugated goat anti-mouse IgG and Alexa 594-conjugated goat anti-mouse IgG were from Molecular Probes (Eugene, OR); Mowiol (4-88) was from Calbiochem (La Jolla, CA); Plasmid DNA isolation kit was from Qiagen (Hilden, Germany); and ABI Prism Big Dye Terminator Cycle Sequencing Ready Reaction Kit was from PE Applied Biosystems (Norwalk, CT). Hematoxylin was from Fluka Biochemika (Buchs, Switzerland). Mouse anti-human VEGF (ab1316) clone VG1) was from Abcam (Cambridge, UK). Human recombinant (hr) VEGF₁₆₅ and rat recombinant (rr) FGF-2, cloned in prokaryotic vector pQE16, were a gift from the Department of Pathology, University Hospital Nijmegen, Nijmegen, The Netherlands. All experiments were performed at ambient temperature (22°C), unless stated otherwise.

Isolation of heparan sulfate from human lung tissue

Lung tissue was collected from 8 individuals, 5 were male, and 3 were female. Small lung specimens were taken from resected lung lobes, not showing any sign of the underlying disease for which the patient underwent surgery (mostly lung cancer) or obstruction pneumonia. Subjects (54 ± 7 ; mean age \pm SD) had spirometric values in the normal range. Per gram (wet weight) of human lung tissue, 4 ml 50mM sodium phosphate

buffer, pH 6.5, containing 2mM EDTA, 2mM cysteine, and 10 U papain were added and digestion was performed for 16 h at 65°C. The digest was centrifuged (16,000g for 20 min at 4°C) and the supernatant containing the GAGs was subjected to mild alkaline borohydride digestion (0.5M NaOH/0.1M NaBH₄ at 4°C) to remove residual peptides from the GAGs. After overnight digestion, the mixture was neutralized by addition of 6M HCl. Proteins were precipitated for 30 min at 0°C by addition of 100% (wt/vol) trichloroacetic acid to a final concentration of 15%. Precipitated proteins were removed by centrifugation (16,000g for 20 min at 4°C), and GAGs were precipitated by addition of 5 vol of 100% ethanol to the supernatant and incubation overnight at -20°C. After centrifugation (16,000g for 30 min at 4°C), the pelleted GAGs were washed with 70% ethanol, dried, and dissolved in MilliQ. To obtain GAG preparations which contained only HS, chondroitinase ABC, which digests chondroitin sulfate and dermatan sulfate, was added (1 IU/100 mg of GAG in 25mM Tris-HCl, pH 8.0) and incubation was performed for 16 h at 37°C. The efficacy of chondroitinase ABC treatment was evaluated by agarose gel electrophoresis¹⁸. HS were further purified using DEAE Sepharose column chromatography¹⁸, using 0.2M, 0.5M, 1.0M and 2.0M NaCl in 10mM Tris-HCl elution steps, pH 6.8. The 0.5M and 1.0M HS fractions were pooled, ethanol-precipitated, and residual salt removed by a 70% (vol/vol) ethanol wash. HS preparations were dissolved in MilliQ, checked for purity (Figure 1) and stored at 4°C.

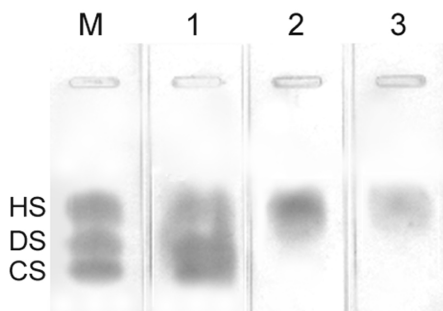


Figure 1. Agarose gel electrophoresis of human lung HS used for biopanning. The gel was run in 50mM Ba(Ac)₂ pH 5.0 and stained by a combined azure A-silver procedure. M, marker; lane 1: total lung GAG; lanes 2 and 3: human lung HS after DEAE sepharose column chromatography (eluting at 0.5M NaCl [2], and 1.0M NaCl [3] followed by chondroitinase ABC digestion). HS, heparan sulfate; DS, dermatan sulfate; CS, chondroitin sulfate.

Selection of anti-GAG antibodies

Phage display-derived antibodies were obtained as described¹⁵ using four rounds of panning against HS (0.5M and 1.0M fraction). Briefly, antibody-expressing phages were added to HS-coated tubes, and bound phages were eluted at high pH to allow for the infection of *E. coli* TG1 cells. After overnight amplification, phages were rescued by the addition of helper phage and used for further rounds of selections.

Screening for bacteria expressing antibodies against glycosaminoglycans

Screening for bacteria expressing anti-HS antibodies was as described¹⁵. Briefly, single colonies picked from the last two rounds of selection were grown in 96-well polystyrene plates until bacterial growth was visible. Antibody production was induced by the addition of isopropyl- β -D-thiogalactopyranoside

(IPTG, final concentration 1mM). Plates were centrifuged, and the supernatant containing soluble antibodies was applied to wells of polystyrene microtiter plates previously coated with HS. Bound antibodies were detected using mouse anti-c-*Myc*, followed by incubation with alkaline phosphatase-conjugated rabbit anti-mouse IgG. Alkaline phosphatase activity was measured using *p*-nitrophenyl phosphate as a substrate. Absorbance was measured at 405 nm. To establish the CDR3 and V_H gene DNA segments, antibody expressing clones were sequenced using PelB-seq (5'-CCGCTGGATTGTTACTC-3') (located within the PelB leader sequence), and For Link-seq (5'-GCCACCTCCGCCTGAACC-3') (located in the linker region between the V_H and the V_L genes). For this purpose, double-stranded DNA was isolated using standard procedures.

Large scale preparation of antibodies

To obtain large amounts of soluble antibodies, periplasmic fractions from infected bacteria were isolated¹⁵. Briefly, bacteria were grown at 37°C until an optical density (OD₆₀₀) of 0.5 was reached. Induction was effectuated by the addition of IPTG. After incubation at 30°C for 3 h, the culture was centrifuged, and the pellet was resuspended in 200mM sodium borate buffer (pH 8.0) containing 160mM NaCl, and an ethylenediaminetetraacetic acid (EDTA)-free protease inhibitor cocktail (1mM). After centrifugation at 5,000g for 30 min at 4°C, the supernatant (representing the periplasmic fraction containing the antibodies) was filtered through a 0.45 μ m filter, dialyzed overnight at 4°C versus PBS, and stored at -20°C.

Characterization of antibodies by ELISA

Affinity of the antibodies to various molecules was evaluated by ELISA as described¹⁵. Briefly, wells were coated with the molecules concerned by incubation with 100 μ l of a 10 μ g/ml solution in wells of a 96-well microtiter plate for 16 h at 4°C. The wells were rinsed with PBS containing 0.1% (vol/vol) Tween-20 (PBST) and blocked with 2% BSA in PBS containing 0.05% (vol/vol) Tween-20. Antibodies were added and allowed to bind for 90 min. Bound antibodies were detected by incubation with 10-fold diluted mouse anti-c-*Myc* monoclonal antibody 9E10, followed by incubation with 1:1,000 diluted alkaline-phosphatase conjugated rabbit anti-mouse IgG. Plates were rinsed six times with PBST following each incubation. Enzyme activity was detected using 100 μ l 1 mg *p*-nitrophenyl phosphate/ml 1M diethanolamine/0.5mM MgCl₂, pH 9.8, as a substrate. Absorbance was read at 405 nm. All assays were performed at least 3 times and representative results are shown. As a control, wells were incubated with an irrelevant antibody TSC01 (CDR3 sequence LGFHS, V_H3 family, germline segment DP40).

To evaluate which chemical groups are important for recognition of the antibodies, an ELISA with modified HS/heparin preparations (from porcine intestine) was performed, including heparins that were desulfated and *N*-sulfated, desulfated and *N*-acetylated, *N*-desulfated and *N*-acetylated, and various HS preparations. Periplasmic fractions containing antibodies were incubated for 90 min in 96-well microtiter plates previously coated with modified heparin/HS preparations. The plates were rinsed with PBST and ELISA was performed as

described above.

Characterization of antibodies and localization of HS epitopes by immunohistochemistry

Human lung cryosections (5 μ m) were fixed in 4% paraformaldehyde. After rinsing in PBS for 10 min, cryosections were incubated in H₂O₂ solution (0.3% in PBS, pH 7.3) to quench endogenous peroxidase activity. Subsequently, cryosections were washed for 10 min in PBS, blocked with PBS containing 0.05% (vol/vol) Tween-20 and 2% (wt/vol) BSA for 10 min, and incubated with 2-fold diluted antibodies containing 3% normal horse serum for 45 min. Bound antibodies were detected by incubation with 1:10 diluted mouse anti-c-*Myc* monoclonal antibody 9E10 containing 3% normal horse serum for 45 min. After washing with PBST (2 \times 10 min), cryosections were incubated with biotinylated anti-mouse IgG containing 3% normal horse serum, for 45 min, washed with PBST (2 \times 10 min), and incubated with Vectastain Elite ABC-kit (Vector, Burlingame, CA) for 45 min. Sections were rinsed in PBST and incubated with 3,3'-diaminobenzidine (DAB) solution to identify bound antibody. After a final wash in PBS, sections were counterstained with Mayers' hematoxylin and mounted with Entellan (Merck, Darmstadt, Germany). As a control, cryosections were incubated with an irrelevant antibody TSC01.

To evaluate the specificity of the antibodies, cryosections were digested with the glycosidases heparinase III, heparinase I (both digest HS) 0.04 IU/ml in 50mM NaAc/50mM Ca(Ac)₂, pH 7.0 or chondroitinase ABC (digests chondroitin sulfate and dermatan sulfate) 0.02 U/ml in 25mM Tris-HCl, pH 8.0, (2 h at 37°C, refreshing the enzyme after

1 h). As a control, cryosections were incubated in reaction buffer without enzyme. After washing three times with PBS and blocking for 30 min with PBS containing 0.05% (vol/vol) Tween-20 and 2% (wt/vol) BSA, cryosections were incubated with antibodies and processed for immunohistochemistry as described above. The efficiency of heparinase III and chondroitinase ABC treatment was evaluated by incubation of cryosections with antibodies against GAG-‘stubs’, generated by the glycosidases. For HS stubs the antibody 3G10 was used. For chondroitin sulfate stubs the antibody 2B6 was used. All tests were performed at least 3 times.

To evaluate whether the antibodies react with heparin or mast cells *in situ*, human lung cryosections were rehydrated, blocked with PBS containing 0.05% (vol/vol) Tween-20 and 2% (wt/vol) BSA for 30 min, and incubated with 2-fold diluted antibodies for 90 min. Bound antibodies were detected using 1:100 diluted anti-c-*Myc* rabbit polyclonal anti-body A-14 and goat anti-rabbit IgG Alexa 488, each for 60 min. For detection of mast cell tryptase, 1:500 diluted mouse anti-human mast cell tryptase and goat anti-mouse IgG Alexa 594 were included in the incubations. Macrophages were detected by 1:500 diluted CD68, and goat anti-mouse IgG Alexa 594. After each incubation, cryosections were washed, fixed in 100% methanol, air-dried, and embedded in Mowiol (10% (wt/vol) in 0.1M Tris-HCl, pH 8.5/25% (vol/vol) glycerol/2.5% (wt/vol) NaN₃). As a control, cryosections were incubated with an irrelevant antibody TSC01.

Inhibition of antibody binding to heparin and HS by FGF-2 and VEGF

To study whether the HS epitope defined by the antibodies is involved in the binding of FGF-2 and/or VEGF, polystyrene microtiter plates were coated with HS from bovine kidney or heparin from porcine intestinal mucosa. Subsequently, 100 µl of a solution containing FGF-2¹⁹ or VEGF₁₆₅ (0.3 µg/ml PBS, containing 0.05% (vol/vol) Tween-20 and 2% (wt/vol) BSA) was applied for 60 min to wells of the polystyrene microtiter plate. At these amounts, a maximum number of FGF-2 or VEGF₁₆₅-binding sites on HS and heparin are occupied, as determined using anti-growth factor antibodies. After washing, antibodies were applied. The amount of antibodies was chosen such that, in an ELISA without growth factors, 50% staining was obtained, 100% being the value obtained using saturating amounts of antibody. This set-up was chosen to sensitively detect a reduction of HS-bound antibodies by growth factors. Bound antibodies were detected as described.

Results

Selection of anti-HS antibodies

A human synthetic phage library containing phages expressing antibodies was biopanned against HS isolated from human lung. After four rounds of panning, seven antibodies were selected (Table 1). The antibodies were different with respect to their amino acid sequence of the complementarity-determining region 3 and/or V_H gene.

Characterization of anti-HS antibodies

Using ELISA, antibodies were shown to be reactive for the lung HS preparation as well as for heparin, a highly sulfated

Table 1: Characteristics of anti-HS antibodies

Antibody	CDR3 sequence	V _H family	Germline segment
EV3A1	GKRRRQ	V _H -3	DP-42
EV3B2*	GKMKLNR	V _H -3	DP-38
EV3C3*	GYRPRF	V _H -3	DP-42
EV3D6	WMHLRVRH	V _H -1	DP-5
EV4D6	GARPRAN	V _H -3	DP-38
EV4D12	HAPLRNTRTNT	V _H -3	DP-38
EV4F8	GMRPRL	V _H -3	DP-38

Given are the antibody code, amino acid sequence of the V_H complementarity-determining region 3 (CDR3), V_H family and the germline segment (DP numbering). CDR3 sequences are shown in single-letter amino acid code. V_H families and DP segments were deduced from the V BASE using DNAPLOT alignment (<http://www.mrc-cpe.cam.ac.uk/imt-doc/restricted/DNAPLOT.html>) by applying the full-length V_H sequences of the anti-HS antibody clones (nomenclature according to Tomlinson and coworkers⁴⁰).

*Antibodies EV3B2 and EV3C3 have been partially described¹⁵.

form of HS. HS from other sources was also recognized, except for EV3A1, which only reacted with heparin (Table 2). None of the antibodies was reactive with other GAGs such as dermatan sulfate and chondroitin 4-sulfate, chondroitin 6-sulfate, hyaluronic acid, keratan sulfate and K5 (similar to the HS precursor polysaccharide), nor with other polyanionic molecules such as dextran

sulfate and DNA.

Analysis of HS epitopes recognized by the antibodies

To determine which chemical groups are important for recognition, we tested all seven antibodies for reactivity with chemically modified heparin and HS preparations (Table 2).

None of the antibodies reacted with K5 capsular polysaccharide from *E. coli* (which is similar to the HS precursor polysaccharide), indicating that additional modifications are essential for binding. Except for antibodies EV4D12 and EV4D4, none of the antibodies reacted with heparin that was completely desulfated/*N*-acetylated, desulfated but *N*-sulfated heparin, or *N*-desulfated/*N*-acetylated, indicating that *N*- and *O*-sulfate groups are essential. Only antibody EV4D12 reacted, although weakly, with heparin that was completely desulfated and *N*-sulfated, suggesting that *N*-sulfation is of major importance for the binding of this antibody. Antibody EV4D6 was the only antibody which partially recognized *N*-desulfated and *N*-acetylated heparin (but not HS), indicating that the presence of *N*-sulfate groups is not absolutely essential for binding.

Figure 2. Immunostaining for HS epitopes defined by anti-HS antibodies. Nontreated and heparinase III-treated cryosections of human lung were incubated with periplasmic fractions containing antibody EV3C3 (a), EV4D12 (b), EV3D6 (c), EV3A1 (d), or anti-heparan sulfate stub antibody (3G10) (e). Bound antibodies were visualized by incubation with anti-*c-Myc* mouse monoclonal antibody 9E10, followed by biotinylated anti-mouse IgG. Sections were counterstained with Mayers' hematoxylin. Untreated tissue (a1-d1, a2-d2) showed HS epitopes differentially distributed throughout parenchymal tissue (for details see text). Staining was lost or strongly decreased after heparinase III-treatment (a3-d3), indicating the HS-nature of the epitopes. Staining of heparan sulfate stubs in heparinase III-treated tissue showed alveolar HS to be present in alveolar and capillary basement membranes (e2-e3). Alveolar macrophages are negative (arrow in e2). Scale bars, 20 μm.

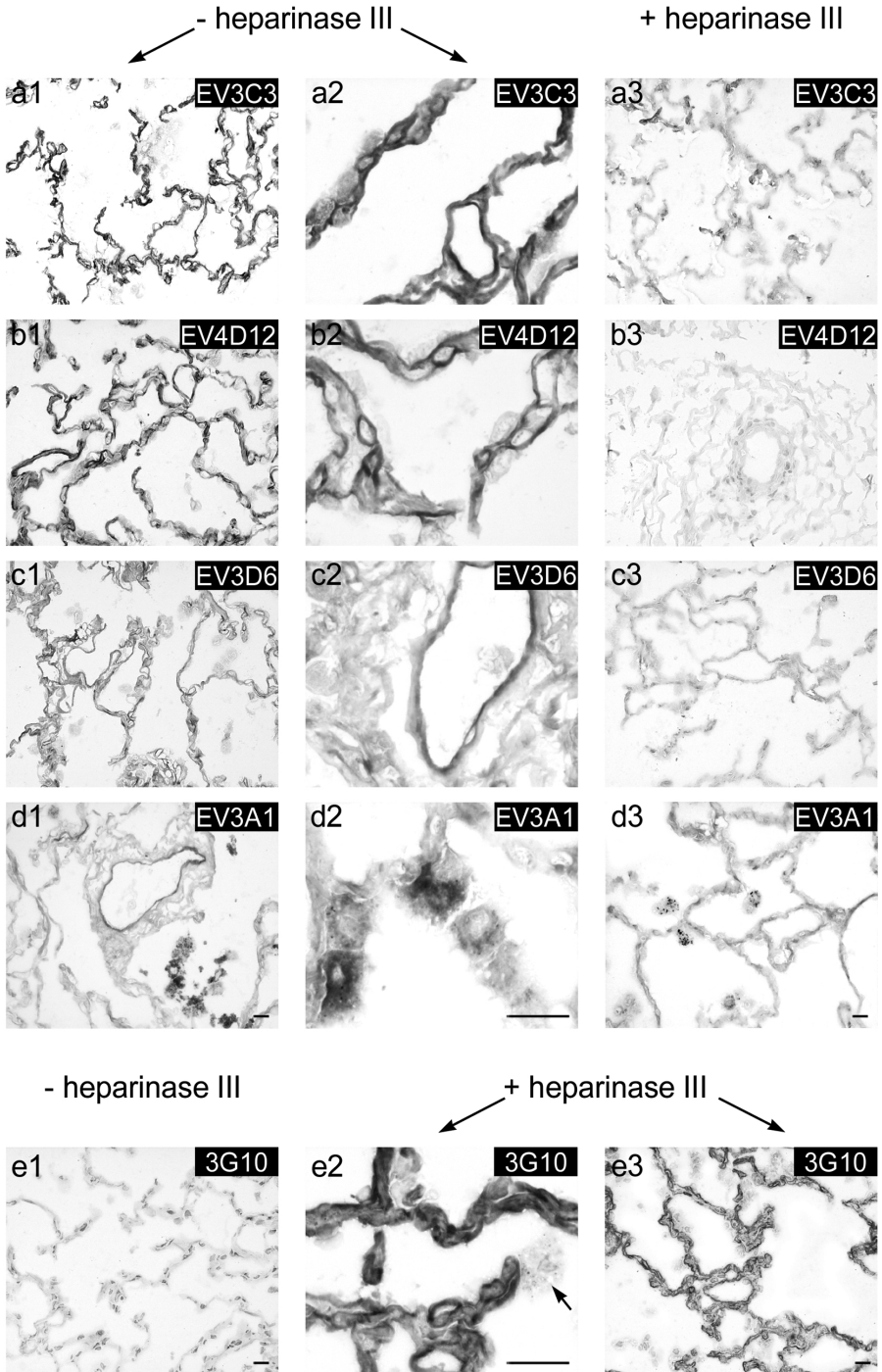


Table 2: Reactivity of anti-HS antibodies with modified HS and heparin molecules

Test substance	Antibody code						
	EV3A1	EV3B2	EV3C3	EV3D6	EV4D6	EV4D12	EV4F8
Heparin, porcine intestinal mucosa	+	++	+	++	++	+	++
Heparin, <i>N</i> -desulfated and <i>N</i> -acetylated	-	-	-	-	+/-	-	-
Heparin, completely desulfated and <i>N</i> -sulfated	-	-	-	-	-	+/-	-
Heparin, completely desulfated and <i>N</i> -acetylated	-	-	-	-	-	-	-
HS (bovine kidney)	-	+	+	+	+	+	+
HS (intestinal mucosa)	-	+	+/-	+/-	+	+	+
HS, <i>N</i> -desulfated and <i>N</i> -acetylated	-	-	-	-	-	-	-
K5 (capsular polysaccharide from <i>E. coli</i>)*	-	-	-	-	-	-	-

Periplasmic fractions of the antibodies were applied to various GAG preparations immobilized on microtiter plates. Bound antibodies were detected using anti-*c-Myc* mouse monoclonal antibody 9E10, followed by alkaline phosphatase-conjugated rabbit anti-mouse IgG, after which enzymatic activity was measured using *p*-nitrophenyl phosphate as a substrate. Substrate affinity: ++, very strong; +, strong; +/-, moderate; -, absent ($n = 3$).

*Similar to the HS precursor polysaccharide.

Localization of HS epitopes in human lung

To study the location of the HS saccharides defined by the antibodies, we performed immunohistochemistry using cryosections of human lung. Each antibody showed a defined pattern of reactivity (Table 3, Figure 2: shown are the antibodies EV3C3 (a), EV4D12 (b), EV3D6 (c), EV3A1 (d), and anti-stub antibody 3G10 (e)). All antibodies, except for EV3A1 and EV3D6, primarily stained basement membranes of alveoli, bronchioli and blood vessels. The antibodies differed in preference toward different types of basement membranes. EV3D6 was the only antibody which was only reactive with basement membranes of bronchioli and blood vessels (Figure 2,

c1-c2). Basement membranes of alveoli were not recognized by EV3D6. For the other antibodies, staining intensity of basement membranes of blood vessel endothelium, bronchioles, and capillaries was identical, or stronger compared to alveolar basement membranes. Basement membranes of smooth muscle cells of blood vessels and bronchioli were recognized by the antibodies EV3C3, EV4D12 (Figure 2, a1-a2, b1-b2), and antibody EV3B2 (not shown), whereas the other antibodies were completely negative. Antibody EV3A1 was primarily reactive with macrophages (Figure 3c and 3d). It stained granules of uneven size, likely lysosomes. It was not reactive with mast cells (Figure 3a and

3b). EV3C3 was the only antibody which clearly stained the epithelial cells of bronchioli (Figure 4a); other antibodies (e.g., EV4D12, Figure 4b) were negative in this respect. Note that EV3C3, but not EV4D12, shows a distinct intracellular staining in bronchiolar epithelium. Nuclei of bronchiolar cells appeared to be reactive with EV3C3 (Figure 4a, *insert*). Macrophages were recognized by all antibodies, except for EV3D6 and EV4D6 (data not shown). Mast cells were recognized by the antibodies EV3B2,

EV3C3 and EV3F8 (data not shown). Thus, the staining patterns of anti-HS antibodies show a unique distribution of HS epitopes in human lung.

To ascertain HS specificity of the antibodies, cryosections of human lung tissue were treated with heparinase III, heparinase I, or chondroitinase ABC, before incubation with the antibody. Staining was absent or strongly decreased after treatment with heparinase III (Figure 2, a3-d3), whereas treatment with chondroitinase ABC had no effect

Table 3: Immunostaining for HS epitopes defined by anti-HS antibodies

Structure	Antibody code						
	EV3A1	EV3B2	EV3C3	EV3D6	EV4D6	EV4D12	EV4F8
Alveoli							
Basement membrane epithelium	-	+/-	+	-	+/-	+/-	+/-
Basement membrane capillaries	-	+	++	-	+	++	+
Bronchioli							
Epithelial cells	-	-	+	-	-	-	-
Basement membrane epithelial cells	+	+	++	+	+	++	+
Basement membrane smooth muscle cells	-	+	+	-	-	+/-	-
Blood vessels							
Basement membrane endothelium	+	+	++	+	+	++	++
Basement membrane smooth muscle cells	-	+/-	+	-	-	+/-	-
Mast cells	-	+	+	-	-	-	+
Macrophages	++	+	+	-	-	+	+/-

Periplasmic fractions of bacteria expressing anti-HS antibodies were applied to cryosections of human lung. Bound antibodies were visualized by incubation with anti-c-*Myc* mouse monoclonal antibody 9E10, followed by biotinylated anti-mouse IgG. Sections were counterstained with Mayers' hematoxylin. Staining: ++, strong; +, moderate; +/-, weak; -, absent ($n = 3$).

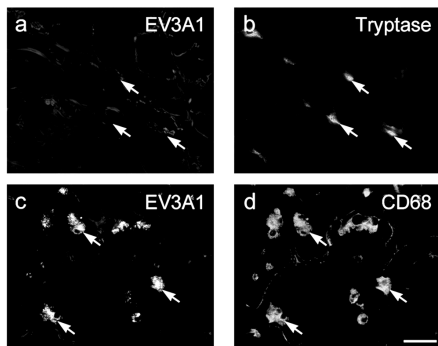


Figure 3. Staining of macrophages by antibody EV3A1. Cryosections of human lung were incubated with periplasmic fractions of antibody EV3A1 (a, c). Bound antibodies were visualized by incubation with rabbit polyclonal anti-c-Myc IgG, followed by Alexa 488-conjugated goat anti-rabbit IgG. Tryptase, identifying mast cells, was visualized using mouse anti-human mast cell tryptase, followed by Alexa 594-conjugated goat anti-mouse IgG (b). Macrophages were visualized using mouse anti-human CD68, followed by Alexa 594-conjugated goat anti-mouse IgG (d). Note that EV3A1 reacted strongly with macrophages, but not mast cells. Scale bar, 50 μ m.

(data not shown). For antibody EV3A1 staining of macrophages was not abolished by treatment with heparinase III, nor with heparinase I. For antibody EV3C3 some staining at discrete, but unidentified, places in the alveolar wall still remained after treatment with heparinase III (Figure 2, a3). After treatment with heparinase I, however, staining was completely lost.

Inhibition of antibody binding by FGF-2 and VEGF

To study if antibody-defined HS saccharides were involved in growth factor binding, the inhibition of antibody binding to HS/heparin by FGF-2 and VEGF

was studied. Using FGF-2, binding of antibody EV3C3 to HS was blocked by $22 \pm 2\%$, EV3B2 by $14 \pm 4\%$, and EV4F8 by $19 \pm 2\%$ (values are mean \pm SD, $n = 4$). In case of heparin, only antibody EV3A1 was blocked by $39 \pm 3\%$. For VEGF, only binding of antibody EV3A1 to heparin could be slightly inhibited ($11 \pm 1\%$). No effect of VEGF was observed for the other antibodies. In tissue, endogenous FGF-2 could be detected at sites of basement membranes (Figure 5, a1), and staining was removed after heparinase III-treatment (Figure 5, a2). After applying recombinant FGF-2, most basement membranes were stained (Figure 5, b1), and staining was decreased after heparinase III-treatment (Figure 5, b2). No endogenous VEGF could be detected. Recombinant VEGF₁₆₅ added to the sections was located in basement membranes of alveoli, blood vessels, bronchioli and macrophages (Figure 5, c1). Heparinase III digestion greatly

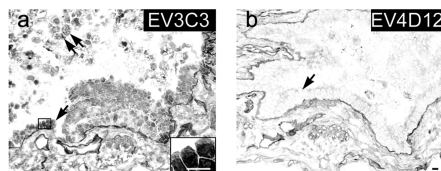


Figure 4. Staining of bronchiolar epithelium by antibody EV3C3. Cryosections were incubated with antibody EV3C3 (a) and EV4D12 (b). Bound antibodies were visualized by incubation with anti-c-Myc mouse monoclonal antibody 9E10, followed by biotinylated anti-mouse IgG. Sections were counterstained with Mayers' hematoxylin. Note that EV3C3, but not EV4D12, shows a distinct intracellular staining in the bronchiolar epithelium, nuclei appearing to be positive (*insert*). Single arrows, epithelial cells of bronchioli; double arrows in a, detached epithelial cells. Scale bars, 10 μ m.

abolished VEGF binding to sections (Figure 5, c2).

Discussion

In this study we describe the selection of seven antibodies against human lung HS from a semi-synthetic phage display library. Phage display has proven to be a very useful technique to select antibodies against poorly immunogenic molecules,

such as HS. All antibodies selected in this study recognize different HS epitopes, as indicated by their staining patterns and reactivity toward various HS preparations. For all antibodies, the CDR3 region of the heavy chain, which is of prime importance for the specificity and affinity of the antibodies, contained two or more basic amino acid residues likely involved in binding to negatively charged HS. HS-binding consensus sites contain basic amino acids, e.g., $XBBXBX$ (B, basic amino acid residue; X, any amino acid residue²⁰). Three out of seven antibodies bear the sequence $'GX_1RPRX_2'$ (X_1 : any amino acid; X_2 : hydrophobic amino acid). We suggest that this sequence forms a potential GAG-binding site.

Of seven antibodies selected against lung HS, two (EV4D12 and EV4F8) are identical to antibodies selected against HS from bovine kidney and human skeletal muscle^{15, 16}. Their CDR3 sequences are HAPLRNTRTNT and GMRPRL, and it indicates that common HS saccharides are present in these organs. The position of sulfate groups is of major importance for the binding of the antibodies. The requirement of both *N*- and *O*-sulfate groups for epitope recognition was indicated by chemically modified heparins. Overall desulfation completely abolished recognition by all antibodies. *N*-resulfation could not restore the heparin-antibody interaction, except (partly) for EV4D12. *N*-desulfation abolished reactivity with all antibodies, except EV4D6. Because CS as well as DS were not bound by any of the antibodies, sulfation patterns specific for HS are likely to be important in the structure of the epitopes involved in binding. For two antibodies (EV3A1 and EV3C3), staining

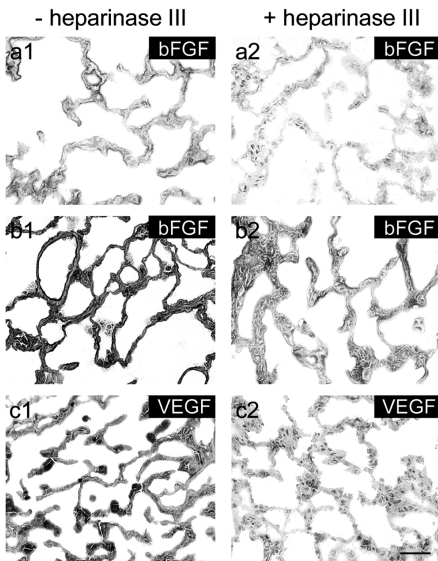


Figure 5. Localization of bFGF and VEGF in human lung. Non-treated (a1-c1) and heparinase III-treated (a2-c2) cryosections of human lung were incubated with an antibody to bFGF (a, b) or VEGF (c). Sections b and c were pretreated with 20 $\mu\text{g}/\text{ml}$ bFGF or VEGF prior to incubation with the antibody to bFGF or VEGF. Heparinase III treatment removed endogenous bFGF (a2), and reduced binding of recombinant bFGF and recombinant VEGF to sections (b2, c2). After digestion with heparinase III endogenous bFGF could not be detected (a2). Staining of sections treated with heparinase III prior to incubation with bFGF or VEGF was markedly decreased (b2 and c2). Scale bar, 50 μm .

could not be completely abolished using heparinase III-treatment. For EV3A1, treatment with heparinase III abolished staining of basement membranes, but not of macrophages (Figure 2, d3). Treatment with heparinase I also did not remove staining. Staining for HS/heparin stubs, generated by heparinases, was positive after treatment with heparinase I, but not III, indicating that the HS/heparin in macrophages is not a substrate for heparinase III and therefore probably not bound to a core protein (heparinase III cleaves HS in a region near the core protein, and HS is then washed away from the tissue section). This situation may be analogous to that of heparin in mast cells. In mast cells heparin is not bound to a core protein (it is cleaved off by an endogenous endoglucuronidase) and also cannot be washed out after treatment with heparinase I, probably because of a tight binding of heparin (fragments) to positively charged molecules (histamine, proteases). Also, 3-*O*-sulfation of glucosamine residues inhibits cleavage of heparin at that site²¹, and heparin with a high degree of 3-*O*-sulfation may be more resistant to heparinase I digestion compared with heparin which is less 3-*O*-sulfated.

For antibody EV3C3, heparinase III abolished basement membrane staining but not staining at some regions in the alveolar wall. Heparinase I, however, abolished all staining. Heparinase III cleaves primarily at unsulfated hexuronic acid residues, especially if there are relatively few sulfate groups on the adjacent residues. In contrast, heparinase I prefers highly sulfated regions including sulfated iduronic acid residues. Therefore, we suggest that EV3C3 recognizes highly sulfated regions in

HS. Possibly, although speculative, free EV3C3-positive HS, not bound to a core protein, stick to positively charged areas in the alveolar wall and can only be removed by more extensive digestion by heparinase I.

Our results implicate that in human lung at least seven different HS epitopes are present. Already in the early seventies it was recognized that pulmonary HS are exceptionally diverse with respect to sulfation²²⁻²⁴. The biosynthesis of HS allows for a large number of different epitopes. First a precursor polysaccharide is formed, which is subsequently subjected to a number of modifications²⁵. Regions where the precursor molecule is not modified consist of D-glucuronic acid-*N*-acetyl-glucosamine (GlcA-GlcNAc) repeats and are known as *N*-acetylated (NA) domains. These act as spacers between the highly modified and sulfated domains (S-domains). In these S-domains, extensive modifications occur, especially additions of sulfate groups and epimerisation of GlcA to IdoA. The bifunctional enzyme *N*-deacetylase/*N*-sulfotransferase (NDST) catalyzes the first modification. Mice deficient in NDST-1, but not -2, die shortly after birth due to respiratory failure caused by immaturity of type II pneumocytes which results in insufficient production of surfactant⁹⁻¹⁰. This indicates that NDST-1, but not 2, is essential for the maturation of type II pneumocytes, and implies the importance of specific sulfate patterns in HS. NDST-1 deficient mice have undersulfated HS in which *N*-sulfation and 2-*O*-sulfation are reduced, but in which 6-*O*-sulfation is normal⁹.²⁶ The antibodies identified in this study recognize specific sulfation patterns and may be valuable tools to study HS sac-

charides in health and disease.

A well recognized feature of HS/heparin is the binding of growth factors. FGF-2 could (partially) prevent three (out of seven) antibodies to bind to HS. This suggests that a number of antibodies are not recognizing domains in HS/heparin involved in binding FGF-2/VEGF. The three antibodies that were blocked cover the sites to which FGF-2 binds in sections. Interestingly, these three antibodies are the only ones reactive with mast cells (see Table 3). In case of VEGF, only antibody EV3A1 could be partially inhibited by VEGF from binding to heparin, and this antibody did not completely cover the structures reactive with exogenously applied VEGF. The binding of growth factors to immobilized HS in ELISA may be quite weak. It should be noticed that in tissue, HS chains are clustered on a core protein in a way that is probably not possible in microtiter plates. In tissue, therefore, a multivalency effect may be expected which results in a stronger binding of growth factors compared to that seen in ELISA. In this respect it is notable that for example for glypican-1 (a HS-proteoglycan) a K_d of 0.12nM has been found for VEGF₁₆₅, which is considerably lower than what is generally found for HS²⁷.

The staining patterns of the antibodies raise curiosity about the function of the distinct HS epitopes involved in human lung. Antibody EV3A1 showed a quite different staining pattern compared with the other antibodies as it reacted strongly with macrophages. Frevort and coworkers²⁸ showed positive staining for HS on the cell surface of alveolar macrophages. Macrophages are distributed throughout connective tissues and participate in both defense- and injury-related processes²⁹.

They are thought to play a central role in the fibroproliferative response, and studies indicate that they produce FGF-2³⁰ and generate an abundant amount of VEGF³¹. Interestingly, EV3A1 was the only antibody that could compete with VEGF for HS. In lung the role of VEGF, which is bound by HS, has recently attracted much attention. In rats, a blockade of the VEGF receptor results in lung alveolar cell apoptosis and emphysema^{32,33}. In humans, lung tissue from patients with emphysema contains less VEGF compared with controls. Also, lower levels of VEGF in sputum correlate well with lower FEV₁ and DL_{co} levels³⁴.

Proteoglycans and GAGs may have a specific role in the pathogenesis of pulmonary diseases. Next to binding and modulation of growth factors/cytokines, GAGs (especially HS) can function as strong inhibitors of neutrophil elastase³⁵⁻³⁷, and may thus influence the protease/antiprotease balance. Alterations in HS would have consequences for the protective HSPG barrier of the alveolus⁷. In the urine of patients with emphysema, a decreased content of the HS epitope JM403 was found together with a normal content of HS³⁸, suggesting a structural alteration in or an altered processing of HS molecules in the lungs of emphysematous patients. Studies on chemically and enzymatically modified HS indicate that the JM403 epitope contains one or more *N*-unsubstituted glucosamine and D-glucuronic acid units, and is located in a region of the HS chain composed of mixed *N*-sulfated and *N*-acetylated disaccharide units³⁹. This is an example of a structural alteration in HS associated with a pulmonary disease. The availability of seven HS epitope-specific antibodies further allows to identify changes in the

fine structure of HS associated with pulmonary conditions.

In conclusion, using phage display technology seven antibodies were selected against HS from human lung. Antibodies recognize different epitopes and some of them compete with growth factor for binding to HS. The binding of bFGF and VEGF to the alveolar matrix of human lung is likely to be mediated via HS. The availability of anti-lung HS antibodies and their encoding DNAs may provide valuable tools to study more accurately alterations in HS in health and disease.

Acknowledgements

The authors express their gratitude to Dr. G. Winter (Cambridge University, Cambridge, United Kingdom) for providing the phage display library. They thank Dr. J.M.H. Raats (Department of Biochemistry, Faculty of Sciences, Nijmegen, The Netherlands) for providing the pUC119 His VSV vector, and IBEX Technologies (Montreal, QC, Canada) for providing recombinant heparinase III derived from *Flavobacterium heparinum*. This work was financially supported by the Netherlands Asthma Foundation (Grants to A.R. and E.V., NAF project 95.44) and the Dutch Cancer Society (Grant to E.W. project KUN 98-1801).

References

1. Stringer, S. E. & Gallagher, J. T. Heparan sulphate. *Int J Biochem Cell Biol* 29, 709-14. (1997).
2. Lindahl, U., Kusche-Gullberg, M. & Kjellen, L. Regulated diversity of heparan sulfate. *J Biol Chem* 273, 24979-82. (1998).
3. Lindahl, U. [The great Scandinavian Jahre Prize 1993. What is the function of heparan sulfate?]. *Nord Med* 109, 4-8 (1994).
4. Bernfield, M. et al. Functions of cell surface heparan sulfate proteoglycans. *Annu Rev Biochem* 68, 729-77 (1999).
5. Gallagher, J. T. Heparan sulfate: growth control with a restricted sequence menu. *J Clin Invest* 108, 357-61 (2001).
6. Li, D., Clark, C. C. & Myers, J. C. Basement membrane zone type XV collagen is a disulfide-bonded chondroitin sulfate proteoglycan in human tissues and cultured cells. *J Biol Chem* 275, 22339-47 (2000).
7. van Kuppevelt, T. H. et al. Ultrastructural localization and characterization of proteoglycans in human lung alveoli. *Eur J Cell Biol* 36, 74-80. (1985).
8. Wang, Y., Sakamoto, K., Khosla, J. & Sannes, P. L. Detection of chondroitin sulfates and decorin in developing fetal and neonatal rat lung. *Am J Physiol Lung Cell Mol Physiol* 282, L484-90 (2002).
9. Ringvall, M. et al. Defective heparan sulfate biosynthesis and neonatal lethality in mice lacking N-deacetylase/N-sulfotransferase-1. *J Biol Chem* 275, 25926-30. (2000).
10. Fan, G. et al. Targeted disruption of NDST-1 gene leads to pulmonary hypoplasia and neonatal respiratory distress in mice. *FEBS Lett* 467, 7-11 (2000).
11. Sannes, P. L., Khosla, J. & Cheng, P. W. Sulfation of extracellular matrices modifies responses of alveolar type II cells to fibroblast growth factors. *Am J Physiol* 271, L688-97 (1996).
12. van Kuppevelt, T. H., Cremers, F. P., Domen, J. G. & Kuyper, C. M. Staining of proteoglycans in mouse lung alveoli. II. Characterization of the Cuprolinic blue-positive, anionic sites. *Histochem J* 16, 671-86 (1984).
13. Sannes, P. L. Differences in basement membrane-associated microdomains of type I and type II pneumocytes in the rat and rabbit lung. *J Histochem Cytochem* 32, 827-33 (1984).
14. Li, Q., Park, P. W., Wilson, C. L. & Parks, W. C. Matrilysin shedding of syndecan-1 regulates chemokine mobilization and transepithelial efflux of neutrophils in acute lung injury. *Cell* 111, 635-46 (2002).
15. Dennissen, M. A. et al. Large, tissue-regulated domain diversity of heparan sulfates demonstrated by phage display antibodies. *J Biol Chem* 277, 10982-6 (2002).
16. Jenniskens, G. J., Oosterhof, A., Brandwijk, R., Veerkamp, J. H. & van Kuppevelt, T. H. Heparan sulfate heterogeneity in skeletal muscle basal lamina: demonstration by phage display-derived antibodies. *J Neurosci* 20, 4099-111. (2000).
17. Winter, G. & Milstein, C. Man-made antibodies. *Nature* 349, 293-9. (1991).
18. van de Lest, C. H., Versteeg, E. M., Veerkamp, J. H. & van Kuppevelt, T. H. Quantification and characterization of glycosaminoglycans at the nanogram level by a combined azure A-silver staining in agarose gels. *Anal Biochem* 221, 356-61. (1994).
19. Pieper, J. S. et al. Loading of collagen-heparan sulfate matrices with bFGF promotes angiogenesis and tissue generation in rats. *J Biomed Mater Res* 62, 185-94 (2002).
20. Cardin, A. D. & Weintraub, H. J. Molecular modeling of protein-glycosaminoglycan interactions. *Arteriosclerosis* 9, 21-32 (1989).
21. Ernst, S., Langer, R., Cooney, C. L. & Sasisekharan, R. Enzymatic degradation of glycosaminoglycans. *Crit Rev Biochem Mol Biol* 30, 387-444 (1995).
22. Linker, A. & Hovingh, P. The heparitin sulfates (heparan sulfates). *Carbohydr Res* 29, 41-62 (1973).

23. Radhakrishnamurthy, B., Jeansonne, N. E. & Berenson, G. S. Heterogeneity of heparan sulfate chains in a proteoglycan from bovine lung. *Biochim Biophys Acta* 802, 314-20 (1984).
24. Linker, A. & Hovingh, P. Structural studies of heparitin sulfates. *Biochim Biophys Acta* 385, 324-33 (1975).
25. Salmivirta, M., Lidholt, K. & Lindahl, U. Heparan sulfate: a piece of information. *Faseb J* 10, 1270-9 (1996).
26. Jenniskens, G. J. et al. Disturbed Ca²⁺ kinetics in N-deacetylase/N-sulfotransferase-1 defective myotubes. *J Cell Sci* 116, 2187-93 (2003).
27. Ali, S., Hardy, L. A. & Kirby, J. A. Transplant immunobiology: a crucial role for heparan sulfate glycosaminoglycans? *Transplantation* 75, 1773-82 (2003).
28. Frevert, C. W. et al. Binding of interleukin-8 to heparan sulfate and chondroitin sulfate in lung tissue. *Am J Respir Cell Mol Biol* 28, 464-72 (2003).
29. Sibille, Y. & Reynolds, H. Y. Macrophages and polymorphonuclear neutrophils in lung defense and injury. *Am Rev Respir Dis* 141, 471-501 (1990).
30. Henke, C. et al. Macrophage production of basic fibroblast growth factor in the fibroproliferative disorder of alveolar fibrosis after lung injury. *Am J Pathol* 143, 1189-99 (1993).
31. Tuder, R. M., Petrache, I., Elias, J. A., Voelkel, N. F. & Henson, P. M. Apoptosis and emphysema: the missing link. *Am J Respir Cell Mol Biol* 28, 551-4 (2003).
32. Kasahara, Y. et al. Endothelial cell death and decreased expression of vascular endothelial growth factor and vascular endothelial growth factor receptor 2 in emphysema. *Am J Respir Crit Care Med* 163, 737-44. (2001).
33. Kasahara, Y. et al. Inhibition of VEGF receptors causes lung cell apoptosis and emphysema. *J Clin Invest* 106, 1311-9. (2000).
34. Kanazawa, H., Asai, K., Hirata, K. & Yoshikawa, J. Possible effects of vascular endothelial growth factor in the pathogenesis of chronic obstructive pulmonary disease. *Am J Med* 114, 354-8 (2003).
35. Walsh, R. L., Dillon, T. J., Scicchitano, R. & McLennan, G. Heparin and heparan sulphate are inhibitors of human leucocyte elastase. *Clin Sci (Lond)* 81, 341-6 (1991).
36. Rao, N. V., Kennedy, T. P., Rao, G., Ky, N. & Hoidal, J. R. Sulfated polysaccharides prevent human leukocyte elastase-induced acute lung injury and emphysema in hamsters. *Am Rev Respir Dis* 142, 407-12 (1990).
37. Brown, G. M., Brown, D. M. & Donaldson, K. Inflammatory response to particles in the rat lung: secretion of acid and neutral proteinases by bronchoalveolar leucocytes. *Ann Occup Hyg* 35, 389-96 (1991).
38. van de Lest, C. H. et al. Altered composition of urinary heparan sulfate in patients with COPD. *Am J Respir Crit Care Med* 154, 952-8. (1996).
39. van den Born, J. et al. Presence of N-unsubstituted glucosamine units in native heparan sulfate revealed by a monoclonal antibody. *J Biol Chem* 270, 31303-9 (1995).
40. Tomlinson, I. M., Walter, G., Marks, J. D., Llewelyn, M. B. & Winter, G. The repertoire of human germline VH sequences reveals about fifty groups of VH segments with different hypervariable loops. *J Mol Biol* 227, 776-98. (1992).



Chapter 4

Submitted

A rare, highly sulfated heparan sulfate sequence (GlcNS6S-IdoA2S)₃ has a strict topography and is involved in cell behavior.

Nicole C. Smits •

Sindhulakshmi Kurup ••

Gerdy B. Ten Dam •

Theo Hafmans •

Jeremy E. Turnbull •••

Dorothe Spillmann ••

Jin-ping Li ••

Richard P.N. Dekhuijzen ••••

Toin H. van Kuppevelt •

- *Department of Biochemistry, Radboud University Nijmegen Medical Centre, NCMLS, Nijmegen, The Netherlands*
- *Department of Medical Biochemistry and Microbiology, Biomedical Center, Uppsala University, Uppsala, Sweden*
- *School of Biological Sciences at University of Liverpool, Liverpool L69 7ZB, UK*
- *Department of Pulmonary Diseases, Radboud University Nijmegen Medical Centre, Nijmegen, The Netherlands*

Heparan sulfate (HS) regulates the activity of various ligands and is involved in molecular recognition on the cell surface and in the extracellular matrix (ECM). Specific binding of HS to ligands depends on sulfation patterns of HS. Tissue and cellular location of specific HS domains have been suggested by immunohistochemistry. However, the location and function of specific HS saccharide sequences have not been reported. In this study, we selected a novel phage display-derived antibody and established the saccharide sequence of its epitope using a combination of biosynthetic HS oligosaccharide libraries, tissues from mice defective in HS biosynthetic enzymes, and a panel of chemically modified heparins. The HS sequence was $(\text{GlcNS6S-I doA2S})_3$ and this highly sulfated sequence was, next to heparin-containing mast cells, only present in a small subset of HS. Blocking this specific HS domain resulted in reduced cell proliferation and enhanced sensitivity to apoptosis, but had no effect on cell adhesion. This is the first time that immuno-blockage reveals the cellular importance of a specific HS sequence.

Introduction

Heparan sulfate proteoglycans (HSPGs), major components of the cell surface and the ECM, are involved in a variety of biological phenomena, including cell adhesion, proliferation, and differentiation. Due to their high negative charge, HS chains interact with a variety of proteins, including growth factors/morphogens and their receptors, chemokines, and extracellular matrix proteins. HS-protein interactions vary with regard to specificity, and may depend on charge density in addition to strict sequence motifs of HS.

The interaction of heparin and HS with FGFs and their receptors (FGFR) has been characterized in great detail. Specific HS structures are predominantly determined by the regulated positioning of *N*-, 2-, 6-, and 3-*O*-sulfate groups along HS chains¹. For example, FGF-2 requires both *N*- and 2-*O*-sulfate groups for binding to HS. The 6-*O*-sulfate group is not essential for binding to FGF-2, but is critical for activation of the FGFR². In contrast, binding of hepatocyte growth factor, platelet-derived growth factor, lipoprotein lipase, and herpes simplex virus glycoprotein C to HS are

all dependent on 6-*O*-sulfation³. The activation of antithrombin III by HS/heparin is mediated by a specific pentasaccharide in which a 3-*O*-sulfate group is crucial. Thus, the biological functions of HSPGs are controlled by biosynthetic events that define HS structures.

Antibodies reactive with HS have been developed and have proven valuable tools to locate HS epitopes in cells and tissues⁴⁻⁸. From the phage display-derived anti-HS antibodies available, some chemical HS modifications crucial for antibody binding have been identified, however, the exact saccharide sequence(s) of the epitope remains elusive^{8,9}. This impedes the assignment of specific HS domains/sequences to cell biological phenomena.

Here, we report on the selection, characterization and application of a novel phage display-derived antibody, NS4F5. The antibody reacted with a specific stretch of highly sulfated GlcNS6S-I doA2S disaccharides, which was very restrictively located in tissues. To study the cell biological relevance of this HS domain, we used the antibody as blocking agent and showed that it is involved in

cell proliferation and apoptosis, but not in cell adhesion. Our study provides new insights into the function of a specific HS domain and shows that specific blockage of a saccharide sequence results in altered cellular behavior.

Experimental methods

ScFv antibodies

Periplasmic fractions of infected bacteria were isolated as described ⁴. Bacteria were grown and induced by IPTG to produce antibodies. Periplasmic fractions, containing antibodies, were isolated, dialyzed against PBS, and stored at -20°C .

Tissues and cells

Rats (Wistar, male, 8 weeks old) were obtained from the Central Animal Laboratory (RUNMC, Nijmegen, The Netherlands).

Hsepi^{+/-} and *Hsepi*^{-/-} mouse embryos (18.5 d.p.c.) were from Dr. J-p. Li (Uppsala, Sweden), *Hs2st*^{+/-} and *Hs2st*^{-/-} mouse embryos (18.5 d.p.c.) were from Dr. C. Merry (Manchester, UK). Human lung epithelial cells (A549; ATTC, Rockville, MD) were cultured in F-12K Nutrient Mixture (Kaighn's modification) (Gibco, Life Technologies, Inc., Grand Island, NY), supplemented with 10% FCS (PAA Laboratories GmbH, Pasching, Austria). CHO-K1 and CHO-*pgsF-17* cells were cultured in Ham's F-12 medium supplemented with 10% FCS.

Antibody treatment

Cells were incubated for 24 h after passage before further manipulation. Medium was removed and replaced with 1% FCS or containing antibodies (10 or 50 $\mu\text{g}/\text{ml}$) in medium with 1%

FCS. Cells were incubated 16 h for immunohistochemistry. As controls, cells were incubated with irrelevant antibody (MPB49) which is $> 95\%$ identical to most antibodies used, but does not bind any GAG.

Polysaccharides

For characteristics of polysaccharides, see Table 1.

Oligosaccharides

Specific activity of ³H-end-labeled products was $\sim 7.5 \times 10^6$ cpm/nmol. Heparin was chemically *O*-desulfated to eliminate all 6-*O*-sulfate and about half of the 2-*O*-sulfate groups, and was subjected to partial deaminative cleavage at low pH followed by end-labeling through reduction with NaB_3H_4 . ³H-end-labeled 8-mer ($\sim 1.4 \times 10^6$ cpm/nmol) was recovered and separated into subfractions with defined numbers of 2-*O*-sulfates. Subfractions were separately incubated with mastocytoma microsomal enzymes in the presence of (unlabeled) PAPS, primarily *de novo* attaching sulfate groups in 6-*O*-position.

Binding assays

Affinity chromatography was performed on columns with 1 mg antibody coupled to 0.5 mg Protein-A-beads in 50mM Tris/HCl, pH 7.4. Radiolabeled polysaccharide samples were eluted with a stepwise gradient of 0.15M - 2M NaCl in 50mM Tris/HCl, pH 7.4. Polysaccharide samples compared for antibody binding were applied in similar amounts, based on specific radioactivity determined by colorimetric analysis. Heparin oligosaccharides and oligosaccharide libraries were separated by affinity chromatography, as described ⁹.

Reactivity of antibodies with K5 polysaccharide derivatives and modified heparin preparations (Table 1) was evaluated by ELISA. Wells of microtiter plates (Greiner, Frickenhausen, Germany) were coated as described ⁵. After blocking with PBS containing 3% (wt/vol) BSA and 1% (vol/vol) Tween-20 for 1 h, anti-HS antibodies (in PBS containing 1% (wt/vol) BSA and 0.1% (vol/vol) Tween-20) were added for 1.5 h. As a control, antibody MPB49 was used. Bound antibodies were detected using mouse IgG anti-VSV tag antibody P5D4 (1:10; Boehringer Mannheim, Mannheim, Germany), followed by incubation with alkaline phosphatase-conjugated rabbit anti-mouse IgG (1:2000; Dako, Glostrup, Denmark), both for 1 h. Enzyme activity was detected using 100 μ l 1 mg *p*-nitrophenyl phosphate (ICN, Aurora, OH)/ml 1M diethanolamine

0.5mM MgCl₂ (pH 9.8) as a substrate. Absorbance was read at 405 nm.

Characterization of NS4F5 oligosaccharide epitopes

For sequencing of epitope motifs, selected library octasaccharides were affinity purified on an NS4F5 column. Binding and nonbinding fragments were separately pooled, desalted, dried, and sequenced ⁶. Samples were subjected to partial HNO₂ cleavage by 2mM NaNO₂ in 20mM HCl and stopped after different time points (0-60 min). Aliquots were pooled, and a fraction of the pool analyzed by anion-exchange chromatography directly while a fraction was subjected to enzymatic digestion with recombinant IdoA2S-sulfatase. Digests were analyzed on a Propac column and sequence information was obtained by detecting shifts in the elution positions

Table 1: Characteristics of K5 polysaccharide derivatives and modified heparin

Test molecule	Characteristics	Source
K5	(GlcNAc-GlcA) ₂₀	Glycores (Milano, Italy)
NdAcNS K5	<i>N</i> -deacetylated/ <i>N</i> -sulfated K5 ²⁰	Glycores (Milano, Italy)
epiNdAcNS K5	epimerized <i>N</i> -deacetylated/ <i>N</i> -sulfated K5	Glycores (Milano, Italy)
OS K5 (low)	low <i>O</i> -sulfated K5: 90% GlcNAc6OS, 10% GlcNAc ²⁰	Glycores (Milano, Italy)
NdAcNS/OS K5 (low)	<i>N</i> -deacetylated/ <i>N</i> -sulfated/low <i>O</i> -sulfated K5: 90% GlcNS6OS, 10% GlcNS ²⁰	Glycores (Milano, Italy)
NdAcNS/OS K5 (high)	<i>N</i> -deacetylated/ <i>N</i> -sulfated/high <i>O</i> -sulfated K5: 100% GlcNS6OS; 70% GlcA2,3OS, 30% GlcA2OS or GlcA3OS ²⁰	Glycores (Milano, Italy)
heparin	11.3% NAc, 88.7% NS, 69% 2OS, 79% 6OS	G. Ronzoni Institute (Milan, Italy)
CdSNAc heparin	completely desulfated/ <i>N</i> -acetylated heparin	Seikagaku (Tokyo, Japan)
CdSNS heparin	completely desulfated/ <i>N</i> -sulfated heparin	Seikagaku (Tokyo, Japan)
NdSNAc heparin	<i>N</i> -desulfated/ <i>N</i> -acetylated heparin: 100% NAc, 0% NS, 69% 2OS, 79% 6OS	G. Ronzoni Institute (Milan, Italy)
2OdS heparin	2- <i>O</i> -desulfated heparin: 13% NAc, 87% NS, 0% 2OS, 79% 6OS	G. Ronzoni Institute (Milan, Italy)
partially 6OdS heparin	6- <i>O</i> -desulfated heparin: 13% NAc, 87% NS, 67% 2OS, 23% 6OS	G. Ronzoni Institute (Milan, Italy)
OdS heparin	<i>O</i> -desulfated heparin	Neoparin (Alameda, CA)
carboxyl-reduced heparin	uronic acid COOH-reduced heparin	Neoparin (Alameda, CA)
HS		Celsus (Cincinnati, OH)

K5 is the non-sulfated precursor polysaccharide of HS/heparin derived from *E. coli*; the modified heparin preparations and HS are from porcine intestinal mucosa. HS, heparan sulfate; (Glc)NAc, *N*-acetyl(glucosamine); (Glc)NS, *N*-sulfated(glucosamine); GlcA, D-glucuronic acid; IdoA, L-iduronic acid; OS, *O*-sulfate.

of the enzyme-treated fragments.

Immunohistochemistry

Sections (4 μm) were air-dried and blocked with PBS containing 2% (wt/vol) BSA and 0.05% (vol/vol) Tween-20 (blocking buffer) for 20 min. Sections were incubated with anti-HS antibodies in blocking buffer for 1 h. As a control, antibody MPB49 was used. Bound antibodies were detected by incubation with mouse anti-VSV tag antibody P5D4 (1:10), followed by Alexa 488-conjugated goat anti-mouse IgG (1:200; Molecular Probes, Eugene, OR), both for 45 min. After each incubation, sections were washed three times 5 min with PBS containing 0.1% (vol/vol) Tween-20. Sections were fixed in 100% (vol/vol) ethanol for 10 s, air-dried, and embedded in 10% (wt/vol) Mowiol.

To evaluate antibody specificity, sections were digested with the glycosidases heparin lyase III (digests HS) 0.04 IU/ml in 50mM NaAc/50mM Ca(Ac)₂, pH 7.0 or chondroitinase ABC (digests CS and dermatan sulfate) 0.02 U/ml in 25mM Tris-HCl, pH 8.0, (2 h at 37°C, refreshing the enzyme after 1 h). As a control, sections were incubated in reaction buffer without enzyme. After washing three times with PBS and blocking for 30 min, sections were incubated with anti-HS antibodies and processed for immunohistochemistry as above. The efficiency of heparin lyase III-, and chondroitinase ABC-treatment was evaluated by incubation of sections with antibodies against GAG-‘stubs’ generated by the glycosidases. For HS stubs the antibody 3G10 (Seikagaku, Tokyo, Japan) was used. For CS stubs the antibody 2B6 (Seikagaku, Tokyo, Japan) was used. All tests were performed at

least three times. Sections were examined using a Leica CTR6000 microscope.

Immuno-electron microscopy

Tissue was fixed for 3 h in Somogyi solution containing 4% (vol/vol) formaldehyde and 0.05% (vol/vol) glutaraldehyde in 0.1M phosphate buffer (PB). Sections (200 μm) were cut and incubated in increasing amounts of glycerol (10-20-30%) in PB for 30 min. Sections were oriented on Thermanox (LAB-TEK DVI., Miles Laboratories Inc., Naperville) and frozen in liquid propane. Freeze substitution was performed as described ⁷. Ultra-thin low-cryl HM20 resin sections were cut on a Reichert Ultracut-E and mounted on one-hole nickel grids coated with a formvar film. Sections were pre-incubated in PBS containing 0.2% BSA and 0.05% cold fish skin gelatin (PBG). Sections were incubated overnight at 4°C in drops of PBG containing antibodies and washed for 20 min in PBG. Bound antibodies were visualized using anti-VSV tag antibody P5D4 and goat anti-mouse IgG labeled with gold spheres (10 nm, Aurion, Wageningen, Netherlands). Sections were washed in PBS and post-fixed with 2.5% (vol/vol) glutaraldehyde in PBS for 5 min. After washing with distilled water, sections were contrasted with uranyl acetate and studied using a Jeol TEM 1010 electron microscope.

Cell proliferation assay

Human lung epithelial cells were incubated at 37°C with or without purified scFv antibodies. Incubation was for 4 days in a humidified atmosphere. Cell proliferation was assessed by measuring the mitochondrial dehydrogenase activity using the tetrazolium salt 4-[3-(4-iodo-

phenyl)-2-(4-nitrophenyl)-2H-5-tetrazolo]-1,3-benzene disulphonate (WST-1) (Boehringer Mannheim, Germany), according to the manufacturer's protocol.

Adhesion assay

Flatbottom 96-well plates (Greiner, Frickenhausen, Germany) were coated with 100 μ l of type I collagen (Symatase, Chaponost, France) for 60 min and washed three times with PBS. Cells were labeled with Calcein-AM (Molecular Probes, Eugene, OR) in PBS for 30 min at 37°C in the dark while shaking. Labeled cells were incubated with scFv antibodies (50 μ g/ml) in medium supplemented with 1% FCS for 30 min and allowed to adhere for 45 min. Non-adherent cells were removed. Attached cells were lysed and fluorescence was quantified in a cytofluorometer (Perseptive Biosystems). Adhesion was expressed as the mean percentage (\pm SD) of bound cells from four wells relative to untreated cells.

Detection of apoptosis in human lung epithelial cells after treatment with scFv antibodies

Cells were treated with scFv antibodies (50 μ g/ml) for 16 h, washed with PBS, fixed in ice cold methanol for 10 min, washed three times with PBS, and blocked with blockingbuffer for 10 min. Permeabilization and TUNEL labeling were performed according to the manufacturer's instructions (In Situ Cell Death Detection kit; Roche), and cells were incubated with DAPI 0.5 μ g/ml for 1 min. Cells were washed with PBS, rinsed with ice cold methanol, air dried and embedded in Mowiol.

In addition to the TUNEL assay, apoptosis

was detected using an M30 CytoDEATH antibody that detects a caspase cleavage site in cytokeratin 18 (CK-18) and labels apoptotic epithelial cells instead of viable or necrotic cells⁸. To detect caspase cleavage, cells were treated with scFv antibodies (50 μ g/ml) for 16 h. After blocking, cells were incubated with M30 antibody for 1 h. Cells were washed with PBS and incubated with goat anti-mouse IgG Alexa 488 for 1 h. Cells were washed with PBS and incubated with 0.5 μ g/ml DAPI. Cells were washed with PBS, air-dried, fixed with ice cold methanol and embedded with Mowiol.

Statistical analysis

Four independent experiments were subjected to statistical analysis. Results were expressed as mean \pm SD. Data were analyzed using Student's t-test, as appropriate. $P < 0.05$ was considered significant for all tests.

Results

Selection of scFv antibody NS4F5

Four rounds of panning were performed against glycosaminoglycans (GAGs) isolated from human lung tissue, using the semi-synthetic scFv library no.1⁹. Panning resulted in an increase of phage titer from 3×10^4 colony-forming units in the first round to 2×10^8 colony-forming units in the fourth round. Supernatants containing antibodies of clones obtained after the third and fourth selection were initially tested for reactivity with various GAGs. Of the clones reactive with heparin/HS, one clone produced an antibody (NS4F5) with a very selective reactivity towards (modified) heparin preparations and a restrictive staining pattern (see below). Therefore, this antibody was selected for further analysis.

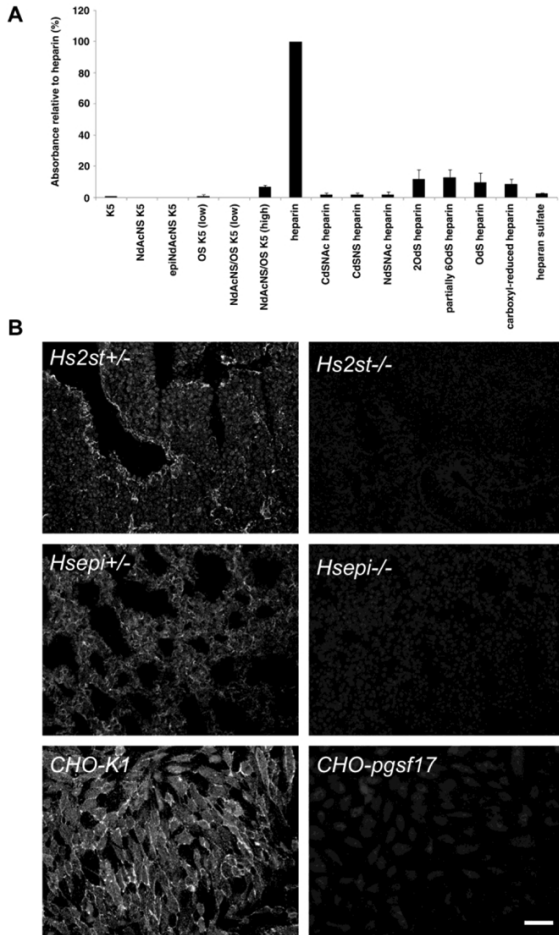


Figure 1. Characterization of the NS4F5 epitope by ELISA and immunohistochemistry. (A) ELISA.

Antibody NS4F5 was applied to various immobilized GAG preparations. Bound antibodies were detected using mouse anti-VSV-tag IgG antibody P5D4, followed by alkaline phosphatase-conjugated rabbit anti-mouse IgG. Enzymatic activity was measured using *p*-nitrophenyl phosphate as a substrate. Bars represent the mean reactivity \pm SD ($n = 4$) of the antibodies in percent relative to the reactivity with heparin. (B) Immunohistochemistry. Cryosections of heterozygous and homozygous knockout embryos deficient for 2-*O*-sulfo-transferase (*Hs2st*^{-/-}, *Hs2st*^{-/-}), and C5-epimerase (*Hsepi*^{-/-}, *Hsepi*^{-/-}) were stained with antibody NS4F5. Bound antibodies were detected using mouse anti-VSV-tag IgG antibody P5D4, followed by Alexa 488-conjugated goat anti-rabbit IgG. CHO K1 (wild type) and *pgsF-17* (*Hs2st*^{-/-}) cells were also used. Scale bar, 50 μ m.

Antibody NS4F5 belongs to the V_H3 family, has a DP53 germline gene segment, and contains a heavy chain complementarity-determining region 3 amino acid sequence of SGRKGRMR.

Characterization of the HS epitope defined by antibody NS4F5

The NS4F5 epitope has a requirement for N-, 2-O- and 6-O-sulfation and epimerization To identify the epitope defined by antibody NS4F5 and characterize its structure in detail different approaches were taken.

Initially, a large set of (modified) heparin and *E. coli* cell wall polysaccharide K5 and other GAG preparations was analyzed for their reactivity with the antibody. NS4F5 reacted strongly with heparin (Figure 1A), but not with other classes of GAGs including HS, chondroitin sulfate, dermatan sulfate, and hyaluronate (not shown). *N*-sulfation was an essential modification since *N*-desulfated heparin did not react with the antibody. In addition, 2-*O*- and 6-*O*-sulfation were crucial because 2-*O*-desulfated, as well

as partially 6-*O*-desulfated heparin were not reactive. Epimerization was also an essential modification since none of the K5 preparations tested (the *E. coli* K5 cell wall polysaccharide is the non-sulfated, non-epimerized precursor polysaccharide of heparin/HS) was reactive, including highly *N*- and *O*-sulfated K5. To substantiate the data obtained by ELISA, immunohistochemistry was performed using embryonic tissues from mice defective in heparin/HS biosynthetic enzymes (Figure 1B). Antibody NS4F5 did not stain tissues from mice lacking, 2-*O*-sulfotransferase [*Hs2st*^{-/-}] ¹⁰, or epimerase [*Hsepi*^{-/-}] ¹¹, further indicating that 2-*O*-sulfation and epimerization are essential modifications. In addition, a cell line lacking 2-*O*-sulfotransferase [CHO *pgsf*-17] ¹² was negative.

The NS4F5 epitope has a defined saccharide sequence: (GlcNS6S-IdoA2S)₃, To further define the epitope and establish its saccharide sequence we turned to heparin-derived oligosaccharide libraries (Figure 2). Using a library containing ³H-end-labeled heparin fragments ranging from 4-12 monosaccharides, it was established by immunoaffinity that the minimal length for binding was an 8-mer, and that longer oligosaccharides did not increase binding affinity (Figure 2A). The binding heparin 8-mer eluted as a homogeneous oligosaccharide from an anion exchange column (Figure 2B upper panel) in contrast to the non-bound fraction which contained a broad spectrum of less charged oligosaccharides (data not shown). Cleavage of the bound, end-labeled 8-mer by (partial) nitrous acid digestion at low pH (selective for *N*-sulfated residues) resulted in three additional fragments corresponding to end-

labeled di-, tetra-, and hexasaccharides. Comparison of the elution characteristics of these saccharides with those of standards with known sequences elucidated the saccharide sequence of the fragments and, by combination, the parent oligosaccharide. The disaccharide corresponded to IdoA2S-anManol6S (2-*O*-sulfated iduronic acid - 6-*O*-sulfated anhydromannitol; note that nitrous acid treatment and subsequent reduction converts the reducing *N*-sulfated glucosamine to an anhydromannitol). The tetrasaccharide corresponded to IdoA2S-GlcNS6S-IdoA2S-anManol6S (GlcNS6S = *N*- and 6-*O*-sulfated glucosamine), the hexasaccharide to IdoA2S-GlcNS6S-IdoA2S-GlcNS6S-IdoA2S-anManol6S, and the octasaccharide, i.e., the original octasaccharide bound by the antibody, to IdoA2S-GlcNS6S-IdoA2S-GlcNS6S-IdoA2S-GlcNS6S-IdoA2S-anManol6S. To substantiate these data, a biosynthetic heparin library was used, consisting of fully *N*-sulfated, epimerized octasaccharides with various numbers of 2-*O*- and/or 6-*O*-sulfation (Figure 2C). Only the highest sulfated octasaccharide present in the library, harboring three 2-*O*-sulfated iduronic acids and three *N*- and 6-*O*-sulfated glucosamines, was able to bind to the antibody (note that during the preparation of the library the glucosamine at the reducing end has been converted to an anhydromannitol which will not be 6-*O*-sulfated). Therefore, and given the notion that IdoA2S residues are clustered in the heparin octasaccharide library (unpublished observation), the binding octasaccharide had two monosaccharide-sequence possibilities: IdoA2S-GlcNS6S-IdoA2S-GlcNS6S-IdoA2S-GlcNS6S-IdoA-anManol and IdoA-GlcNS6S-IdoA2S-GlcNS6S-

IdoA2S-GlcNS6S-IdoA2S-anManol. The latter sequence is more likely since the library has been constructed by partial nitrous acid that preferentially cleaves at sites of non-sulfated iduronic acid residues (unpublished observation). Combined, data show that the epitope

defined by antibody NS4F5 contains three *N*-sulfates, three 2-*O*-sulfates and three 6-*O*-sulfate groups. Taken into account the data obtained from the oligosaccharide libraries it can be deduced that antibody NS4F5 defines the sequence (GlcNS6S-IdoA2S)₃, 3-*O*-

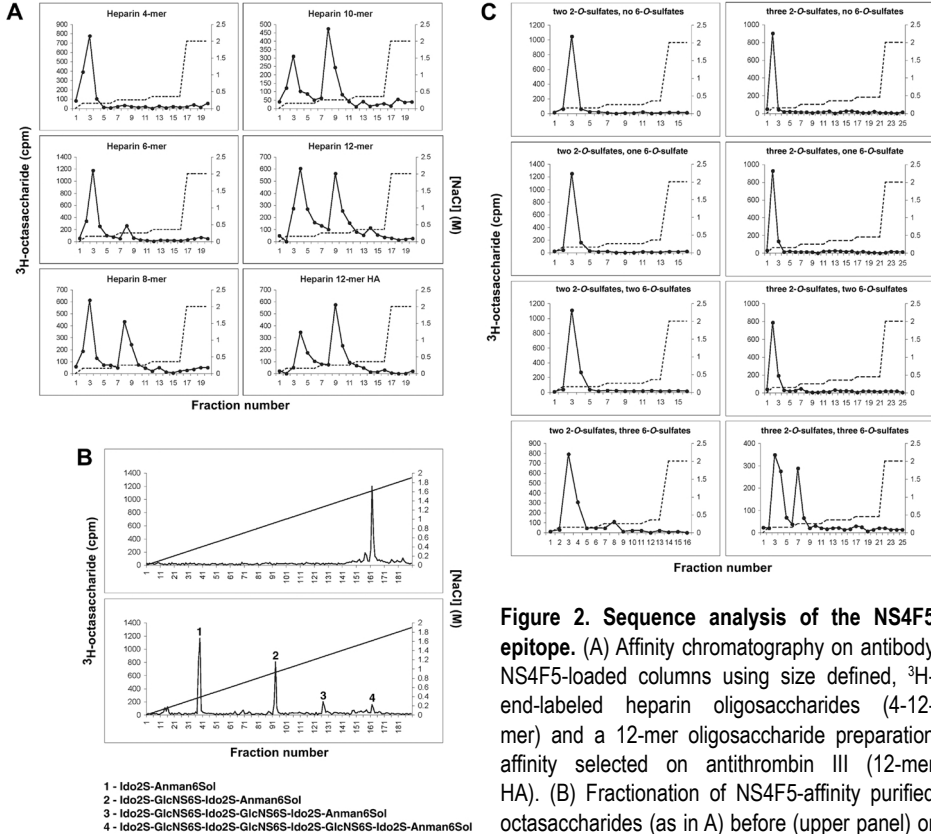


Figure 2. Sequence analysis of the NS4F5 epitope. (A) Affinity chromatography on antibody NS4F5-loaded columns using size defined, ³H-end-labeled heparin oligosaccharides (4-12-mer) and a 12-mer oligosaccharide preparation affinity selected on antithrombin III (12-mer HA). (B) Fractionation of NS4F5-affinity purified octasaccharides (as in A) before (upper panel) or after partial deaminative cleavage (lower panel) by anion-exchange HPLC on a Propac column, using a linear salt gradient for elution (---). (C) Reactivity of immobilized antibody NS4F5 with heparin-derived, ³H-end-labeled octasaccharide libraries with defined numbers of 2-*O*- and variable numbers of 6-*O*-sulfate groups using a stepwise increasing salt gradient as indicated (---). The left panel shows affinity separation of oligosaccharides with two 2-*O*-sulfate groups and zero, one, two, or three added 6-*O*-sulfate groups, respectively. The right panel displays corresponding patterns for octasaccharides containing three 2-*O*-sulfate groups. Note that only the highest sulfated octasaccharides harboring three 2-*O*-sulfated iduronic acids and three *N*- and 6-*O*-sulfated glucosamines are able to bind the antibody.

sulfation, a rare modification in heparin, is of no importance since 3-*O*-sulfate containing 12-mers (the antithrombin III high affinity fraction 'heparin 12-mer HA', Figure 2A) do not bind any better than oligosaccharides without this modification.

The NS4F5-defined sequence (GlcNS6S-IdoA2S)₃ is present in HS and has a restricted tissue distribution In rat renal tissue antibody NS4F5 only stains the medullary part and not the cortex (Figure 3). This is highly unusual since all anti-HS antibodies studied so far strongly reacted with the cortical region, which includes

the glomerulus^{4, 16, 17}. Treatment of renal sections with heparin lyase III, which removes HS from the tissue section, abolished staining indicating that the (GlcNS6S-IdoA2S)₃ sequence is present in HS, be it only in a subset of HS. To identify the renal tubules positive for antibody NS4F5, we performed colocalization studies with an antibody raised against aquaporin-1 (AQP-1), a marker for proximal tubules and descending thin limbs of the loops of Henle. Staining for the NS4F5 epitope was restricted to the descending thin limbs (Figure 3D, asterisk) and to small blood vessels (Figure 3D, arrows). In the

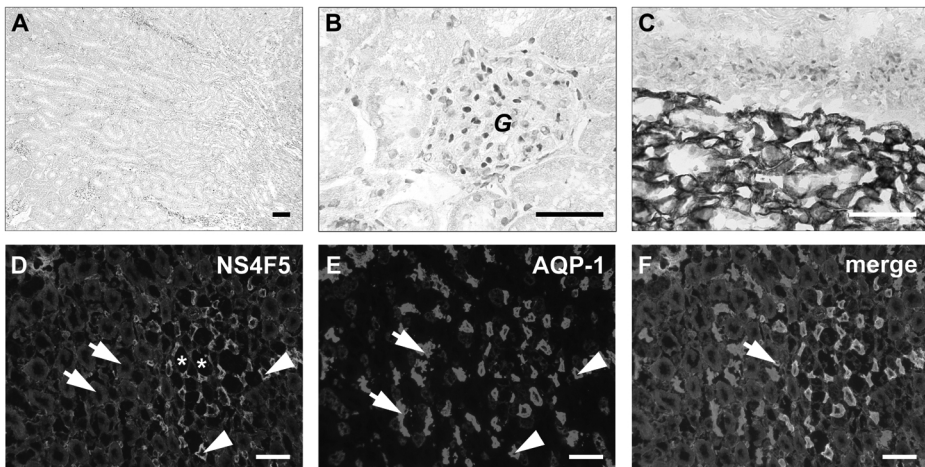


Figure 3. Restricted location of the antibody NS4F5-defined heparan sulfate domain in rat kidney. A, B Cortical area. C. Cortical-medullary area. D-F. Medullary area. D-F Identification of antibody NS4F5-reactive structures by colocalization. Medullary areas were incubated with antibody NS4F5 (D, green) and with an antibody against aquaporin-1 (E, AQP), a marker for descending thin limbs of the Loops of Henle and proximal tubules (red). F: overlay. Note that the specific HS domain is only present in descending thin limbs and some small blood vessels. Scale bars, 50 μ m.

G, Glomerulus

Asterisks in D, ascending thin limbs of the loops of Henle; arrows in D, ascending thick limbs of the loops of Henle; arrow heads in D, descending thin limbs of the loops of Henle

Arrows in E, proximal tubules; arrow heads in E, descending thin limbs of the loops of Henle

Arrow in F, small blood vessel

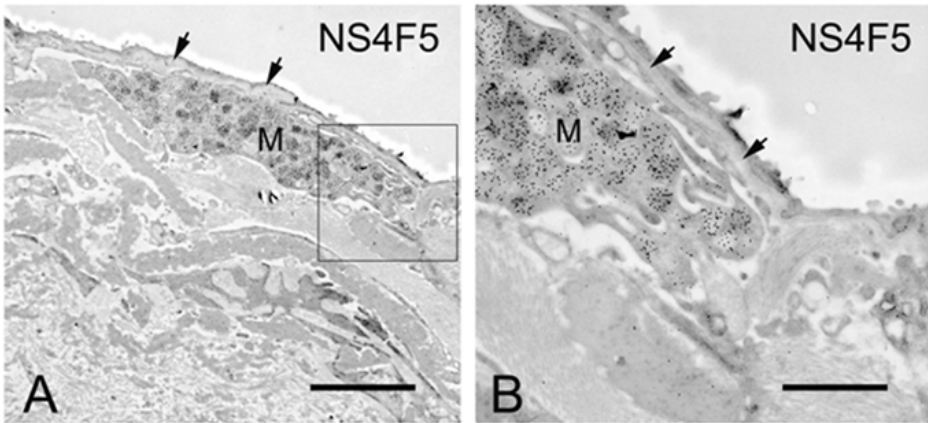


Figure 4. Immuno-electron microscopical localization of the antibody NS4F5 epitope in human lung. For experimental details, see text. Only heparin-containing granules in mast cells (M) are clearly positive. Note that basement membranes (arrows), a rich source of HS, are completely negative. Bar in A represents 15 μm ; bar in B, 5 μm .

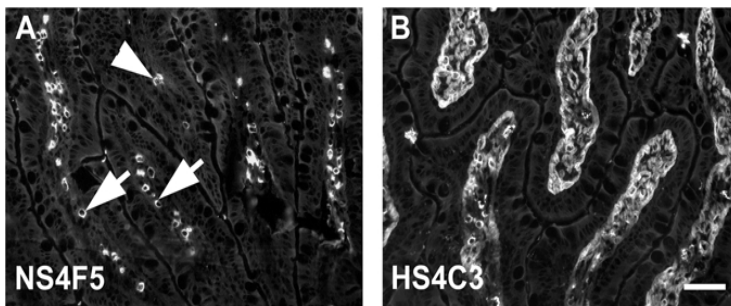


Figure 5. Immunolocalization of the epitope recognized by antibody NS4F5 in rat intestine. Cryosections of rat intestine were incubated with the NS4F5 antibody (A) or with anti-HS antibody HS4C3 (B). Bound antibodies were visualized by incubation with anti-VSV mouse monoclonal antibody P5D4, followed by Alexa 488-conjugated goat anti-mouse IgG. Capillaries of the villi are clearly positive (A, arrows), along with mast cells (A, arrow head) Basement membranes of epithelia were negative (compare with basement membrane staining using anti-HS antibody HS4C3). Scale bar, 50 μm .

descending thin limbs, water is passively absorbed from the tubular lumen and highly sulfated HS may play a role in this process since it will be osmotic active (by binding sodium ions), thereby providing the osmotic conditions associated with

water uptake. In the lung, only heparin-containing mast cells were positive (Figure 4, M), the staining being confined to the heparin-containing granules. Strikingly, basement membranes—a rich source of HS—were completely negative

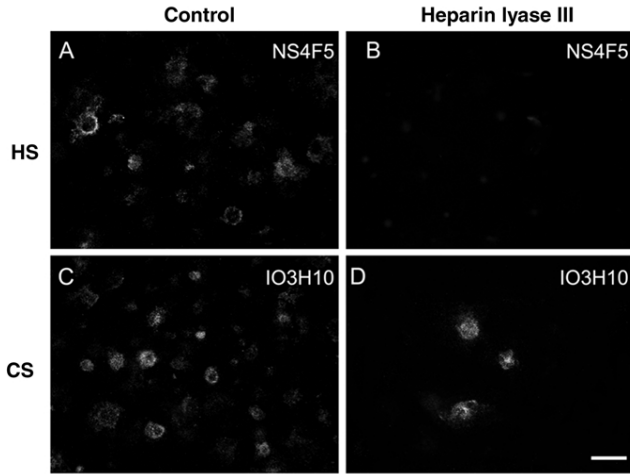


Figure 6. Expression of NS4F5 epitopes by human lung epithelial cells. Human lung epithelial cells were stained with antibody NS4F5 (A) or anti-CS antibody IO3H10 (C). Bound antibodies were detected using mouse monoclonal antibody P5D4 followed by Alexa 488-conjugated goat anti-rabbit IgG. Human lung epithelial cells produce NS4F5 epitopes (A) which can be removed by heparin lyase III-treatment (B),

indicating the epitope to be present in HS. Note that heparin lyase III-treatment had no effect on CS (C, D). Scale bar, 50 μ m.

(Figure 4, arrows). In the intestine, the capillaries of the villi were clearly positive, along with mast cells (Figure

5). The basement membrane of the epithelia was negative (compare with the staining of the basement membrane

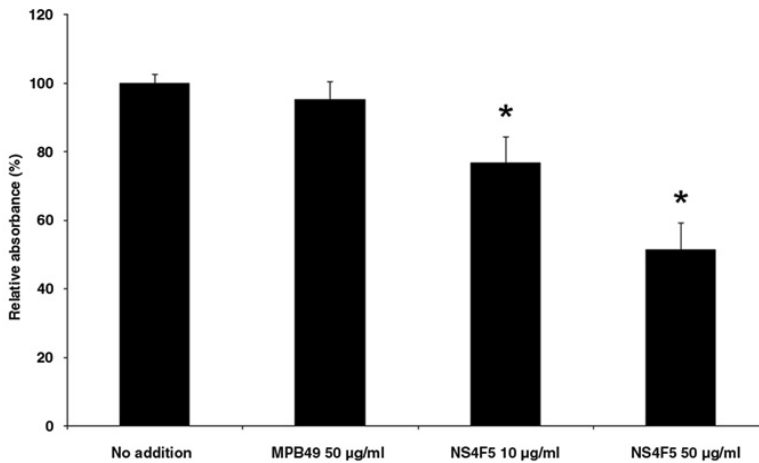


Figure 7. Immunoblocking using antibody NS4F5 antibody reduces cell proliferation. Human lung epithelial cells were incubated with or without the NS4F5 antibody (10 and 50 μ g/ml) for 16 h. Proliferation was measured at 450 nm using the WST-1 assay (see Experimental Methods). Values are expressed as means \pm SD, $n = 5$). Note that the effect of the NS4F5 antibody is dose dependent. As a control, cells were incubated with an irrelevant antibody MPB49. *, $P < 0.05$

using anti-HS antibody HS4C3). Combined, immunohistochemical data show that the specific NS4F5-defined HS do-

main is present in heparin (most cells) and a small subset of HS.

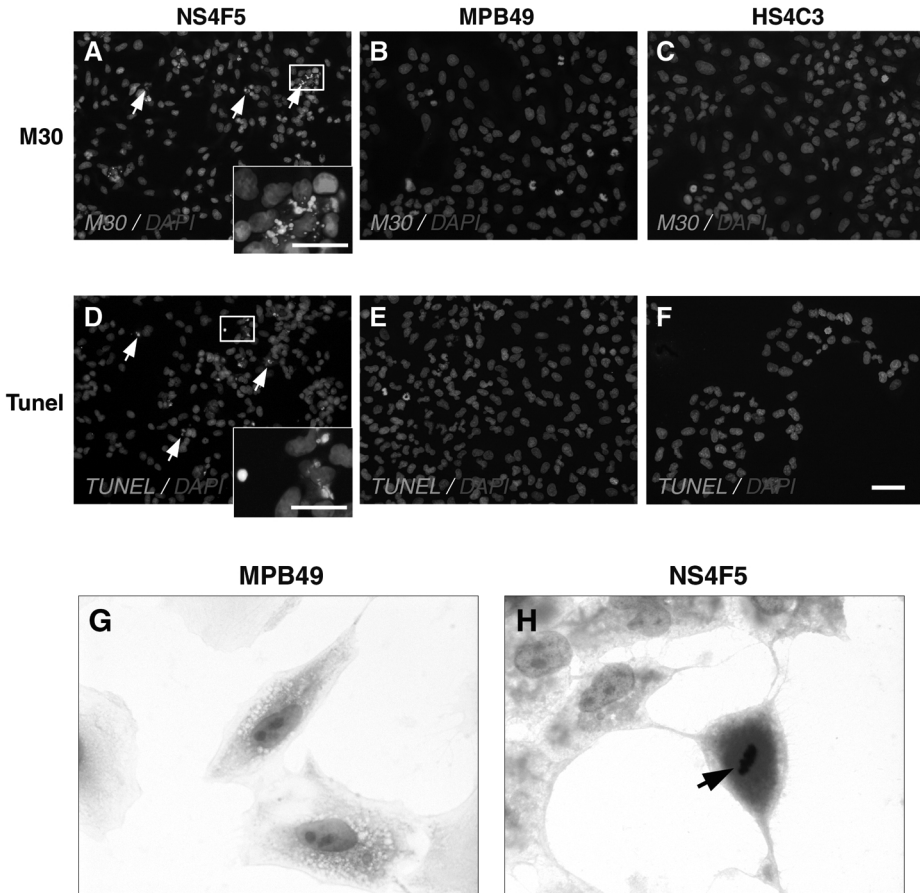


Figure 8. Immuno blocking using antibody NS4F5 induces morphologic changes consistent with apoptosis. Human lung epithelial cells were treated with purified NS4F5 (A, D), irrelevant antibody MPB49 (B, E) or anti-HS antibody HS4C3 (C, F). Cells were fixed and concomitantly stained with M30 antibody (A-C) which recognizes caspase-cleaved cytokeratin 18 (CK-18) in the cytoplasm of epithelial cells, or with TUNEL (D-F) which labels DNA strand breaks ('nicks') generated by apoptosis. DAPI was used to identify nuclei. The arrows in A identify caspase-cleaved CK-18 in the cytoplasm of epithelial cells, whereas arrows in D identify TUNEL positive cells. Cells treated with the control antibody show normal nuclei (G), whereas cells treated with antibody NS4F5 cells show nuclear condensation (H, arrow). Scale bar, 50 μ m.

Blocking of NS4F5 epitopes decreased cell proliferation and stimulated apoptosis but had no influence on cell adhesion

HSPGs have many roles in cell physiology¹³. To study the effect of blockage of the NS4F5 epitope on cellular behavior, human lung epithelial cells were used. These cells produce the NS4F5 epitope (Figure 6A), which can be removed by heparin lyase III-treatment (Figure 6B), indicating that the epitope is present in HS. Note that heparin lyase III has no effect on CS detected by an anti-CS antibody (Figure 6, C and D).

Dose dependent effect of antibody NS4F5 on cell proliferation

To study the effect of the NS4F5 epitope on cell proliferation, human lung epithelial cells were treated with purified NS4F5 antibody and the proliferation analyzed (Figure 7). Treatment of cells with 10 μg antibody/ml resulted in a reduced cell proliferation to $76.6\% \pm 7.7\%$. Treatment with 50 $\mu\text{g}/\text{ml}$ further reduced proliferation to $51.4\% \pm 7.8\%$. The irrelevant phage display-derived antibody MPB49¹⁴ had no effect on cell proliferation.

Effect of antibody NS4F5 on apoptosis

To determine whether the NS4F5 epitope plays a role in apoptosis, human lung epithelial cells were treated with purified NS4F5 antibody. As controls, the irrelevant antibody MPB49 and anti-HS antibody HS4CS, which has a different specificity than antibody NS4F5⁹ were used. After treatment with NS4F5, a number of cells were positive for immunostaining with antibody M30 (Figure 8A), which detects caspase-cleaved CK-18 and which is a marker for the process of apoptosis. Staining was

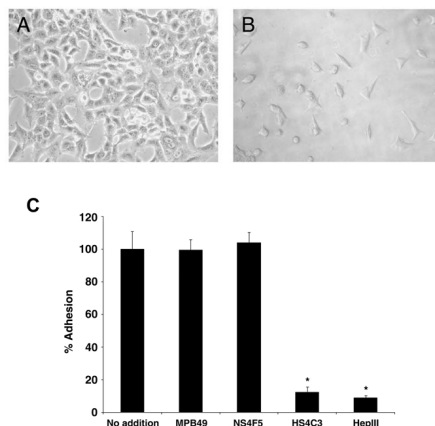


Figure 9. Immunoblocking using antibody NS4F5 has no effect on cell adhesion. Calcein-AM labeled human lung epithelial cells were incubated for 60 min with or without, purified antibody NS4F5, MPB49 or HS4C3 (50 $\mu\text{g}/\text{ml}$) or heparin lyase III (HepIII), and plated in wells pre-coated with type I collagen. After washing off non-adherent cells, phase contrast images of remaining adherent cells were taken (A, without heparin lyase III; B, with heparin lyase III), or cells were lysed and fluorescence was quantified using a cytofluorometer (C). Values are expressed as means \pm SD, $n = 5$). Note that adhesion is HS dependent, but that antibody NS4F5 has no effect on cell adhesion, in contrast to antibody HS4C3.

*, $P < 0.05$

observed in the cytoplasm and exhibited a discrete punctuate distribution (Figure 8A, arrows). In addition, nuclear condensation was observed (Figure 8H). NS4F5-treated cells were also positive for the TUNEL staining (Figure 8D), which detects 3'-OH DNA ends nuclei, further indicating that blockage with NS4F5 induced apoptosis. Cells treated with purified irrelevant antibody MPB49 (Figure 8, B and E), and with anti-HS antibody HS4C3 (Figure 8, C and F) did not show signs of apoptosis.

Effect of antibody NS4F5 on cell adhesion

To study the effect of NS4F5 epitopes on cellular adhesion, Calcein-AM-labeled human lung epithelial cells were treated without (Figure 9A) and with (Figure 9B) heparin lyase III or with purified NS4F5 antibody, and allowed to attach to type I collagen-coated wells. As controls, cells were incubated with purified irrelevant antibody MPB49 or with purified anti-HS antibody HS4C3. Digestion of HS by heparin lyase III decreased the number of adherent cells to $8.9 \pm 1.6\%$ (Figure 9C). Antibody HS4C3 had a similar effect ($12.3 \pm 3.4\%$). Antibody NS4F5, however, did not have any effect on cell adhesion. These data indicated that, although cell adhesion is HS dependent, the HS epitope recognized by antibody NS4F5 does not play a major role.

Discussion

In this study, we describe the selection, characterization and application of the novel phage display-derived anti-HS antibody NS4F5. This antibody defines a specific stretch of highly sulfated disaccharides (GlcNS6S-IdoA2S)₃, which is common in heparin¹⁵, but very rare in HS, and has a restrictively location in tissues. Antibody NS4F5 was used as a blocking agent to study the cell biological relevance of such a highly sulfated HS domain, and it was demonstrated that the defined HS sequence is involved in cell proliferation and apoptosis, but not in cell adhesion. These findings provide new insights into the function of a specific HS domain and strengthen the importance of HS sequences (or very high HS charge densities),¹⁶ in cellular behavior.

The chemical heterogeneity of HS, coupled with the lack of appropriate tools to study the fine structure of HS has

seriously limited the investigations into the roles of HS in cell biological phenomena. Using phage display technology, we have generated a large panel of epitope-specific antibodies against HS^{4, 5, 22-25}. Although these antibodies are unique in their preference for specific modification patterns on HS molecules (for example 2-*O*-sulfation, 6-*O*-sulfation, 3-*O*-sulfation and/or epimerization)^{4, 7, 8}, the exact saccharide sequence remains elusive. Antibody NS4F5 is the first antibody of which the epitope could be described in terms of a saccharide sequence. For this a number of tools were used including chemo-enzymatically prepared heparin oligosaccharide libraries, chemically modified heparin preparations and tissues from mice defective in HS biosynthetic enzymes. Knowing the specificity of antibody NS4F5 makes it a powerful tool to investigate the role of HS domains in cell biological phenomena.

HS-protein interactions have recently attracted much interest and it is now widely recognized that HS is a modulator of protein function¹³. HS-protein interactions vary with regard to specificity, and often seem to depend on specific HS domains, the degree of sulfation being of major importance^{1, 26}. For instance, the binding of both FGF-2 and VEGF depends on the sulfation state of HS, as does for instance the process of tumor cell proliferation^{27-29, 17}.

Blocking of HS domains recognized by antibody NS4F5 induced cell apoptosis and inhibited cell proliferation, but had no effect on cell attachment. Another anti-HS antibody (HS4C3), however, did affect cell attachment, but had no effect on the process of apoptosis. Clearly, different HS domains can mediate

different cellular responses. The cell biological function of the highly sulfated HS domain defined by the antibody is in line with previous work on the effect of sulfation on cellular behavior. HS 6-*O*-endosulfatase, an enzyme which removes 6-*O*-sulfate groups from (highly) sulfated HS domains, resulted in decreased proliferation and increased apoptosis of breast cancer cells³¹. Likewise, highly sulfated HS fragments, derived from a melanoma cell line and prepared by heparin lyase III digestion, decreased cell proliferation and increased apoptosis whereas low sulfated HS fragments, prepared by heparin lyase I had the opposite effect¹⁸. Finally, apoptosis was noticed in blood vessels of mice with a targeted deletion of the HS biosynthetic enzyme *N*-deacetylase/*N*-sulfotransferase 1 which results in a lower degree of HS sulfation³³. Thus, highly sulfated HS domains generally promote cell proliferation and inhibit apoptosis. This study pin-points these effects to a specific HS domain (IdoA2S-GlcNS6S)₃ defined by antibody NS4F5 and strongly suggests a role for (IdoA2S-GlcNS6S)₃ sequences in critically important pathways of cellular growth control. Such specific HS domains may be main targets for the development of novel therapeutic approaches. Some analogy may be drawn here with the drug fondaparinux, a synthetic heparin-based pentasaccharide that binds and activates anti-thrombin III, thereby reducing blood clot formation. The development of fondaparinux was based on the identification of the active domain within heparin responsible for its anticoagulant characteristics¹⁹. Our findings may be generalizable to pathologies that are de-

pendent on HS/heparin-mediated pathways and may have implications for the development of therapeutic interventions. Sequence analysis of other antibody-defined HS domains and analysis of their cell biological function, may thus provide a window to develop defined oligosaccharides with therapeutic potential.

Acknowledgements

Supported by grants from the International Human Frontier Science Program Organization (HFSP, grant RGP00-62/2004-C101), and the Swedish Foundation for Strategic Research (A303:156e), Swedish Research Council Grant 32X-15023, Swedish Cancer Society Grant 4708-B02-01XAA and Polysackaridforskning AB (Uppsala, Sweden).

The authors thank Dr. P. Oreste (Glycores, Milan, Italy) for modified K5 polysaccharides, Dr. A. Naggi (G. Ronzoni Institute for Chemical and Biochemical Research, Milan, Italy) for modified heparin preparations, Dr. J-p Li (Department of Medical Biochemistry and Microbiology, University of Uppsala, The Biomedical Center, Uppsala, Sweden) the *Hsepi*^{+/-} and *Hsepi*^{-/-} mouse embryos, Dr. C. Merry for the *Hs2st*^{+/-} and *Hs2st*^{-/-} mouse embryos, Dr. J. Esko for providing wild type and mutant CHO cells, Dr. J. Gallagher for providing modified heparin oligosaccharides, Dr. J.M.H. Raats for the pUC119 His-VSV vector and IBEX Technologies (Montreal, Canada) for providing recombinant heparin lyase III derived from *F. heparinum*. We thank P.H.K. Jap for his advice in the field of tissue morphology, and G. Pettersson for expert technical assistance.

References

1. Esko, J. D. & Selleck, S. B. Order out of chaos: assembly of ligand binding sites in heparan sulfate. *Annu Rev Biochem* 71, 435-71 (2002).
2. Nakato, H. & Kimata, K. Heparan sulfate fine structure and specificity of proteoglycan functions. *Biochim Biophys Acta* 1573, 312-8 (2002).
3. Lindahl, U., Kusche-Gullberg, M. & Kjellen, L. Regulated diversity of heparan sulfate. *J Biol Chem* 273, 24979-82. (1998).
4. Smits, N. C. et al. Heterogeneity of heparan sulfates in human lung. *Am J Respir Cell Mol Biol* 30, 166-73 (2004).
5. van Kuppevelt, T. H., Dennissen, M. A., van Venrooij, W. J., Hoet, R. M. & Veerkamp, J. H. Generation and application of type-specific anti-heparan sulfate antibodies using phage display technology. Further evidence for heparan sulfate heterogeneity in the kidney. *J Biol Chem* 273, 12960-6 (1998).
6. Kreuger, J., Salmivirta, M., Sturiale, L., Gimenez-Gallego, G. & Lindahl, U. Sequence analysis of heparan sulfate epitopes with graded affinities for fibroblast growth factors 1 and 2. *J Biol Chem* 276, 30744-52 (2001).
7. Muller, M., Marti, T., and Kriz, S. Improved structural preservation by freeze-substitution. 7th European Congress on Electron Microscopy, 720-721 (1980).
8. Leers, M. P. et al. Immunocytochemical detection and mapping of a cytokeratin 18 neo-epitope exposed during early apoptosis. *J Pathol* 187, 567-72 (1999).
9. Nissim, A. et al. Antibody fragments from a 'single pot' phage display library as immunochemical reagents. *Embo J* 13, 692-8 (1994).
10. Merry, C. L. et al. The molecular phenotype of heparan sulfate in the Hs2st^{-/-} mutant mouse. *J Biol Chem* 276, 35429-34 (2001).
11. Li, J. P. et al. Targeted disruption of a murine glucuronyl C5-epimerase gene results in heparan sulfate lacking L-iduronic acid and in neonatal lethality. *J Biol Chem* 278, 28363-6 (2003).
12. Bai, X. & Esko, J. D. An animal cell mutant defective in heparan sulfate hexuronic acid 2-O-sulfation. *J Biol Chem* 271, 17711-7 (1996).
13. Lindahl, U. Heparan sulfate-protein interactions - A concept for drug design? *Thromb Haemost* 98, 109-15 (2007).
14. Smits, N. C. et al. Phage display-derived human antibodies against specific glycosaminoglycan epitopes. *Methods Enzymol* 416 (2006).
15. Conrad, H. E. (Academic Press, San Diego, 1998).
16. Kreuger, J., Spillmann, D., Li, J. P. & Lindahl, U. Interactions between heparan sulfate and proteins: the concept of specificity. *J Cell Biol* 174, 323-7 (2006).
17. Fuster, M. M. & Esko, J. D. The sweet and sour of cancer: glycans as novel therapeutic targets. *Nat Rev Cancer* 5, 526-42 (2005).
18. Liu, D., Shriver, Z., Venkataraman, G., El Shabrawi, Y. & Sasisekharan, R. Tumor cell surface heparan sulfate as cryptic promoters or inhibitors of tumor growth and metastasis. *Proc Natl Acad Sci U S A* 99, 568-73 (2002).
19. Petitou, M. et al. Synthesis of thrombin-inhibiting heparin mimetics without side effects. *Nature* 398, 417-22 (1999).
20. Leali, D. et al. Fibroblast growth factor-2 antagonist activity and angiostatic capacity of sulfated *Escherichia coli* K5 polysaccharide derivatives. *J Biol Chem* 276, 37900-8 (2001).



Chapter 5

Submitted

Overexpression of heparanase and loss of heparan sulfate: initiating events in pulmonary emphysema

Nicole C. Smits •

Antoine A. Robbesom •

Mieke M.J.F. Koenders •

Elly M.M. Versteeg •

Johan van der Vlag ••

Jo Berden ••

Israel Vlodavsky •••

Eyal Zcharia •••

Jin-ping Li ••••

Johan Bulten •••••

Richard P.N. Dekhuijzen ••••••

Toin H. van Kuppevelt •

- *Department of Biochemistry, Radboud University Nijmegen Medical Centre, NCMLS, Nijmegen, The Netherlands*
- *Department of Nephrology, Radboud University Nijmegen Medical Centre, NCMLS, Nijmegen, The Netherlands*
- *Cancer and Vascular Biology Research Centre, The Bruce Rappaport Faculty of Medicine, Haifa, Israel*
- *Department of Medical Biochemistry and Microbiology, Biomedical Centre, Uppsala University, Uppsala, Sweden*
- *Department of Pathology, Radboud University Nijmegen Medical Centre, Nijmegen, The Netherlands*
- *Department of Pulmonary Diseases, Radboud University Nijmegen Medical Centre, Nijmegen, The Netherlands*

Rationale Emphysema, together with chronic bronchitis, forms chronic obstructive pulmonary disease (COPD) which is worldwide an important and increasing cause of morbidity and mortality. At the time of clinical diagnosis, the process of parenchymal destruction - characteristic for emphysema - is already in an advanced state, and this seriously hampers the identification of early molecular alterations. **Methods** Using immunohistochemistry, a survey of early changes in the extracellular matrix was performed in lungs from subjects without clinically evident emphysema, but with early signs of emphysema as morphologically established by the destructive index, the most sensitive parameter for emphysema. The changes found in human lungs were mimicked in genetically modified mice and it was studied if the changes could induce the formation of emphysematous lesions. **Results** In men, an increase in destructive index correlated with an increase in heparanase and a specific decrease in heparan sulfate proteoglycans (both side chain and core protein). Alterations in other matrix components like elastin, collagens and laminin were not found. Importantly, overexpressing of heparanase in transgenic mice, accompanied by loss of heparan sulfate, initiated the development of emphysematous lesions, which became more severe with increasing age, resembling the human situation. **Conclusions** Heparanase overexpression and loss of heparan sulfate are crucial and early events in the development of emphysema. Inhibitors of heparanase activity may be evaluated as potential drugs to slow down the process of emphysema.

Introduction

Pulmonary emphysema is defined as ‘a condition of the lung characterized by abnormal permanent enlargement of airspaces distal to the terminal bronchioles, accompanied by the destruction of their walls, and without obvious fibrosis’¹. Emphysema is a disabling progressive disease that takes many years to develop, cigarette smoking being a main risk factor. Together with chronic bronchitis, it constitutes chronic obstructive pulmonary disease (COPD), which affects over 16 million people in the United States and whose prevalence has risen by 41% since 1982². COPD is the fifth leading cause of death worldwide and an increase in its prevalence and mortality are expected in the coming decades³.

The pathogenesis of emphysema remains elusive. A major problem in research to early pathogenic events of emphysema is the time span between initiation and clinical manifestation. At the

time of clinical diagnosis the process of parenchymal destruction is already in an advanced state, precluding identification of early molecular events. Morphological analysis of lung parenchyma allows for early identification of emphysematous lesions. This especially holds for the destructive index (DI), which is a measure for early parenchymal destruction and has a high sensitivity towards mild forms of emphysema⁴. The DI is a more sensitive parameter in comparison to the mean linear intercept (MLI), which is a parameter for airspace enlargement and which is generally used for morphometrical analysis of emphysema.

Except for the well-characterized $\alpha 1$ anti-trypsin deficiency, which accounts for about 1% of the cases of emphysema, the etiology and pathogenesis of emphysema are not understood. Several hypotheses have been proposed, and they include the protease/anti-protease

concept⁵, the oxidant/anti-oxidant theory⁶, aberrant tissue repair⁷, malfunctioning of the extracellular matrix (ECM)⁸, and emphysema as an immunological disorder⁹. The prevailing hypothesis involves a protease/anti-protease imbalance in the lung. Due to chronic cigarette smoke exposure, an influx of inflammatory cells releases proteases that overwhelm anti-proteolytic defenses¹⁰, resulting in degradation of the ECM. Most attention has focused on elastin as the main target of destruction, especially since loss of elasticity is a hallmark of emphysema. However, little is known about destruction of individual ECM components at the early onset of emphysema. Currently, research interest is changing from the abundant fibrillar components like elastin and collagen to the more regulatory molecules in the ECM like glycosaminoglycans, including heparan sulfate (HS). In an official statement of the *American Thoracic Society* on future research on pulmonary emphysema it was stated that: 'Future directions should explore the specific role of pulmonary parenchymal glycosaminoglycans in maintaining alveolar integrity'¹¹.

Here, we evaluated ECM components in lung specimens and found that overexpression of heparanase and loss of HS (proteoglycans) were associated with the initial stages of emphysema in men, and could initiate emphysematous lesions in mice.

Experimental methods

Chemicals and antibodies

All chemicals were purchased from Merck (Darmstadt, Germany), unless stated otherwise. Alexa 594-conjugated goat anti-rabbit IgG, Alexa 488-conjugated

goat anti-mouse IgM (μ chain), and Alexa 594-conjugated goat anti-mouse IgG2b were from Molecular Probes (Eugene, OR). FITC-conjugated donkey anti-goat IgG, mouse anti-elastin (clone BA-4), and rabbit anti-laminin were from Sigma Immuno Chemicals (St. Louis, MO). Rabbit anti-type I collagen was from Chemicon International, Inc. (Temecula, CA). Goat anti-type IV collagen was from Southern Biotechnology Associates (Birmingham, AL). Mouse anti-human heparanase 1 (clone HP3/17) was from Insight Biopharmaceuticals Ltd. (Rehovot, Israel). Mowiol (4-88) was obtained from Calbiochem (La Jolla, CA). Aminoethyl carbazole (red) substrate kit was from Zymed Laboratories Inc. (San Francisco, CA). Mouse monoclonal antibody 6B6, directed against decorin, a dermatan sulfate proteoglycan, was from Seikagaku (Tokyo, Japan). Goat polyclonal antibody B131¹² was directed against the core protein of agrin (a HS proteoglycan). Mouse monoclonal antibody JM72¹³ was directed against domain AGR10 of the core protein of agrin. Mouse monoclonal anti-HS antibody JM403 was directed against a HS domain containing glucuronic acid-rich sequences with *N*-unsubstituted glucosamine units^{14,15}. All incubations were performed at ambient temperature (22°C) unless stated otherwise.

Human lung specimens

Lung specimens were obtained from patients undergoing lobectomy or pneumonectomy for a localized malignant pulmonary process at the University Lung Centre Nijmegen or the Rijnstate Hospital Arnhem, the Netherlands. Specimens (1 cm³) were taken from resected lung lobes, not showing any sign of the underlying

disease for which the patient underwent surgery. Subjects were studied according to guidelines of the Committee of Medical Ethics of the Radboud University Nijmegen Medical Centre, and gave informed consent. Lung function tests were performed before surgery. Static and dynamic lung function tests were performed with a wet spirometer and with a closed circuit helium-dilution method (Pulmonet III, Sensormedics, Bilthoven, The Netherlands). Diffusion capacity for carbon monoxide per liter/lung (alveolar) volume (DL_{CO}/VA) was measured with the single breath-holding carbon monoxide method (Sensormedics 2450), and was corrected for actual hemoglobin. Measurements were performed at least 12 h after smoking. Predicted spirometric values were derived from the ERS standards. Both smokers and ex-smokers were included and patient groups were comparable with respect to age and pack years (Table 1). None of the patients could be classified as having COPD according to the GOLD criteria¹⁶.

Tissue processing

Each specimen (about 1 cm³) was cut into pieces of equal size. One part was immersed in PBS (pH 7.2), inflated under vacuum (13kPa) for 20 min using a routine water stream-driven device (water aspirator) to restore alveolar dimensions¹⁷, frozen in liquid nitrogen, and stored at -80°C. This part was used for immunohistochemistry (see below). The other part was similarly inflated in PBS containing 4% formalin and further processed for paraffin embedding. From this part, sections (5 μm) were cut and hematoxylin-eosin stained, and used for morphological characterization. All sec-

tions were blinded and scored independently by two observers.

Morphological characterization of lung specimens

Parenchymal destruction

The degree of emphysema was evaluated by the DI, using a microscopic point count technique⁴. Microscopic fields devoid of large bronchi(oli), vessels, collapsed tissue, or extensive fibrosis were selected. From each lung specimen, an average of 5 different sections was used, and representative non-overlapping fields were selected. Alveolar, and duct spaces lying underneath the counting points were evaluated for the presence of destruction. Destruction was defined on base of one or more of the following criteria: [1] at least two alveolar wall defects, [2] at least two intraluminal parenchymal rags in alveolar ducts, [3] clearly abnormal morphology, or [4] classic emphysematous changes⁴. The percentage of all the points falling into the several categories of destroyed airspaces was computed to reveal the DI. In general, 750 counting points were analyzed per specimen.

Airspace enlargement

Enlargement of the airspaces was determined by the MLI measurement technique, which represents the average size of alveoli originally described by Dunnill¹⁸. To determine the MLI, the same images as described above were used. A transparent sheet with 10 horizontal and 11 vertical lines was laid over the images, and intercepts of alveolar walls with these lines were counted. Values were corrected for tissue shrinkage by measuring the dimensions before and after histological processing. The correction factor was 0.832, in ac-

Table 1: Characteristics of study groups

	Normal* (n = 7) (DI < 30%)	Slightly affected* (n = 9) (DI 30 - 80%)	Moderately affected* (n = 7) (DI > 80%)
Age (yr)	53±9 (47-63)	59±9 (50-76)	57±8 (54-75)
Male/female	6/1	8/1	7/0
Smoking (Ex/C)	3/4	2/7	2/5
Pack-years	26±9 (15-45)	37±19 (20-84)	37±15 (12-55)
K _{CO} , % pred	85±23 (59-132)	77±21 (45-106)	73±18 (59-108)
DI, %	21±8 (11-29)	56±8 (41-65)	85±4 (80-90)
MLI, mm	0.28±0.03 (0.23-0.34)	0.29±0.03 (0.24-0.35)	0.37±0.08 (0.29-0.49)

Ex, ex-smokers, not smoking for at least one year; C, current smokers; DI, Destructive Index; MLI, Mean Linear Intercept; KCO, diffusion capacity for CO.

*All values are presented as means ± SD, with ranges in parentheses.

cordance with data from Weibel¹⁹.

Immunohistochemistry

Cryosections (5 μm) were rehydrated for 10 min in PBS, blocked in PBS containing 2% (wt/vol) BSA for 20 min, and incubated with the primary antibody for 60 min. Following each incubation, cryosections were washed in PBS (3 times 5 min). Antibody JM72 was used at 1:250 dilution, anti-heparanase 1 antibody was used at 1:200 dilution, anti-type I collagen, antibody B131, antibody JM403, and all secondary antibodies were used at 1:100 dilution. All other primary antibodies were used at 1:50 dilution. Cryosections were fixed in 96% ethanol, air-dried, and embedded in Mowiol (10% (wt/vol) in 0.1M Tris-HCl, pH 8.5/25% (vol/vol) glycerol/2.5% (wt/vol) NaN₃). Additionally, heparanase expression was detected using aminoethyl carbazole (red) substrate kit. Briefly, sections were rehydrated for 10 min in tris-buffered saline (TBS), blocked in TBS containing 1% (wt/vol) BSA for 30 min, and incuba-

ted with the anti-heparanase 1 antibody for 60 min. Sections were washed in TBS, and incubated with 1000-fold diluted peroxidase labeled goat anti-mouse for 60 min. Sections were washed in PBS for 5 min, rinsed in NaAc buffer, and peroxidase activity was detected using aminoethyl carbazole (red) substrate kit. Sections were rinsed in water, counterstained with hematoxylin, washed with running tap water for 10 min, and with demineralized water for 5 min, and embedded in Kaiser's gelatin. As controls, primary or conjugated antibodies were omitted. Digital images were processed using Adobe Photoshop 7.0 software. Lung sections were randomly coded, and immunoreactivity was scored independently using semi-quantitative criteria (-, no reactivity; +/-, weak reactivity; +, strong reactivity; ++ very strong reactivity) by two observers.

Animals

Homozyous transgenic mice overexpressing mammalian heparanase were gene-

rated as described²⁰. In brief, full-length human heparanase cDNA was subcloned into pCAGGS plasmid at *EcoRI-XbaI* sites under constitutive control of the chicken β -actin promoter. The plasmid was digested with *SaII-PstI* and the resulting linear fragment was microinjected to fertilized eggs of C57BL/6 \times Balb/c origin to produce transgenic mice over-expressing the heparanase cDNA. Of the forty-two pups four were positive human heparanase founder transgenic mice as identified by tail tip genotyping. Founder mice were mated with C57BL/6 mice to create F1 mice and those were mated among themselves to create F2 mice. Homozygous F2 mice from each of the four founder lines were identified by Southern blot analysis and quantitative PCR. Expression of the heparanase protein in the four founder lines was verified by Western blot analysis of tissues derived from F2 homozygous heparanase transgenic mice. Homogenized tissue samples were subjected to SDS-PAGE, and heparanase was identified with an antibody specifically directed against the human enzyme. Heparanase over-expression was found in the lungs of all founder lines. Lung specimens were processed as described above.

Statistical analysis

Results were subjected to statistical analysis using Spearman's coefficient of rank correlation, and the Mann-Whitney U test for multiple comparisons. Data were analyzed with the Statistical Package for the Social Sciences 12.01 (SPSS Inc., Chicago, IL), and GraphPad Prism[®], version 4.0 (GraphPad Software Inc., San Diego, CA) computer programs. Statistical significance was regarded when $P < 0.05$.

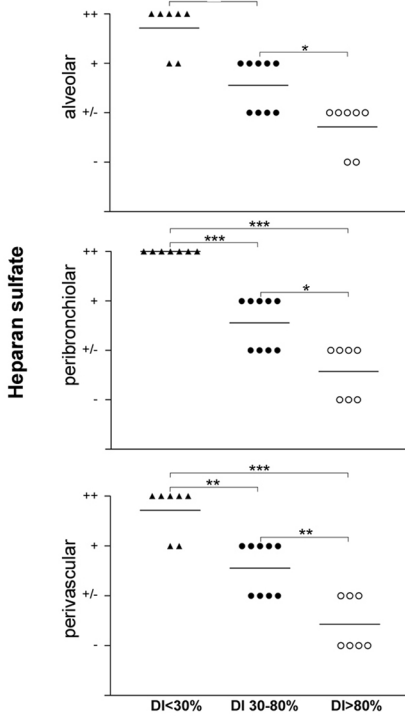
Results

Morphological data

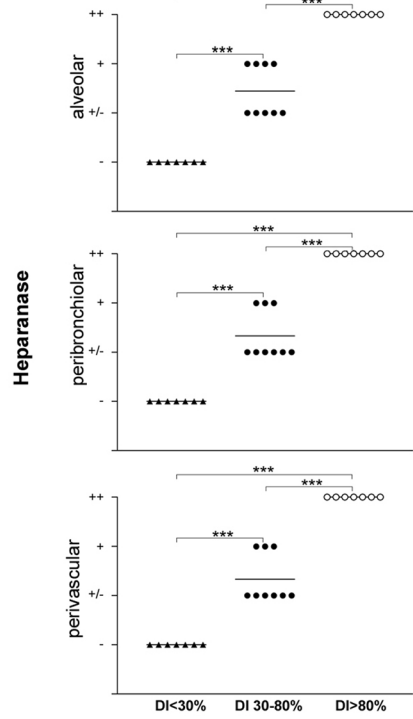
Lung specimens from 23 subjects were morphologically characterized for emphysematous lesions using the DI as a marker for early parenchymal destruction and the MLI as a marker for airspace enlargement (Table 1)²¹. Based on the DI and MLI, three groups were created: (a), normal tissue (DI < 30%, MLI normal); (b), slightly affected lung tissue (DI 30 - 80%, MLI normal) and (c), moderately affected lung tissue (DI > 80%, MLI increased). Please note that for normal, unaffected lungs of non-smoking individuals in the fifth-sixth decade of life, the DI is between 0 - 30%⁴. Using the lung specimens we evaluated early changes in the ECM of lung parenchyma.

Figure 1. Scatter plots showing the relation between staining for extracellular matrix (ECM) components and the destructive index (DI). Morphologically analyzed sections of subjects without clinically evident emphysema and with normal (DI < 30%, MLI normal), slightly affected (DI 30 - 80%, MLI normal), or moderately affected (DI > 80%, MLI increased) lung parenchyma were incubated with antibodies against heparan sulfate (HS; A), heparanase (B), elastin (C), decorin (D), type IV collagen (E), and laminin (F). Immunoreactivity was scored using semi-quantitative criteria (-, no reactivity; +/-, weak reactivity; +, strong reactivity; +/-, very strong reactivity). Note that staining intensity for HS decreased with increasing DI, whereas staining for heparanase increased with increasing DI. There were no differences in staining for other ECM components like elastin, decorin, type IV collagen, and laminin between the three groups. *, $P < 0.05$; **, $P < 0.01$; ***, $P < 0.005$; NS, not significant

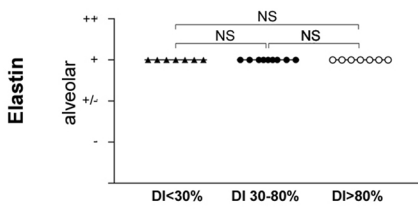
A



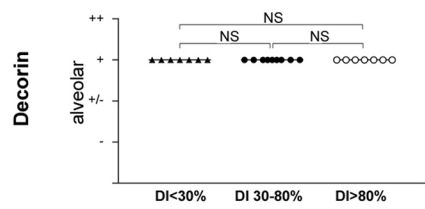
B



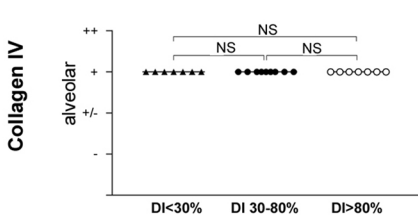
C



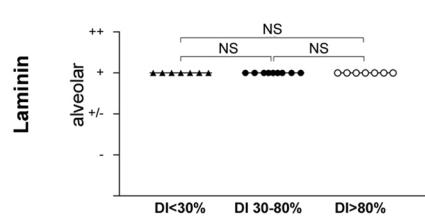
D



E



F



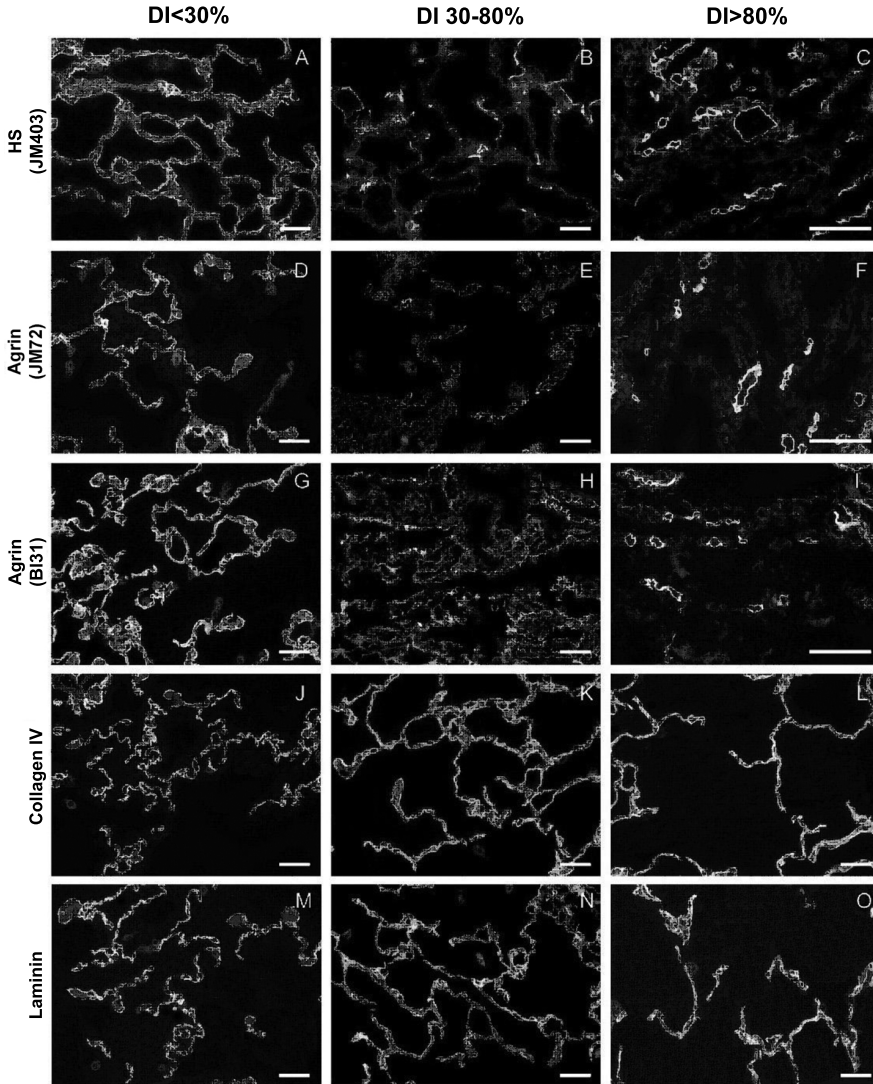


Figure 2. Immunostaining for matrix components in human lung tissue. Morphologically analyzed human lung tissue with Destructive Index (DI) < 30% and normal MLI (A, D, G, J, and M), DI 30 - 80% but normal MLI (B, E, H, K, and N), and DI > 80%, increased MLI (C, F, I, L, and O) were incubated with antibodies against the alveolar basement membrane components heparan sulfate (HS; (A-C)), agrin (antibody JM72 (D-F), and antibody BI31 (G)), type IV collagen (J-L), and laminin (M-O). Note the diminished and discontinuous immunoreactivity for HS (B-C), and agrin (JM72, E-F, and BI31, H-I) in lung tissue with DI 30 - 80%, and DI > 80% compared to strong and continuous immunoreactivity for HS (A), and agrin (D and G) in lung tissue with DI < 30%. Staining for other basement membrane associated components (type IV collagen (J-L) and laminin (M-O) remained unaltered. Scale bars, 50 μ m.

Reduced heparan sulfate and increased heparanase expression are associated with early signs of parenchymal destruction

A set of antibodies which recognize specific ECM components was used to evaluate the lung specimens. HS was abundantly present in normal lung tissue (DI < 30%, MLI normal) in alveolar walls as well as in peribronchiolar and perivascular areas (Figure 1A, Figure 2A, and Figure 4D). However, in slightly affected tissue, with a DI 30 - 80%, but with a normal MLI, a reduced and discontinuous staining for HS was observed in alveolar basement membranes, as well as in peribronchiolar and perivascular areas (Figures 1A, 2B, and 4E). In moderately affected tissue (DI > 80%, MLI increased), the reduction of HS in alveolar basement membranes was more pronounced (Figure 2C and 4F), whereas capillaries remained strongly positive (Figure 2C). Staining for the basement membrane components type IV collagen and laminin, and for the interstitial matrix components elastin and decorin (a dermatan sulfate proteoglycan) did not reveal any differences in staining among the three groups (Figure 1, C-F and Figure 2, J-O). The same was true for type I collagen (data not shown). In normal human lung tissue heparanase expression could not be detected (Figure 1B and Figure 4A). However, heparanase expression was markedly increased in slightly as well as moderately affected lung tissue (Figure 1B and Figure 4, B and C). Heparanase expression was found in alveolar and peribronchiolar areas (primarily associated with epithelial cells), and in perivascular areas. Colocalization studies demonstrated that heparanase expression was associated with reduced or lack of HS expression,

which strongly suggests that heparanase is involved in cleavage of HS (data not shown).

Staining for the core protein of agrin, a major HS proteoglycan, revealed a continuous basement membrane staining in alveolar tissue, and in bronchiolar and vascular areas in normal tissue (Figure 2, D and G). Discontinuous and reduced staining was observed in slightly affected tissue (Figure 2, E and H), and was more prominent in moderately affected tissue (Figure 2, F and I). However, staining of capillaries remained strongly positive in tissues of all three groups (Figure 2, F and I). We next investigated whether HS and the core protein of the HS proteoglycan agrin were affected simultaneously or in sequence. In normal lung tissue, HS side chains and the agrin core protein always colocalized, but in slightly affected lung tissue the core protein could be identified at places where HS was absent, suggesting that HS is degraded prior to the core protein (data not shown).

Heparanase overexpression induces emphysematous lesions in mice

Since our data suggest a role for heparanase in emphysema, lungs of transgenic mice overexpressing mammalian heparanase were studied at different ages from 3 months up to 3 years. We used the MLI as a measure for airspace enlargement (Figure 3). The MLI increased 1.6-fold (1.59 ± 0.13 versus 0.97 ± 0.07 ; $P < 0.0001$, $n = 6$) in heparanase overexpressing mice at 3 months of age, and increased up to 2.2-fold (2.61 ± 0.13 versus 1.17 ± 0.06 ; $P < 0.0001$, $n = 6$) in 3-year old mice (Figure 3). In wild type mice, no heparanase expression in lung tissue could be detected (Figure 4G), in contrast to heparanase overexpressing

mice (Figure 4H), in which the expression was located throughout the lung. HS expression was greatly reduced in the lungs of heparanase overexpressing mice (Figure 4J) as compared to lungs of wild type mice (Figure 4I). Staining patterns for other basement membrane specific

components like the core protein of agrin (Figure 4, K and L) and laminin (Figure 4, M and N), and interstitial components such as elastin (data not shown) and collagen (type IV collagen Figure 4, O and P) did not differ between wild type and heparanase overexpressing mice.

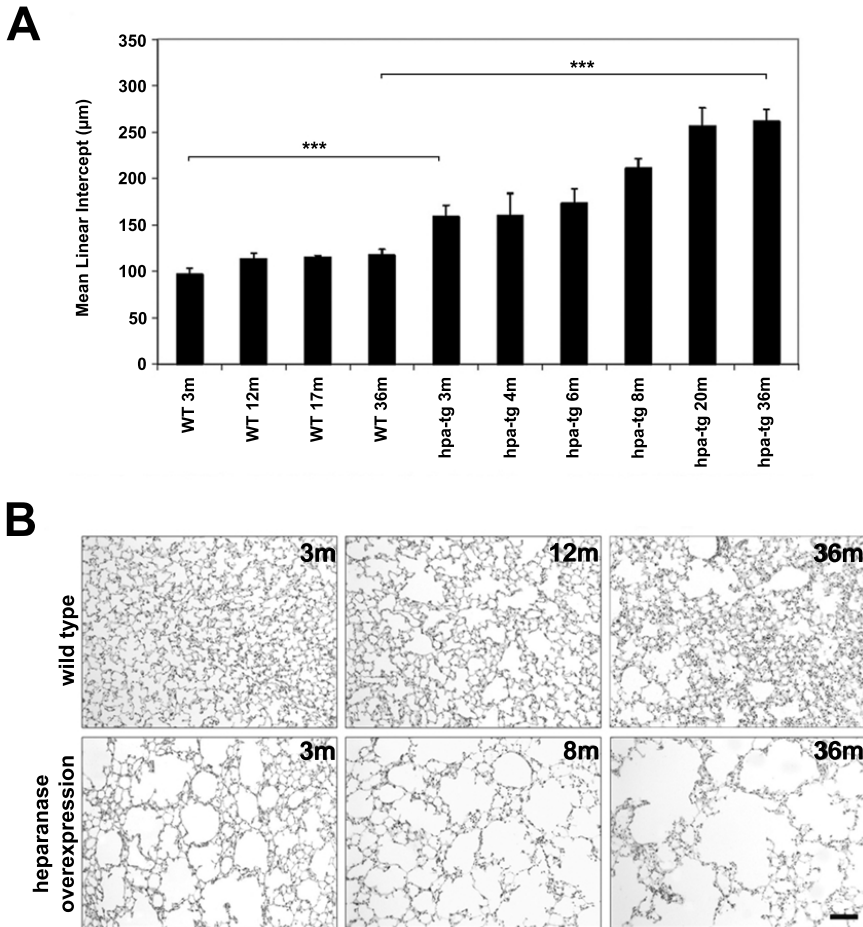


Figure 3. Overexpression of heparanase initiates emphysematous lesions in mice. A, Mean Linear Intercept (MLI) values (mean \pm SD, $n = 6$) of lungs of wild type (WT) and heparanase overexpressing mice (hpa-tg mice) at different ages. ***, $P < 0.0001$. B, hematoxylin-eosin stained sections of lungs from wild type and hpa-tg mice at different ages. In heparanase overexpressing mice enlargement of airspaces was already seen in lungs of 3 months old mice, and increased with age. Scale bar, 50 μ m. m = months

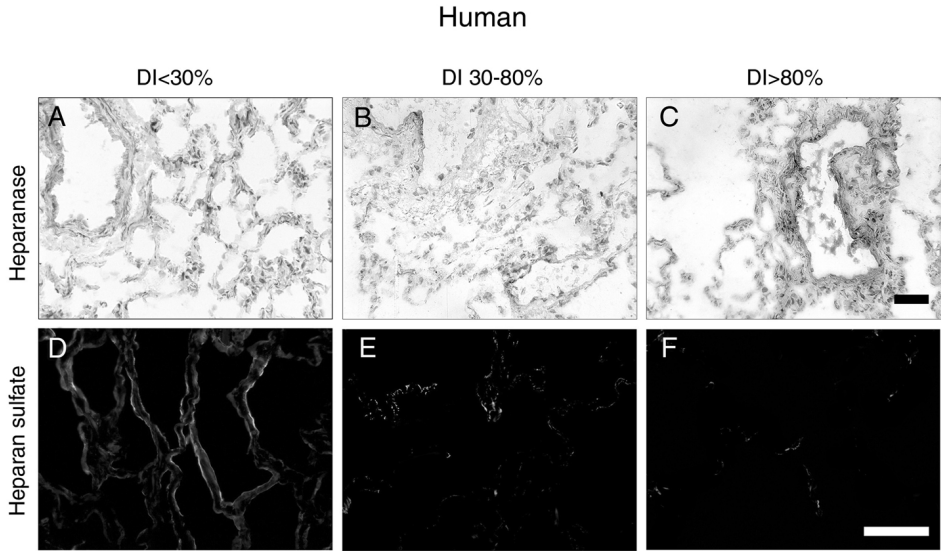
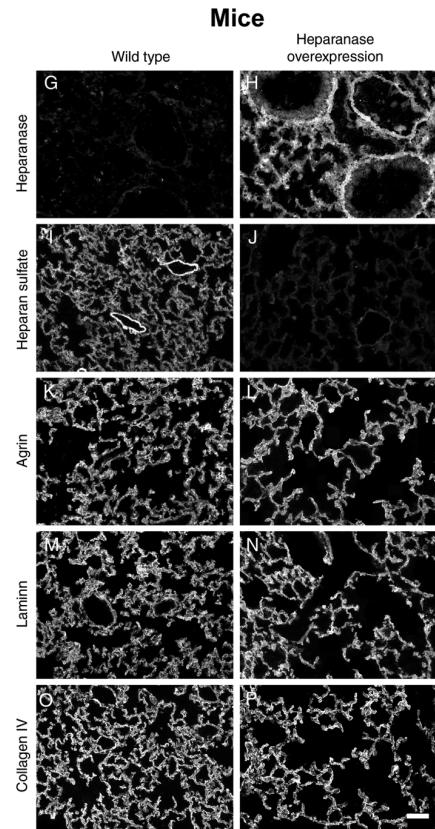


Figure 4. Overexpression of heparanase is associated with loss of heparan sulfate (HS). A-F: morphologically analyzed sections of subjects without clinically evident emphysema and with normal (DI < 30%, MLI normal A, D), slightly affected (DI 30 - 80%, MLI normal B, E), or moderately affected (DI > 80%, increased MLI C, F) lung parenchyma were incubated with antibodies against human heparanase (A-C) or HS (D-F). Heparanase expression increased with DI in alveolar basement membranes (arrows), perivascular areas (arrowheads), and peribronchiolar areas (not shown) whereas HS decreased. Scale bars, 50 μ m.

Lung tissue from wild type mice (G-O), and transgenic mice overexpressing heparanase were stained with antibodies against heparanase (G, H), HS (I, J), agrin core protein (K, L), laminin (M, N), and type IV collagen (O, P). Note the increase in heparanase and loss of HS in transgenic mice. Staining for other matrix components was not affected. Scale bar, 50 μ m.

DI, destructive index



Discussion

The two main findings of this study are the close association of a decreased HS/increased heparanase expression with early parenchymal destruction in human lung tissue, and the initiation of emphysematous lesions by heparanase overexpression in mice. Both data suggest a central role for HS/heparanase in the pathogenesis of emphysema.

HS is increasingly considered as a regulatory polysaccharide, binding and modulating a number of effector molecules and ECM components. It has been coined 'master regulator of interactions'. HS interacts with various classes of proteins that are involved in the pathogenesis of emphysema. These include proteases/protease inhibitors⁵, enzymes involved in neutralizing reactive oxygen species like superoxide dismutase²² and xanthine oxidase^{6,23}, chemokines²⁴, and growth factors/cytokines⁷. In addition, HS proteoglycans interact with basement membrane components, which is necessary for basement membrane barrier integrity in pulmonary tissue. Diminished presence of HS and agrin in the lungs may therefore affect basement membrane integrity. In animal models, HS proteoglycans have been implicated in the pathogenesis of emphysema. Specific inhibition of proteoglycan synthesis induces emphysematous lesions in rats²⁵. In elastase-induced emphysema in rats, HS is readily removed from the lung by degradation of the protein core of the HS proteoglycans⁸, and as a consequence the protective protease (elastase) inhibiting capacity of HS²⁶ is lost. Elastase-induced emphysema can be prevented by administration of HS²⁶. The only long-lasting change (one year) observed in elastase-induced emphysema

is a decrease in the ratio HS/collagen and HS/elastin²⁷. HS can be depolymerized by reactive oxygen and nitrogen species²⁸, both present in cigarette smoke, and expression of heparanase can be induced by reactive oxygen species²⁹. Rats exposed to cigarette smoke show a decrease in HS content in the lung³⁰. In lungs of human emphysematous patients alterations in glycosaminoglycans, including HS, have also been observed^{31,32}, but the results are contradictory. A structurally altered HS has been found in urine samples of patients with emphysema³³ and a diminished HS staining has been reported in alveolar lung tissue from patients with clinically diagnosed mild and severe emphysema³⁴. A diminished peribronchiolar staining for the interstitial proteoglycan decorin has been observed in this patient group³⁴, but in our study, using patients without clinical emphysema, we did not find a reduced staining, perhaps because our specimens were at a very early stage of tissue destruction. This furthermore underscores the importance of characterization of the tissue studied.

Loss of HS staining already occurred at the initial stage of tissue destruction, when the MLI was not increased. Therefore a number of HS dependent phenomena such as vascular endothelial growth factor signaling may be affected early on, and this may be relevant in emphysematogenesis. Blockade of the vascular endothelial growth factor receptor results in the development of emphysematous lesions in rats³⁵, and vascular endothelial growth factor and related proteins have been associated with the pathogenesis of emphysema³⁶. In lung, vascular endothelial growth factor and a number of other growth

factors are bound by HS ³⁷. HS is degraded from the lungs ECM prior to the core protein and this suggests a sequential breakdown of the alveolar wall and puts emphasis on heparanase. Degradation of HS may leave the core protein unprotected from e.g., proteases, resulting in their breakdown. Core proteins are vulnerable to proteolytic digestion ³⁸, and may therefore be prime targets for excess of proteolytic activity when HS is removed ³⁹.

In conclusion, our results provide for the first time a clear link between heparanase and emphysema. Heparanase is overexpressed in human lung parenchyma at an early stage of tissue destruction. Also, overexpression of heparanase in mice causes emphysematous lesions, which become more severe in time as they do in humans. Increased heparanase expression may therefore be a crucial early pathogenic event in emphysema, and may be a promising pharmacological target.

Heparanase has been identified in a variety of cells including endothelial cells, platelets, mast cells, neutrophils, macrophages and T and B lymphocytes ⁴⁰. Currently, a number of heparanase inhibitors such as PI-88 are in clinical trials for their capacity to inhibit angiogenesis and metastasis ⁴¹. Heparanase may be an attractive pharmacological target because it appears that only one form of heparanase is present, in contrast to e.g., the family of matrix metalloproteinases. Understanding the role of heparanase and HS in the onset of emphysema may lead to new therapeutic approaches to control this disease.

Acknowledgements

The authors wish to express their gratitude to the staff and members of the Department of Lung Diseases, University Lung Center Nijmegen, and Canisius-Wilhelmina Hospital, Nijmegen, The Netherlands for providing the lung specimens.

References

1. Snider, G. L., J., K., Thurlbeck, W. M. & Bengali, Z. H. The definition of emphysema. Report of a National Heart, Lung, and Blood Institute, Division of Lung Diseases Workshop. *Am rev respir dis* 132, 182-185 (1985).
2. Murray, C. J. & Lopez, A. D. Alternative projections of mortality and disability by cause 1990-2020: Global Burden of Disease Study. *Lancet* 349, 1498-504 (1997).
3. Pauwels, R. A. & Rabe, K. F. Burden and clinical features of chronic obstructive pulmonary disease (COPD). *Lancet* 364, 613-20 (2004).
4. Saetta, M. et al. Destructive index: a measurement of lung parenchymal destruction in smokers. *Am Rev Respir Dis* 131, 764-9. (1985).
5. Snider, G. L. Emphysema: the first two centuries--and beyond. A historical overview, with suggestions for future research: Part 2. *Am Rev Respir Dis* 146, 1615-22 (1992).
6. Repine, J. E., Bast, A. & Lankhorst, I. Oxidative stress in chronic obstructive pulmonary disease. Oxidative Stress Study Group. *Am J Respir Crit Care Med* 156, 341-57. (1997).
7. Timens, W., Coers, W., Van Straaten, J.F.M., Postma, D.S. Extracellular matrix and inflammation: a role for fibroblast-mediated defective tissue repair in the pathogenesis of emphysema? *Eur Respir Rev* 7, 119-123 (1997).
8. van de Lest, C. H., Versteeg, E. M., Veerkamp, J. H. & van Kuppevelt, T. H. Digestion of proteoglycans in porcine pancreatic elastase-induced emphysema in rats. *Eur Respir J* 8, 238-45. (1995).
9. Snider, G. L. Understanding inflammation in chronic obstructive pulmonary disease: the process begins. *Am J Respir Crit Care Med* 167, 1045-6 (2003).
10. Mahadeva, R. & Shapiro, S. D. Chronic obstructive pulmonary disease * 3: Experimental animal models of pulmonary emphysema. *Thorax* 57, 908-14 (2002).
11. Update: future directions for research on diseases of the lung. The American Thoracic Society. *Am J Respir Crit Care Med* 158, 320-34 (1998).
12. van den Heuvel, L. P. et al. Isolation and partial characterization of heparan sulphate proteoglycan from the human glomerular basement membrane. *Biochem J* 264, 457-65 (1989).
13. van den Born, J. et al. Monoclonal antibodies against the protein core and glycosaminoglycan side chain of glomerular basement membrane heparan sulfate proteoglycan: characterization and immunohistological application in human tissues. *J Histochem Cytochem* 42, 89-102 (1994).
14. van den Born, J. et al. A monoclonal antibody against GBM heparan sulfate induces an acute selective proteinuria in rats. *Kidney Int* 41, 115-23 (1992).
15. van den Born, J. et al. Novel heparan sulfate structures revealed by monoclonal antibodies. *J Biol Chem* 280, 20516-23 (2005).
16. Bellamy, D. et al. International Primary Care Respiratory Group (IPCRG) Guidelines: management of chronic obstructive pulmonary disease (COPD). *Prim Care Respir J* 15, 48-57 (2006).
17. van Kuppevelt, T. H. et al. Restoration by vacuum inflation of original alveolar dimensions in small human lung specimens. *Eur Respir J* 15, 771-7. (2000).
18. Dunnill, M. S. Quantitative Methods in the Study of Pulmonary Pathology. 17, 320-328 (1962).
19. Weibel, E. R. Principles and methods for the morphometric study of the lung and other organs. *Lab Invest* 12, 131-55 (1963).
20. Zcharia, E. et al. Transgenic expression of mammalian heparanase uncovers physiological functions of heparan sulfate in tissue morphogenesis, vascularization, and feeding behavior. *Faseb J* 18, 252-63 (2004).
21. Robbesom, A. A. et al. Morphological quantification of emphysema in small human lung specimens: comparison of methods and relation with clinical data. *Mod Pathol* 16, 1-7 (2003).

22. Tibell, L. A., Sethson, I. & Buevich, A. V. Characterization of the heparin-binding domain of human extracellular superoxide dismutase. *Biochim Biophys Acta* 1340, 21-32 (1997).
23. Adachi, T., Fukushima, T., Usami, Y. & Hirano, K. Binding of human xanthine oxidase to sulphated glycosaminoglycans on the endothelial-cell surface. *Biochem J* 289 (Pt 2), 523-7 (1993).
24. Finkelstein, R., Fraser, R. S., Ghezzi, H. & Cosio, M. G. Alveolar inflammation and its relation to emphysema in smokers. *Am J Respir Crit Care Med* 152, 1666-72. (1995).
25. van Kuppevelt, T. H., van de Lest, C. H., Versteeg, E. M., Dekhuijzen, P. N. & Veerkamp, J. H. Induction of emphysematous lesions in rat lung by beta-D-xyloside, an inhibitor of proteoglycan synthesis. *Am J Respir Cell Mol Biol* 16, 75-84. (1997).
26. Rao, N. V., Kennedy, T. P., Rao, G., Ky, N. & Hoidal, J. R. Sulfated polysaccharides prevent human leukocyte elastase-induced acute lung injury and emphysema in hamsters. *Am Rev Respir Dis* 142, 407-12 (1990).
27. Karlinsky, J. et al. The balance of lung connective tissue elements in elastase-induced emphysema. *J Lab Clin Med* 102, 151-62 (1983).
28. Raats, C. J., Bakker, M. A., van den Born, J. & Berden, J. H. Hydroxyl radicals depolymerize glomerular heparan sulfate in vitro and in experimental nephrotic syndrome. *J Biol Chem* 272, 26734-41 (1997).
29. Kramer, A. et al. Induction of Glomerular Heparanase Expression in Rats with Adriamycin Nephropathy Is Regulated by Reactive Oxygen Species and the Renin-Angiotensin System. *J Am Soc Nephrol* (2006).
30. Latha, M. S., Vijayammal, P. L. & Kurup, P. A. Changes in the glycosaminoglycans and glycoproteins in the tissues in rats exposed to cigarette smoke. *Atherosclerosis* 86, 49-54. (1991).
31. Konno, K. et al. Biochemical study on glycosaminoglycans (mucopolysaccharides) in emphysematous and in aged lungs. *Am Rev Respir Dis* 126, 797-801 (1982).
32. Lafuma, C., Moczar, M., Lange, F. & Robert, L. Biosynthesis of hyaluronic acid, heparan sulfate and structural glycoproteins in hamster lung explants during elastase induced emphysema. *Connect Tissue Res* 13, 169-79 (1985).
33. van de Lest, C. H. et al. Altered composition of urinary heparan sulfate in patients with COPD. *Am J Respir Crit Care Med* 154, 952-8. (1996).
34. van Straaten, J. F. et al. Proteoglycan changes in the extracellular matrix of lung tissue from patients with pulmonary emphysema. *Mod Pathol* 12, 697-705. (1999).
35. Kasahara, Y. et al. Inhibition of VEGF receptors causes lung cell apoptosis and emphysema. *J Clin Invest* 106, 1311-9. (2000).
36. Kasahara, Y. et al. Endothelial cell death and decreased expression of vascular endothelial growth factor and vascular endothelial growth factor receptor 2 in emphysema. *Am J Respir Crit Care Med* 163, 737-44. (2001).
37. Smits, N. C. et al. Heterogeneity of heparan sulfates in human lung. *Am J Respir Cell Mol Biol* 30, 166-73 (2004).
38. Gadek, J. E., Fells, G. A., Zimmerman, R. L. & Crystal, R. G. Role of connective tissue proteases in the pathogenesis of chronic inflammatory lung disease. *Environ Health Perspect* 55, 297-306 (1984).
39. Laros, C. D. The pathogenesis of lung emphysema. A hypothesis. *Respiration* 29, 442-57 (1972).
40. Vlodavsky, I. et al. Expression of heparanase by platelets and circulating cells of the immune system: possible involvement in diapedesis and extravasation. *Invasion Metastasis* 12, 112-27 (1992).
41. Simizu, S., Ishida, K. & Osada, H. Heparanase as a molecular target of cancer chemotherapy. *Cancer Sci* 95, 553-8 (2004).



Chapter 6

Modern Pathology 2008, 21(3):297-307

Aberrant fibrillin-1 expression in early emphysematous human lung: a proposed predisposition for emphysema

Antoine A. Robbesom •, *

Mieke M.J.F. Koenders •, *

Nicole C. Smits •

Theo Hafmans •

Elly M.M. Versteeg •

Johan Bulten ••

Jacques H. Veerkamp •

Richard P.N. Dekhuijzen •••

Toin H. van Kuppevelt •

** These authors contributed equally to this work*

- Department of Biochemistry, Radboud University Nijmegen Medical Centre, NCMLS, Nijmegen, The Netherlands
- Department of Pathology, Radboud University Nijmegen Medical Centre, Nijmegen, The Netherlands
- Department of Pulmonary Diseases, Radboud University Nijmegen Medical Centre, Nijmegen, The Netherlands

Parenchymal destruction, airspace enlargement, and loss of elasticity are hallmarks of pulmonary emphysema. Although the basic mechanism is unknown, there is a consensus that malfunctioning of the extracellular matrix is a major contributor to the pathogenesis of emphysema. In this study, we analyzed the expression of the elastic fiber protein fibrillin-1 in a large number ($n = 69$) of human lung specimens with early-onset emphysema. Specimens were morphologically characterized by the Destructive Index, the Mean Linear Intercept, and the Panel Grading. We observed a strong correlation ($P < 0.001$) of aberrant fibrillin-1 staining with the degree of destruction of lung parenchyma ($r = 0.71$), airspace enlargement ($r = 0.47$), and emphysema-related morphological abnormalities ($r = 0.69$). There were no obvious correlations with age and smoking behavior. Staining for three other extracellular matrix components (type I collagen, type IV collagen, and laminin) was not affected. The aberrant fibrillin-1 staining observed in this study is similar to that observed in Marfan syndrome, a syndrome caused by mutations in the gene encoding fibrillin-1. Strikingly, emphysema is noticed in a number of Marfan patients. This, together with the notion that disruption of the fibrillin-1 gene in mice results in emphysematous lesions, makes fibrillin-1 a strong candidate to be involved in the etiology and pathogenesis of emphysema.

Introduction

Pulmonary emphysema is a progressive lung disease that is defined by an abnormal permanent enlargement of airspaces distal to the terminal bronchioles, accompanied by destruction of their walls and without obvious fibrosis¹. The prevailing theory is that emphysema develops through an imbalance between the proteolytic activity, due to proteases released from inflammatory cells, and the anti-proteolytic defense of the lung. This protease/anti-protease imbalance results in the destruction of lung extracellular matrix (ECM) and eventually leads to emphysema². Another theory is the oxidant/anti-oxidant concept, which postulates that an excess of oxidants and free radicals in the lung directly promotes tissue damage and emphysema³. Firm evidence for either of these concepts is lacking and consequently the pathogenesis of emphysema is still an area of intense investigation.

The pathogenesis of emphysema is characterized by the loss of elasticity. The

network of elastic fibers is an important structural element in lung parenchyma and is, to a major extent, responsible for the elastic recoil properties of the lung⁴.⁵ Elastic fibers are composed of 10-12 nm microfibrils located in and around amorphous elastin⁶⁻⁸. Elastin, the major component of elastic fibers, has attracted much attention in emphysema research. However, evidence that associates elastin to the pathology of emphysema is lacking, although an amino-acid substitution in the elastin gene has been associated with chronic obstructive pulmonary diseases (COPDs), which include emphysema, in one family⁹. Therefore, other molecules present in the elastic fiber may play important roles in the process of emphysema.

Fibrillin-1 is the major component of the microfibrillar part of the elastic fibers, although many other components, including fibulins¹⁰⁻¹², microfibril-associated glycoproteins¹³⁻¹⁵, and emilins¹⁶⁻¹⁸, are present. A number of observations

have associated fibrillin-1 with developmental emphysema. In man, developmental emphysema has been noticed in patients with Marfan syndrome, an autosomal disorder caused by mutations in the gene encoding fibrillin-1¹⁹⁻²⁷. In mice, disruption of the fibrillin-1 gene results in developmental emphysema. The tight skin mouse, characterized by tandem duplication of 30–40 kb in the gene encoding fibrillin-1, develops emphysematous lesions that are in many ways similar to those observed in humans²⁸⁻³². In addition, mice harboring a targeted deletion of 6 kb of the fibrillin-1 gene also display emphysematous lesions³³. Both Marfan syndrome and the two mouse models share a mutated form of fibrillin-1 that gives rise to developmental emphysema. It is, however, unknown if fibrillin-1 also plays a role in the onset of adult emphysema.

This study reports on the role of fibrillin-1 in early-onset emphysema in adult humans. A major problem in the research into the onset of emphysema is the large time span between the initiation of the degenerative disease process and its clinical manifestations. At the time of clinical diagnosis, the process of parenchymal destruction is already in an advanced state, impeding the identification of initiating molecular events. Detailed morphological analysis of lung parenchyma allows for early identification of emphysema, especially since the definition of emphysema is based on morphological parameters. Therefore, we used lung specimens from patients without clinical emphysema but with microscopical emphysema, as defined by destruction of the alveolar wall and enlargement of the airspaces³⁴. On the basis of our data, a new concept

for the onset of emphysema is proposed.

Experimental Methods

Lung tissue

Lung specimens were obtained from patients undergoing a lobectomy or pneumonectomy, for a localized malignant process, at the University Lung Center Nijmegen. All subjects were studied according to the guidelines of the Medical Ethical Committee of the Radboud University Nijmegen Medical Center. Specimens were sampled distantly from the tumor or in an unaffected lobe. Upon histological analysis, specimens did not show any sign of the underlying disease. Lung function tests were performed before surgery. Lung function data for all patients studied were within normal range, according to ERS standards³⁵.

Tissue processing

Small tissue specimens were taken from resected lung lobes. Each specimen was cut into pieces of equal size. One part was immersed in phosphate-buffered saline (PBS) and inflated under vacuum (13 kPa) for 20 min using a routine water stream-driven device (water aspirator) to restore alveolar dimensions³⁶. This part was used for immunohistochemistry (see below). The other -adjacent- part was similarly inflated in PBS containing 4% formalin, embedded in paraffin, and used for morphological analysis (see below).

Morphological analysis

Three morphological parameters have been used to characterize human lung parenchyma and establish the severity of emphysema: the Destructive Index (DI, a measure for early parenchymal destruction)³⁷, the Mean Linear Intercept

(MLI, a measure for airspace enlargement)³⁸, and Panel Grading (PG, morphological grading of emphysematous lesions)³⁹. Hematoxylin and eosin (Sigma-Aldrich, St Louis, MO, USA)-stained sections (5 μ m) were used.

Destructive Index

Using a microscopic point count technique, the DI was evaluated. Microscopic fields devoid of large bronchioli, large blood vessels, collapsed tissue, or extensive fibrosis were selected. For each lung specimen, an average of five different sections was used, and representative non-overlapping fields were selected. Alveoli lying underneath the counting points were evaluated for the presence of destruction. Destruction was defined on the basis of one or more of the following criteria: (a) at least two alveolar wall defects, (b) at least two intraluminal parenchymal rags in alveolar ducts, (c)

clearly abnormal morphology, or (d) classic emphysematous changes³⁷. The percentage of all the points falling into these categories was computed to yield the DI. Generally, 750 points were analyzed per specimen with maxima up to 5000 points. A DI value of 0–30% was considered normal³⁷.

Mean Linear Intercept

The MLI is a measure for airspace enlargement. To determine the MLI, the same images as described above were used. A transparent sheet with 10 horizontal and 11 vertical lines was laid over the images, and intercepts of alveolar walls with these lines were counted. Values were corrected for tissue shrinkage by measuring the dimensions before and after histological processing. The correction factor was 0.82, which is in accordance with earlier studies⁴⁰. A total of 2,500 intercepts were counted

Table 1: Characteristics of the study group and morphological data of the specimens studied

	Normal (n = 12)	Moderate degree of microscopical emphysema (n = 27)	High degree of microscopical emphysema (n = 30)
<i>Study group</i>			
Age (year)	60 \pm 9	61 \pm 8	65 \pm 6
Pack years	29 \pm 9	38 \pm 20	39 \pm 21
FEV ₁ (% pred.)	74 \pm 15	82 \pm 19	77 \pm 17
FEV ₁ /VC (% pred.)	82 \pm 1	91 \pm 1	78 \pm 2
K _{CO} (% pred.)	81 \pm 26	82 \pm 22	75 \pm 19
TLC (% pred.)	93 \pm 23	95 \pm 17	102 \pm 13
RV/TLC (% pred.)	105 \pm 21	106 \pm 21	108 \pm 18
<i>Morphological data specimens</i>			
DI (%)	25 \pm 10	58 \pm 8	83 \pm 7
MLI (μ m)	290 \pm 41	319 \pm 43	394 \pm 55
PG (%)	31 \pm 11	57 \pm 9	78 \pm 8

DI, Destructive Index; MLI, Mean Linear Intercept; PG, Panel Grading; FEV₁, forced expiratory volume in 1 s; % pred., percentage of predicted value; VC, vital capacity; K_{CO}, diffusion capacity for CO; TLC, total lung capacity; RV, residual volume.

All values are means \pm SD.

per specimen with maxima up to 18,000 intercepts.

Panel Grading

The degree of emphysema in the images described above was analyzed by comparing the images with a panel of reference images. The grading ranged from 0 (normal tissue) to 100% (complete destruction). The PG value was expressed as an average percentage of severity of the lesions. The average number of measured slides per specimen was six.

Study Group

Sixty-nine lung parenchymal specimens, derived from patients without clinical emphysema, were selected on the basis of the three morphological parameters (DI, MLI, and PG). All of the specimens studied were derived from patients with a history of smoking, ranging from 10 to 100 pack years. The characteristics of this study group are depicted in Table 1. Specimens originating from patients who had never smoked and had values within the normal range were used as a control ($n = 7$). Specimens originating from patients with other pulmonary diseases (large cell carcinoma ($n = 2$) and sarcoidosis ($n = 2$)) were studied to evaluate the specificity of the data.

Immunohistochemistry

All incubations were performed at room temperature, unless stated otherwise. Cryosections of 2 μm were cut and endogenous peroxidase was blocked with 0.3% (v/v) H_2O_2 in PBS for 1 h. Subsequently, sections were washed in PBS and incubated for 30 min with 1% (w/v) bovine serum albumin (fraction V; Sigma-Aldrich) in PBS (block buffer). Sections were incubated overnight with

mouse anti-fibrillin-1 (mAb 1919, raised against bovine zonular fibrils; Chemicon International, Temecula, CA, USA) diluted 1:1000 in block buffer. After three washes in PBS, the primary antibody was detected with a biotinylated horse anti-mouse IgG antibody (Jackson Immuno Laboratories, West Grove, PA, USA) for 1 h, followed by enhancement with the avidin–biotin–peroxidase complex (Vectastain ABC Elite kit; Vector Laboratories Inc., Burlingame, CA, USA) for 1.5 h. After three washes in PBS, the sections were incubated with diaminobenzidine substrate (DAB) (Sigma-Aldrich), enhanced with nickel. After a final wash in PBS, the sections were counterstained with hematoxylin (Sigma-Aldrich) and mounted in entellan (Merck, Darmstadt, Germany).

Using the method described above, three other antibodies were used, namely, rabbit anti-laminin (L9393, 1:100 dilution; Sigma Immuno Chemicals, St Louis, MO, USA), a rabbit antibody against bovine type I collagen (1:100 dilution; Chemicon International), and a goat antibody against human type IV collagen (1340-01, 1:100 dilution; Southern Biotechnology Associates, Birmingham, AL, USA). Biotinylated donkey anti-rabbit IgG and donkey anti-goat IgG (Jackson Immuno Laboratories) were used to detect the primary antibodies.

All sections were randomly coded, and immunoreactivity was scored independently by two observers using a semiquantitative scale ranging from 0 (linear staining, no fragmentation) to 6 (punctuate staining, extensive fragmentation).

Statistics

Results were calculated with SPSS 11.0 (SPSS Inc., Chicago, IL, USA) using Spearman's two-sided ranked correlation and plotted in a scatter diagram.

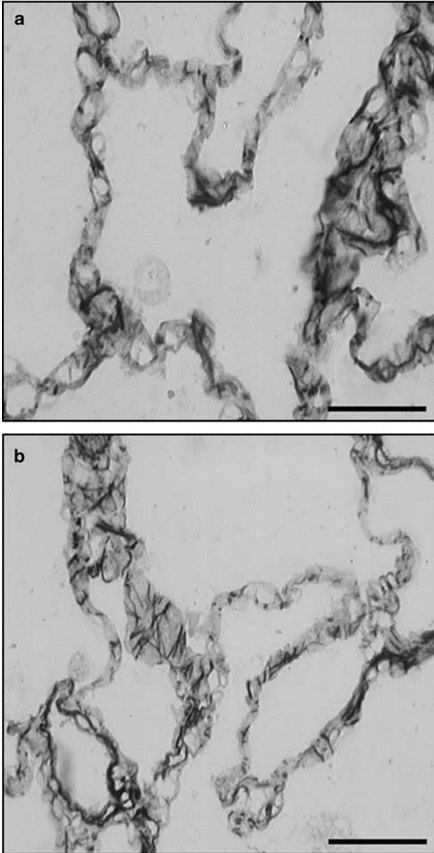


Figure 1. Fibrillin-1 immunostaining in normal human lung parenchyma. Two cryosections, derived from a 21-year-old patient who had never smoked and had no aberrant morphological parameters, were incubated with an antibody against fibrillin-1 (a, b). Bound antibody was visualized with biotinylated anti-mouse IgG followed by DAB incubation. Note the abundant fibrillar fibrillin-1 staining, which meandered throughout the alveolar septa. Scale bar, 50 μ m.

Results

Study Group

As depicted in Table 1, lung function of the patients studied did not meet the GOLD (Global Initiative for Chronic Obstructive Lung Disease) criteria⁴¹ for the diagnosis of emphysema. Sixty-nine lung specimens were morphologically characterized for their degree of microscopical emphysema using the DI as a marker for early parenchymal destruction, the MLI as a marker for airspace enlargement, and the PG index as a value for emphysematous lesions. Three groups were formed: normal specimens, specimens with a moderate degree of microscopical emphysema, and specimens with a high degree of microscopical emphysema (Table 1).

General

To study fibrillin-1 expression, parenchymal lung specimens were stained with an antibody against fibrillin-1. In control specimens, fibrillin-1 was abundantly expressed in a characteristic fibrillar pattern (Figure 1a and b). Fibrillin-1 was identified in alveoli as elongated fibers meandering throughout the septa. No significant disruption of the linear fibrillin-1 staining was observed. In contrast, in specimens with a high degree of microscopical emphysema, the linear fibers were (almost completely) fragmented and had a punctuate appearance (Figure 2f).

Next to fibrillin-1, we studied other ECM components, namely, type IV collagen and laminin (both confined to basement membranes) and type I collagen. Type IV collagen and laminin showed a typical linear basement membrane staining (Figure 3d–f and g–i, respectively), whereas type I collagen was

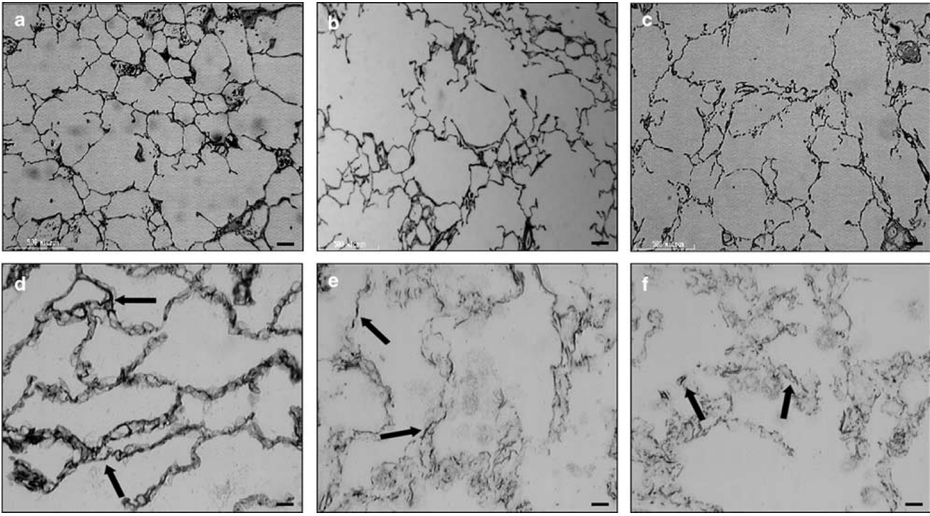


Figure 2. Fibrillin-1 immunostaining. Cryosections derived from a normal lung specimen (63 years, DI = 18%, MLI = 231 μm , PG = 12%) (a, d), a specimen with a moderate degree of microscopical emphysema (58 years, DI = 60%, MLI = 273 μm , PG = 52%) (b, e), and a specimen with a high degree of microscopical emphysema (68 years, DI = 87%, MLI = 317 μm , PG = 85%) (c, f) were incubated with an antibody against fibrillin-1. Bound antibody was visualized with biotinylated anti-mouse IgG followed by DAB incubation. Note the parenchymal destruction and airspace enlargement in specimens with a moderate/high degree of microscopical emphysema (b, c). Compared to the lung specimens with no manifestations of alveolar destruction (d), where an abundant and branched fibrillin-1 staining was seen, a reduced fibrillin-1 staining was apparent in lung specimens with moderate manifestation of alveolar destruction (e). The staining showed fragmented fibers (*arrows*) instead of elongated fibers. In specimens with severe manifestations of alveolar destruction, fibrillin-1 staining was markedly reduced and had a dot-like or punctuate appearance (f, *arrows*). Scale bar, 50 μm .

present as a typical fibrillar staining (Figure 3a–c). Staining for these ECM components did not reveal any differences in abundance or distribution for all specimens examined (Figure 3).

Aberrant fibrillin-1 staining is associated with early parenchymal destruction

The DI reflects the degree of parenchymal destruction and is considered the most sensitive marker for early emphysematous lesions. Lung specimens characterized by a low DI (normal lung specimens), indicating no parenchymal

destruction, expressed fibrillin-1 abundantly (Figure 2d). This expression was comparable to the fibrillin-1 expression seen in control tissue (Figure 1). In lung specimens with moderate manifestations of parenchymal destruction (moderate degree of microscopical emphysema), fibrillin-1 expression was moderately disrupted and slightly reduced (Figure 2e). Lung specimens, characterized by severe manifestations of parenchymal destruction (high degree of microscopical emphysema), displayed a markedly reduced and frag-

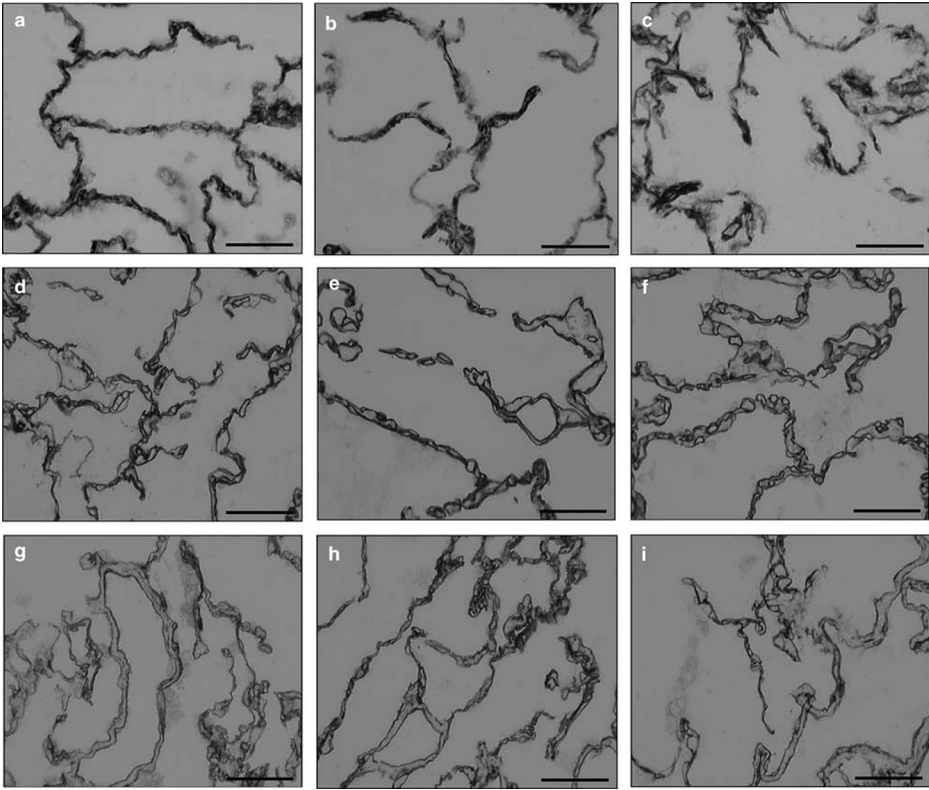


Figure 3. Type I collagen, type IV collagen, and laminin immunostaining. Cryosections derived from a normal lung specimen (63 years, DI = 18%, MLI = 231 μm , PG = 12%) (a, d, g), a specimen with a moderate degree of microscopical emphysema (58 years, DI = 60%, MLI = 273 μm , PG = 52%) (b, e, h), and a specimen with a high degree of microscopical emphysema (68 years, DI = 87%, MLI = 317 μm , PG = 85%) (c, f, i) were incubated with an antibody against type I collagen (a–c), type IV collagen (d–f), and laminin (g–i). Bound antibody was visualized with biotinylated IgG followed by DAB incubation. Note the fibrillar staining pattern for type I collagen and the liner basement membrane staining for type IV collagen and laminin. Type I collagen, type IV collagen, and laminin staining in specimens with a moderate or high degree of microscopical emphysema was similar to the staining in observed normal lung specimens. Scale bar, 50 μm .

mented fibrillin-1 staining, characterized by a punctuate appearance (Figure 2f). To semiquantify the degree of fragmentation, we used an arbitrary scale from 0 (no fragmentation) to 6 (complete fragmentation). When the degree of fibrillin-1 fragmentation was

plotted against the degree of parenchymal destruction, that is, the DI, a significant correlation ($P < 0.001$) was observed (Figure 4).

Aberrant fibrillin-1 staining is associated with airspace enlargement and emphysematous

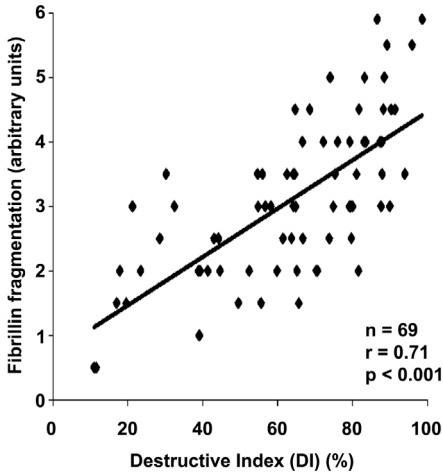


Figure 4. Fibrillin-1 fragmentation as a function of the Destructive Index (DI). By means of an arbitrary scale ranging from no fragmentation (0) to maximal fragmentation (6), fibrillin-1 fragmentation was plotted against the DI. A significant correlation was found between fibrillin-1 fragmentation and DI ($P < 0.001$). The regression coefficient equals 0.71. Each point represents an individual patient.

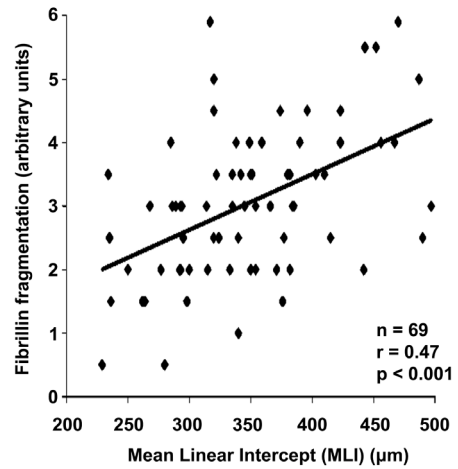


Figure 5. Fibrillin-1 fragmentation as a function of mean linear intercept (MLI). By means of an arbitrary scale ranging from no fragmentation (0) to maximal fragmentation (6), fibrillin-1 fragmentation was plotted against the MLI. A significant correlation was found between fibrillin-1 fragmentation and MLI ($P < 0.001$). The regression coefficient equals 0.47. Each point represents an individual patient.

abnormalities

The MLI is a parameter for airspace enlargement. The presence of fragmented fibrillin-1 staining was plotted against the MLI (Figure 5), and a significant correlation ($P < 0.001$) was observed. The PG value reflects the overall degree of emphysematous abnormalities. A significant correlation ($P < 0.001$) was observed between the amount of fibrillin-1 fragmentation and PG (Figure 6).

Aberrant fibrillin-1 staining is not associated with age

The process of emphysema is age-dependent. Therefore, it may be assumed that the fibrillin-1 fragmentation is dependent on age. However, this appears

not to be the case. When fibrillin-1 fragmentation was plotted against age (Figure 7a), no significant correlation was observed. Fibrillin-1 fragmentation was present at the same level in all age categories. For instance, staining derived in a specimen from a young individual (42 years) with a high DI (70%) was highly fragmented, as was staining in a specimen from an older individual (68 years) with a high DI (87%) (Figure 7c and e). Likewise, a young individual (41 years) with a low DI (11%) displayed a normal fibrillin-1 staining, as did an older individual (78 years) with a low DI (23%) (Figure 7b and d).

Aberrant fibrillin-1 staining is not associated with smoking behavior

The degree of clinical emphysema is strongly correlated with smoking behavior. However, when fibrillin-1 fragmentation was plotted against smoking behavior, as expressed in pack years (one pack year is equal to smoking one pack of cigarettes per day during one year), no correlation was detected (Figure 8).

Aberrant fibrillin-1 staining is not associated with other lung diseases

To evaluate the specificity of the aberrant fibrillin-1 staining for the process of emphysema, specimens derived from patients with other lung diseases (large cell carcinoma and sarcoidosis) were immunostained for fibrillin-1 (Figure 9, for large cell carcinoma). Fibrillin-1 expression in these specimens was abundant with a striking absence of fibrillin-1 fragmentation, indicating the specificity of our observations.

Discussion

In this study, we showed that an aberrant fibrillin-1 staining in lung specimens was significantly associated with the three most important morphometric parameters for emphysema: the DI (alveolar destruction), the MLI (airspace enlargement), and the PG (emphysema-related morphological abnormalities). Since emphysema is defined by an abnormal permanent enlargement of airspaces and by destruction of their walls, characterization of the disease with morphological parameters such as DI and MLI is a prerequisite to study the pathogenesis of emphysema. We collected lung specimens that had microscopical emphysema, as judged by morphometric analysis³⁴. Despite

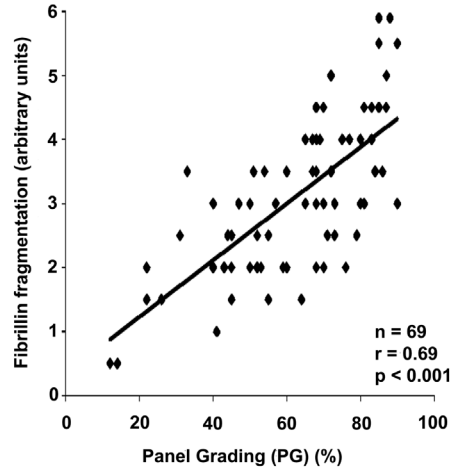


Figure 6. Fibrillin-1 fragmentation as a function of panel grading (PG) value. By means of an arbitrary scale ranging from no fragmentation (0) to maximal fragmentation (6), fibrillin-1 fragmentation was plotted against the PG. A significant correlation was found between fibrillin-1 fragmentation and PG ($P < 0.001$). The regression coefficient equals 0.69. Each point represents an individual patient.

these morphological abnormalities, lung function tests were still within normal range, indicating that the process of lung destruction is still at an early stage. Lung function tests are a useful tool to diagnose COPD, a collective term including chronic bronchitis and emphysema. However, because lung function tests reflect airway obstruction and not loss of pulmonary parenchyma, the use of these tests to merely establish emphysema is controversial⁴²⁻⁴⁴. Besides that, the relationship between lung function data and the morphological assessment of emphysema has been described as poor⁴⁵⁻⁴⁸. Owing to this insensitivity, lung function tests are of limited value to identify the onset of emphysema.

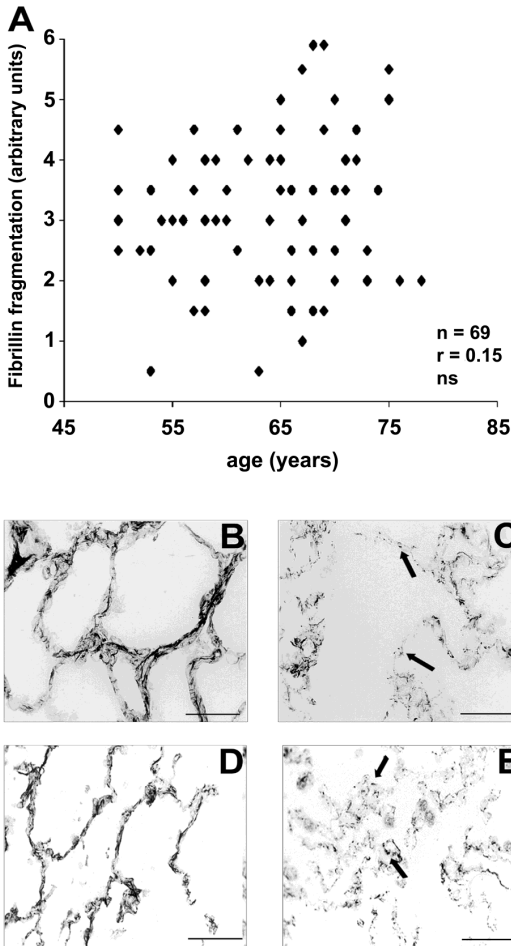


Figure 7. Lack of correlation between fibrillin-1 fragmentation and age. (a) Fibrillin-1 as a function of age. By means of an arbitrary scale ranging from no fragmentation (0) to maximal fragmentation (6), fibrillin-1 fragmentation was plotted against age. No significant correlation was found between fibrillin-1 fragmentation and age. The regression coefficient equals 0.15. Each point represents an individual patient. (b–e) Fibrillin-1 immunostaining in specimens from patients with similar age, but different DIs. Cryosections derived from a young patient (41 years) with a low DI (11%) (b) and a young patient (42 years) with a high DI (70%) (c) were incubated with an antibody against fibrillin-1. Likewise, cryosections from an older patient (78 years) with a low DI (23%) (d) and an older patient (68 years) with a high DI (87%) (e) were immunostained for fibrillin-1. Bound antibody was visualized with biotinylated anti-mouse IgG followed by DAB incubation. Note the abundant, helical, fibrillin-1 staining in the young patient and older patient with a low DI (a, d) and the small, dot-like fibrillin-1 structures (arrows) in the young patient and older patient with a high DI (b, e). Scale bar, 50 μ m.

Therefore, clinical manifestations of emphysema are only evident in patients with a wide spread and advanced emphysema^{46, 49–55}. Indeed, autopsy studies have indicated that one-third of the lung can be affected by emphysema before respiratory function is impaired⁵⁶. The onset of emphysema is a process that can only be measured accurately by microscopic measurements. Therefore, this study used lung specimens from patients without clinical manifestations, but with morphological abnormalities

indicative of early-onset emphysema. This unique data set allowed us to analyze initiating molecular events in the pathogenesis of emphysema.

Our data suggest that fibrillin-1 is an important player in the onset of adult emphysema. This notion is underlined by the observation that staining for other ECM molecules (laminin, type I collagen, and type IV collagen) was not aberrant. The hypothesis that fibrillin-1 is a major player in the onset of emphysema is corroborated by other lines of research

that have correlated fibrillin-1 with developmental emphysema. Mutated forms of fibrillin-1 are causative for developmental emphysema in mouse models^{30, 32}. Tight skin mice, characterized by a tandem duplication of 30–40 kb in the gene encoding fibrillin-1³¹, have an abnormal immunostaining for fibrillin-1²⁹. Fibroblasts from these mice synthesize and secrete normal as well as oversized fibrillin-1 protein^{28, 29}. The resulting abnormal fibrillin-1 assembly results in emphysema that is in many ways similar to that observed in humans. Emphysematous lesions are also observed in another mouse model harboring a targeted deletion of 6 kb in the fibrillin-1

gene³³. As a result, elastic fibers have less tensile strength, resulting in mechanical collapse, overstretching, and fracturing. At such sites, the influx of inflammatory cells is noted. In man, mutations in the fibrillin-1 gene are causative for Marfan syndrome, an autosomal disorder affecting the cardiovascular, skeletal, and ocular system^{20, 22, 24}. To date, over 500 fibrillin-1 mutations have been identified⁵⁷. Mutations are found throughout the gene and result in a reduced fibrillin-1 synthesis, a delayed secretion, and thus an impaired fibrillin-1 deposition into the matrix. The fragmented fibrillin-1 staining observed in our lung specimens is similar to the fibrillin-1 staining observed in skin specimens from Marfan patients^{58, 59}. Strikingly, developmental emphysema has been noticed in a number of Marfan syndrome patients, although studies are scarce. In one study, three out of four autopsied cases (44, 23, and 25 years of age) displayed emphysema on microscopical examination, as indicated by dilatation of alveolar spaces and rupture of alveolar walls. Fragmented elastic fibers, with a granular appearance, and microfibrils were noticed²⁶. In another study, four out of four infants with Marfan syndrome had microscopic emphysema similar to that observed in older patients with emphysema but without Marfan syndrome¹⁹. In yet another study, four out of four infants with Marfan syndrome had microscopical features of emphysema, with interrupted, fragmented, and clumped fibers that were not observed in 13 control infants²⁵. About 5% of the Marfan patients develop bullous emphysema, as detected by chest radiography²⁷. In neonatal Marfan syndrome, a severe form of the disease, emphysema, is common^{21, 23}. It should

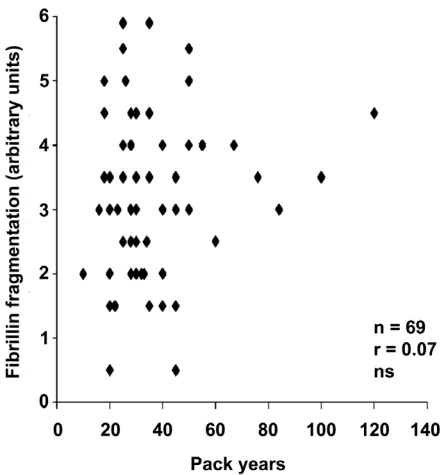


Figure 8. Fibrillin-1 fragmentation as a function of smoking. By means of an arbitrary scale ranging from no fragmentation (0) to maximal fragmentation (6), fibrillin-1 fragmentation was plotted against smoking (expressed in pack years). No significant correlation was found between fibrillin-1 fragmentation and smoking. The regression coefficient equals 0.07. Each point represents an individual patient.

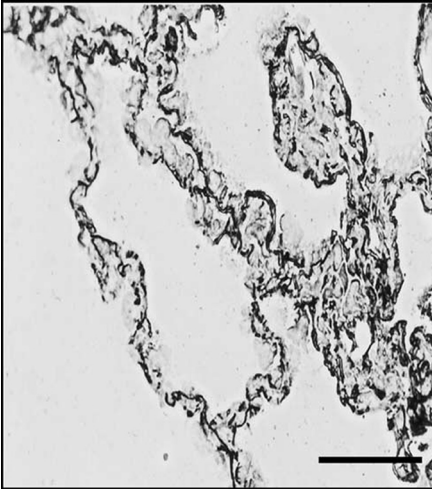


Figure 9. Fibrillin-1 immunostaining in a lung specimen derived from large cell carcinoma. A cryosection from non-emphysematous tissue (DI = 20%, MLI = 264 μ m, PG = 22%; age of patient: 57 years, and 40 pack years), affected by large cell carcinoma, was incubated with an antibody against fibrillin-1. The section contains alveolar fibrosis, due to a desmoplastic reaction, and infiltrated cells. Bound antibody was visualized with biotinylated anti-mouse IgG followed by DAB incubation. Note the abundant fibrillin-1 staining, which was present throughout the alveolar septa. Scale bar, 50 μ m.

be noted that the presence of emphysema in patients with Marfan syndrome may very well be underestimated. Patients are generally not examined for emphysema/COPD. Before the use of β -blockers and cardiovascular surgery, patients generally died in their late 30s, an age at which clinical emphysema is generally not manifest.

The observation that fibrillin-1 fragmentation is not correlated with smoking behavior or age is intriguing. Smoking is considered the most important risk factor for emphysema, but, for unknown reasons, only 15% of smokers actually

develop clinical emphysema⁶⁰. This paradox suggests that, besides smoking, another factor must be involved in the susceptibility to emphysema. Is there another risk factor for emphysema besides smoking? Familial aggregation, implying a genetic predisposition, has been observed for emphysema⁶¹⁻⁶⁴. This suggests that next to environmental causes, genetic influences are of importance for the susceptibility to emphysema. Clinical emphysema would thus result from combined external risk factors and intrinsic host factors. Emphysema has been associated with polymorphisms in genes encoding epoxide hydrolase⁶⁵, vitamin D-binding protein⁶⁶, and heme oxygenase⁶⁷. However, strong associations between these polymorphisms and the elastic recoil properties of the lung are lacking and correlations with protein levels in human lung have not been reported^{68, 69}.

Our study presents data that correlate fibrillin-1 to the onset of adult emphysema. This, together with the notion that mutations in the fibrillin-1 gene may result in emphysematous lesions in man (Marfan syndrome) as well as mice, makes the fibrillin-1 gene a strong candidate for the predisposition of smokers to emphysema. The following hypothesis may now be put forward: a mutation in the gene encoding fibrillin-1 results in a (moderately) affected fibrillin-1 protein in the lung. Once the lung is challenged, for example, by smoking, the affected fibrillin-1 will lead to defective elastic fibers and to the loss of elasticity, which is the major hallmark of emphysema. Owing to the loss of elastic fibers, breathing will be compromised and clinical emphysema will develop.

Acknowledgements

The authors express their gratitude to The Netherlands Asthma Foundation for financial support (NAF project 95.44). The lung specimens were kindly provided by the Department of Lung Diseases, University Lung Center Nijmegen, and the Department of Lung Diseases, Canisius-Wilhelmina Hospital Nijmegen.

References

1. Snider, G. L., J., K., Thurlbeck, W. M. & Bengali, Z. H. The definition of emphysema. Report of a National Heart, Lung, and Blood Institute, Division of Lung Diseases Workshop. *Am rev respir dis* 132, 182-185 (1985).
2. Gadek, J. E., Fells, G. A., Zimmerman, R. L. & Crystal, R. G. Role of connective tissue proteases in the pathogenesis of chronic inflammatory lung disease. *Environ Health Perspect* 55, 297-306 (1984).
3. Repine, J. E., Bast, A. & Lankhorst, I. Oxidative stress in chronic obstructive pulmonary disease. Oxidative Stress Study Group. *Am J Respir Crit Care Med* 156, 341-57. (1997).
4. Kiely, C. M., Sherratt, M. J. & Shuttleworth, C. A. Elastic fibres. *J Cell Sci* 115, 2817-28 (2002).
5. Rosenbloom, J., Abrams, W. R. & Mecham, R. Extracellular matrix 4: the elastic fiber. *Faseb J* 7, 1208-18 (1993).
6. Kiely, C. M. et al. Fibrillin: from microfibril assembly to biomechanical function. *Philos Trans R Soc Lond B Biol Sci* 357, 207-17 (2002).
7. Ramirez, F. & Pereira, L. The fibrillins. *Int J Biochem Cell Biol* 31, 255-9 (1999).
8. Robinson, P. N. & Godfrey, M. The molecular genetics of Marfan syndrome and related microfibrilopathies. *J Med Genet* 37, 9-25 (2000).
9. Kelleher, C. M. et al. A functional mutation in the terminal exon of elastin in severe, early-onset chronic obstructive pulmonary disease. *Am J Respir Cell Mol Biol* 33, 355-62 (2005).
10. Roark, E. F. et al. The association of human fibulin-1 with elastic fibers: an immunohistological, ultrastructural, and RNA study. *J Histochem Cytochem* 43, 401-11 (1995).
11. Yanagisawa, H. et al. Fibulin-5 is an elastin-binding protein essential for elastic fibre development in vivo. *Nature* 415, 168-71 (2002).
12. Zhang, R. Z. et al. Fibulin-2 (FBLN2): human cDNA sequence, mRNA expression, and mapping of the gene on human and mouse chromosomes. *Genomics* 22, 425-30 (1994).
13. Gibson, M. A., Hughes, J. L., Fanning, J. C. & Cleary, E. G. The major antigen of elastin-associated microfibrils is a 31-kDa glycoprotein. *J Biol Chem* 261, 11429-36 (1986).
14. Gibson, M. A., Kumaratilake, J. S. & Cleary, E. G. The protein components of the 12-nanometer microfibrils of elastic and nonelastic tissues. *J Biol Chem* 264, 4590-8 (1989).
15. Gibson, M. A. et al. Further characterization of proteins associated with elastic fiber microfibrils including the molecular cloning of MAGP-2 (MP25). *J Biol Chem* 271, 1096-103 (1996).
16. Bressan, G. M. et al. Emilin, a component of elastic fibers preferentially located at the elastin-microfibrils interface. *J Cell Biol* 121, 201-12 (1993).
17. Colombatti, A. et al. The EMILIN protein family. *Matrix Biol* 19, 289-301 (2000).
18. Doliana, R. et al. EMILIN, a component of the elastic fiber and a new member of the C1q/tumor necrosis factor superfamily of proteins. *J Biol Chem* 274, 16773-81 (1999).
19. Bolande, R. P. & Tucker, A. S. Pulmonary Emphysema And Other Cardiorespiratory Lesions As Part Of The Marfan Abiotrophy. *Pediatrics* 33, 356-66 (1964).
20. Collod-Beroud, G. & Boileau, C. Marfan syndrome in the third Millennium. *Eur J Hum Genet* 10, 673-81 (2002).
21. Jacobs, A. M. et al. A recurring FBN1 gene mutation in neonatal Marfan syndrome. *Arch Pediatr Adolesc Med* 156, 1081-5 (2002).
22. Maslen, C. L. & Glanville, R. W. The molecular basis of Marfan syndrome. *DNA Cell Biol* 12, 561-72 (1993).
23. Milewicz, D. M. & Duvic, M. Severe neonatal Marfan syndrome resulting from a de novo 3-bp insertion into the fibrillin gene on chromosome 15. *Am J Hum Genet* 54, 447-53 (1994).

24. Pyeritz, R. E. The Marfan syndrome and other microfibrillar disorders. In: Royce PM, Steinmann B (eds). *Connective Tissue and Its Heritable Disorders*. Wiley-Liss: New York, 585-626 (2002).
25. Reye, R. D. & Bale, P. M. Elastic tissue in pulmonary emphysema in Marfan syndrome. *Arch Pathol* 96, 427-31 (1973).
26. Sayers, C. P., Goltz, R. W. & Mottiaz, J. Pulmonary elastic tissue in generalized elastolysis (cutis laxa) and Marfan's syndrome: a light and electron microscopic study. *J Invest Dermatol* 65, 451-7 (1975).
27. Wood, J. R., Bellamy, D., Child, A. H. & Citron, K. M. Pulmonary disease in patients with Marfan syndrome. *Thorax* 39, 780-4 (1984).
28. Gayraud, B., Keene, D. R., Sakai, L. Y. & Ramirez, F. New insights into the assembly of extracellular microfibrils from the analysis of the fibrillin 1 mutation in the tight skin mouse. *J Cell Biol* 150, 667-80 (2000).
29. Kielty, C. M. et al. The Tight skin mouse: demonstration of mutant fibrillin-1 production and assembly into abnormal microfibrils. *J Cell Biol* 140, 1159-66 (1998).
30. Rossi, G. A. et al. Hereditary emphysema in the tight-skin mouse. Evaluation of pathogenesis. *Am Rev Respir Dis* 129, 850-5 (1984).
31. Siracusa, L. D. et al. A tandem duplication within the fibrillin 1 gene is associated with the mouse tight skin mutation. *Genome Res* 6, 300-13 (1996).
32. Szapiel, S. V. et al. Hereditary emphysema in the tight-skin (Tsk/+) mouse. *Am Rev Respir Dis* 123, 680-5 (1981).
33. Pereira, L. et al. Targetting of the gene encoding fibrillin-1 recapitulates the vascular aspect of Marfan syndrome. *Nat Genet* 17, 218-22 (1997).
34. Robbesom, A. A. et al. Morphological quantification of emphysema in small human lung specimens: comparison of methods and relation with clinical data. *Mod Pathol* 16, 1-7 (2003).
35. Quanjer, P. H. et al. Lung volumes and forced ventilatory flows. Report Working Party Standardization of Lung Function Tests, European Community for Steel and Coal. Official Statement of the European Respiratory Society. *Eur Respir J Suppl* 16, 5-40 (1993).
36. van Kuppevelt, T. H. et al. Restoration by vacuum inflation of original alveolar dimensions in small human lung specimens. *Eur Respir J* 15, 771-7. (2000).
37. Saetta, M. et al. Destructive index: a measurement of lung parenchymal destruction in smokers. *Am Rev Respir Dis* 131, 764-9. (1985).
38. Dunnill, M. S. *Quantitative Methods in the Study of Pulmonary Pathology*. 17, 320-328 (1962).
39. Nagai, A., Yamawaki, I., Thurlbeck, W. M. & Takizawa, T. Assessment of lung parenchymal destruction by using routine histologic tissue sections. *Am Rev Respir Dis* 139, 313-9. (1989).
40. Weibel, E. R. Principles and methods for the morphometric study of the lung and other organs. *Lab Invest* 12, 131-55 (1963).
41. Pauwels, R. A., Buist, A. S., Ma, P., Jenkins, C. R. & Hurd, S. S. Global strategy for the diagnosis, management, and prevention of chronic obstructive pulmonary disease: National Heart, Lung, and Blood Institute and World Health Organization Global Initiative for Chronic Obstructive Lung Disease (GOLD): executive summary. *Respir Care* 46, 798-825 (2001).
42. Nagai, A., West, W. W., Paul, J. L. & Thurlbeck, W. M. The National Institutes of Health Intermittent Positive-Pressure Breathing trial: pathology studies. I. Interrelationship between morphologic lesions. *Am Rev Respir Dis* 132, 937-45 (1985).
43. Nagai, A., West, W. W. & Thurlbeck, W. M. The National Institutes of Health Intermittent Positive-Pressure Breathing trial: pathology studies. II. Correlation between morphologic findings, clinical findings, and evidence of expiratory air-flow obstruction. *Am Rev Respir Dis* 132, 946-53 (1985).
44. Thurlbeck, W. M. Overview of the pathology of pulmonary emphysema in the human. *Clin Chest Med* 4, 337-50 (1983).
45. Saito, K., Cagle, P., Berend, N. & Thurlbeck, W. M. The "destructive index" in nonemphysematous

- and emphysematous lungs. Morphologic observations and correlation with function. *Am Rev Respir Dis* 139, 308-12. (1989).
46. McLean, A., Warren, P. M., Gillooly, M., MacNee, W. & Lamb, D. Microscopic and macroscopic measurements of emphysema: relation to carbon monoxide gas transfer. *Thorax* 47, 144-9 (1992).
 47. Gevenois, P. A. et al. Comparison of computed density and microscopic morphometry in pulmonary emphysema. *Am J Respir Crit Care Med* 154, 187-92 (1996).
 48. Gurney, J. W. Pathophysiology of obstructive airways disease. *Radiol Clin North Am* 36, 15-27 (1998).
 49. Thurlbeck, W. M. & Angus, G. E. The relationship between emphysema and chronic bronchitis as assessed morphologically. *Am Rev Respir Dis* 87, 815-9 (1963).
 50. Sobonya, R. E. & Burrows, B. The epidemiology of emphysema. *Clin Chest Med* 4, 351-8 (1983).
 51. Nicklaus, T. M., Stowell, D. W., Christiansen, W. R. & Renzetti, A. D., Jr. The accuracy of the roentgenologic diagnosis of chronic pulmonary emphysema. *Am Rev Respir Dis* 93, 889-99 (1966).
 52. Knott, J. M. & Christie, R. V. Radiological diagnosis of emphysema. *Lancet* 1, 881-3 (1951).
 53. Park, S. S., Janis, M., Shim, C. S. & Williams, M. H., Jr. Relationship of bronchitis and emphysema to altered pulmonary function. *Am Rev Respir Dis* 102, 927-36 (1970).
 54. Snider, G. L. Distinguishing among asthma, chronic bronchitis, and emphysema. *Chest* 87, 35S-39S (1985).
 55. Gelb, A. F., Gold, W. M., Wright, R. R., Bruch, H. R. & Nadel, J. A. Physiologic diagnosis of subclinical emphysema. *Am Rev Respir Dis* 107, 50-63 (1973).
 56. Uppaluri, R., Mitsa, T., Sonka, M., Hoffman, E. A. & McLennan, G. Quantification of pulmonary emphysema from lung computed tomography images. *Am J Respir Crit Care Med* 156, 248-54 (1997).
 57. Collod-Beroud, G. et al. Marfan Database (third edition): new mutations and new routines for the software. *Nucleic Acids Res* 26, 229-3 (1998).
 58. Godfrey, M. et al. Unilateral microfibrillar abnormalities in a case of asymmetric Marfan syndrome. *Am J Hum Genet* 46, 661-71 (1990).
 59. Hollister, D. W., Godfrey, M., Sakai, L. Y. & Pyeritz, R. E. Immunohistologic abnormalities of the microfibrillar-fiber system in the Marfan syndrome. *N Engl J Med* 323, 152-9 (1990).
 60. Fletcher, C. & Peto, R. The natural history of chronic airflow obstruction. *Br Med J* 1, 1645-8 (1977).
 61. Cohen, B. H. et al. A genetic-epidemiologic study of chronic obstructive pulmonary disease. I. Study design and preliminary observations. *Johns Hopkins Med J* 137, 95-104 (1975).
 62. Hankins, D., Drage, C., Zamel, N. & Kronenberg, R. Pulmonary function in identical twins raised apart. *Am Rev Respir Dis* 125, 119-21 (1982).
 63. Kueppers, F. & Christopherson, M. J. Alpha1-antitrypsin: further genetic heterogeneity revealed by isoelectric focusing. *Am J Hum Genet* 30, 359-65 (1978).
 64. Larson, R. K., Barman, M. L., Kueppers, F. & Fudenberg, H. H. Genetic and environmental determinants of chronic obstructive pulmonary disease. *Ann Intern Med* 72, 627-32 (1970).
 65. Smith, C. A. & Harrison, D. J. Association between polymorphism in gene for microsomal epoxide hydrolase and susceptibility to emphysema. *Lancet* 350, 630-3 (1997).
 66. Horne, S. L., Cockcroft, D. W. & Dosman, J. A. Possible protective effect against chronic obstructive airways disease by the GC2 allele. *Hum Hered* 40, 173-6 (1990).
 67. Yamada, N. et al. Microsatellite polymorphism in the heme oxygenase-1 gene promoter is associated with susceptibility to emphysema. *Am J Hum Genet* 66, 187-95 (2000).
 68. Schellenberg, D. et al. Vitamin D binding protein variants and the risk of COPD. *Am J Respir Crit Care Med* 157, 957-61 (1998).
 69. Yim, J. J. et al. Genetic susceptibility to chronic obstructive pulmonary disease in Koreans: combined analysis of polymorphic genotypes for microsomal epoxide hydrolase and glutathione S-transferase M1 and T1. *Thorax* 55, 121-5 (2000).



Chapter 7

Summary / Future perspectives



Samenvatting / Toekomstvisie

Heparan sulfate proteoglycans (HSPGs) are cell surface and extracellular matrix (ECM) components that control numerous cell processes. These glycoprotein molecules are comprised of a protein core to which linear polysaccharide chains of heparan sulfate (HS) are attached. Structural diversity is imparted by the HS component, which shows large structural complexity. Such complexity results in a number of sequence motifs that selectively bind and activate distinct effector proteins, including growth factors, proteases and lipoproteins. HS is a linear co-polymer of alternating glucosamine and uronic acid residues. Distinct HS domains are, in large part, defined by the number and position of sulfate groups that decorate the HS chain. Due to the presence of carboxylic and sulfate groups, HS molecules are highly negatively charged, and this property endows HSPGs with unique characteristics that are important in the integrity and functioning of the ECM. Today, evidence is accumulating for the involvement of HSPGs in the pathogenesis of pulmonary emphysema, a smoking-related lung disease, characterized by an imbalance of proteases/protease-inhibitors, oxidants/antioxidants and ECM components.

The relevance of proteoglycans for the development of emphysema is demonstrated in several studies. First, proteoglycans bind and modulate growth factors and cytokines and act, mainly through HS, as strong protease inhibitors. Furthermore, proteoglycans play an important role in the neutralization of oxidants and free radicals. This, together with their strong association with collagen- and elastin fibers and their strategic location in the alveolar wall indicates the importance of proteoglycans in the alveolar matrix. Changes in the synthesis and/or composition of proteoglycans/glycosaminoglycans (GAGs) could result in a disturbance of the alveolar matrix, which may eventually lead to emphysema. In the research towards the pathogenesis of emphysema, proteoglycans, especially agrin and perlecan, have been studied. However, these studies primarily focused on the protein core, ignoring the GAG moiety because of the lack of appropriate tools such as antibodies.

The aim underlying the study described in this thesis was to select antibodies against HS isolated from human lung,

to investigate the distribution of HS in normal versus diseased (emphysematous) lung tissue, and to get a better view of the ECM molecules associated with the onset of emphysema.

In **Chapter 1** an overview is given on the present knowledge concerning proteoglycans in the lung. Special attention is given to the structure, biosynthesis and function of HS, including its role in development and patho-(physiology). In **Chapter 2** is described how phage display-derived antibodies directed against human GAG epitopes can be generated and selected. We have used this phage display technology to select seven unique antibodies against human lung HS, as described in **Chapter 3**. Using these novel antibodies, the expression of distinct HS epitopes in human lung tissue was evaluated. HS epitopes were found to be differentially distributed in human lung tissue. Whereas some HS epitopes were generally present in basement membranes, others had a more restricted distribution, especially with regard to macrophages and bronchiolar epithelial cells. We demonstrated that

some antibodies blocked a FGF-2-binding site in HS, and that one antibody blocked a VEGF-binding site in heparin. Antibodies defining specific HS epitopes can be used as tools to study the structural dynamics of HS on a (sub)cellular level. In **Chapter 4**, the epitope recognized by phage display-derived antibody NS4F5 was studied in more detail. Using a combination of biosynthetic HS oligosaccharide libraries, tissues from mice defective in HS biosynthetic enzymes, and a panel of chemically modified heparins we were able to establish the monosaccharide sequence of its epitope. The HS sequence was (GlcNS6S-IdoA-2S)₃ and this sequence was, next to heparin-containing mast cells, only present in a very small subset of HS. A highly sulfated HS sequence suggests a specific role in cell behavior, and therefore we studied the cell biological relevance of this HS epitope. We have used the antibody as a blocking agent in cultures of human epithelial cells and showed that its HS epitope is involved in cell proliferation and apoptosis, but not in cell adhesion. The NS4F5 antibody is the first phage display-derived antibody against HS described in the literature of which the monosaccharide sequence could be revealed. In **Chapter 5** we evaluated lung tissue from subjects with early signs of emphysema as revealed by the Destructive Index (DI), the most sensitive parameter for emphysema. We focused on early changes in the ECM, and found that in emphysematous lung tissue the expression of HSPGs (both side chain and core protein) was reduced, in contrast to other matrix components such as collagens and laminin. In addition, an upregulation of the HS-degrading enzyme heparanase was observed. To in-

vestigate whether heparanase expression could induce emphysematous lesions, lungs of transgenic mice overexpressing this enzyme were investigated. We demonstrated that lungs of heparanase-overexpressing mice indeed developed emphysematous lesions, which became more severe at increasing age, resembling the human situation. From the results described in this chapter, we conclude that increase in heparanase expression and loss of HS in the lung are early events in the development of emphysema. These new findings argue that inhibitors of heparanase activity might be evaluated as potential drugs to slow down the process of emphysema. In **Chapter 6** we turned to another ECM molecule, fibrillin-1. Fibrillin-1 is a major component of the microfibrillar part of elastic fibers, and binds to HS. We used lung specimens from patients with microscopical emphysema, as defined by destruction of alveolar walls and enlargement of the airspaces. The hypothesis that fibrillin-1 is a player in the onset of emphysema is corroborated by several lines of research. Mutated forms of fibrillin-1 are causative for developmental emphysema in mouse models, including the tight skin mice, characterized by a tandem duplication of 30–40 kb in the gene encoding fibrillin-1, and mice harboring a targeted deletion of 6 kb in the fibrillin-1 gene. We demonstrated that in controls, fibrillin-1 was abundantly expressed in a characteristic fibrillar pattern. In contrast, in specimens with a high degree of microscopical emphysema, the linear fibers were almost completely fragmented and had a punctuate appearance. Staining for other ECM components as collagen type I and IV and laminin did not reveal any differences in abun-

dance or distribution. Aberrant fibrillin-1 staining was associated with early parenchymal destruction. We also showed that aberrant fibrillin-1 staining was associated with airspace enlargement and emphysematous abnormalities. In conclusion, we showed that an aberrant fibrillin-1 staining in lung specimens was significantly associated with the three most important morphometric parameters for emphysema: the DI (alveolar destruction), the MLI (airspace enlargement), and the PG (emphysema-related morphological abnormalities). This, together with the notion that mutations in the fibrillin-1 gene may result in emphysematous lesions in men (Marfan syndrome) as well as mice, makes the fibrillin-1 gene an important player in the onset of pulmonary emphysema.

Future perspectives

In this thesis the role of HS in human lungs, including emphysematous lungs was addressed. Antibodies against HS were selected, and used to study the distribution of specific HS epitopes in normal lung. The panel of antibodies can now be used to study the involvement of specific HS epitopes in lung pathology. There are clear indications that HS is associated with early events, ultimately resulting in emphysema. It will be challenging to identify the exact structures within HS that are important for the development of emphysema. To this end, HS from both emphysematous lungs and controls should be isolated and the chemical make-up should be

determined by mass spectrometry and HS disaccharide analysis. As an alternative for the structural analysis of the total HS, partially digested HS derived from human lung may be affinity purified by anti-HS antibodies and then followed by HS structural analysis. Ultimately, this could lead to the rational development of defined HS-based therapeutics. The potential role of such HS-based glycomimetics in treating emphysema should be evaluated in *in vivo* experimental models of emphysema.

The present set of data offers new insights in the diversity and function of a number of novel HS epitopes. It has become clear that anti-HS antibodies have a strong preference for specific modification patterns on the HS chain. However, it still remains to be elucidated whether these HS epitopes are unique for specific core proteins. Besides this, it would also be challenging to elucidate the exact monosaccharide sequences of the HS epitopes recognized by the antibodies.

GAGs, as HS, could play an important role in the neutralization of oxidants and free radicals. Given that cigarette smoke greatly increases the risk for the development of emphysema, it would be interesting to investigate the effect of cigarette smoke on alveolar proteoglycans. It would be interesting to apply fully characterized phage display-derived antibodies to lungs of rats exposed to cigarette smoke to investigate the effect of smoking on HS (degradation).

Heparansulfaat proteoglycanen (HSPGs) zijn celoppervlak- en extracellulaire matrix (ECM) gerelateerde componenten die verschillende cellulair processen controleren. Deze glycoproteïnen bestaan uit een eiwitketen waaraan lineaire polysaccharideketens van heparansulfaat (HS) zijn gekoppeld. Structurele diversiteit wordt voornamelijk teweeg gebracht door de HS component, welke een enorme structurele complexiteit vertoont. Een dergelijke complexiteit resulteert in een aantal sequenties welke selectief verschillende effectormoleculen kunnen binden en activeren, zoals groeifactoren, proteasen en lipoproteïnen. HS is een co-polymeër dat bestaat uit repeterende eenheden van glucosamine en uronzuur. Verscheidenheid in HS domeinen wordt grotendeels bepaald door de hoeveelheid en positie van sulfaatgroepen in de HS keten. Door de aanwezigheid van carboxyl- en sulfaatgroepen zijn HS moleculen sterk negatief geladen. Deze eigenschap zorgt ervoor dat HSPGs unieke eigenschappen bezitten die belangrijk zijn voor de integriteit en het functioneren van de ECM. Er zijn steeds meer aanwijzingen die duiden op de betrokkenheid van HSPGs bij de pathogenese van longemfyseem, een aan roken gerelateerde longaandoening, die gekenmerkt wordt door een onbalans van proteasen/proteaseremmers, oxidanten/anti-oxidanten en ECM componenten.

De relevantie van proteoglycanen bij de ontwikkeling van longemfyseem is aangetoond in verschillende studies. Ten eerste binden en moduleren proteoglycanen talrijke groeifactoren en cytokinen en fungeren zij, voornamelijk via HS, als krachtige proteaseremmers. Bovendien spelen proteoglycanen een belangrijke rol bij de neutralisatie van oxidanten en vrije radicalen. Dit, alsmede de nauwe associatie met collageen- en elastinevezels en de strategische locatie in de alveolaire wand, geeft het belang van proteoglycanen in de alveolaire matrix aan. Veranderingen in de synthese en/of samenstelling van proteoglycanen/glycosaminoglycanen (GAGs) kunnen resulteren in verstoring van de alveolaire matrix hetgeen uiteindelijk kan leiden tot longemfyseem. Onderzoek naar de pathogenese van longemfyseem heeft zich in de afgelopen jaren voornamelijk gericht op proteoglycanen, in het bijzonder agrine en perlecan. Deze studies waren echter hoofdzakelijk gericht op de eiwitketens, aangezien er nauwelijks hulpmiddelen, zoals antilichamen, be-

stonden om individuele GAG-ketens te onderzoeken.

Het doel van de in dit proefschrift beschreven studie was om antilichamen te genereren tegen HS geïsoleerd uit humaan longweefsel, de distributie van HS te bestuderen in normaal versus afwijkend (emfysemateus) longweefsel en een algemeen beter inzicht te krijgen in de ECM moleculen die geassocieerd zijn bij het ontstaan van emfyseem.

In **Hoofdstuk 1** wordt een overzicht gegeven van de huidige kennis van proteoglycanen in de long. Hierbij is voornamelijk aandacht geschonken aan de structuur, biosynthese en functie van HS, alsmede aan de rol bij ontwikkeling en patho(fysiologie). In **Hoofdstuk 2** wordt beschreven hoe antilichamen gericht tegen specifieke GAG epitopen gegenereerd en geselecteerd kunnen worden met behulp van de phage display techniek. We hebben deze phage display techniek gebruikt om 7 unieke antilichamen te selecteren die gericht zijn tegen HS geïsoleerd uit humane long, zoals beschreven in **Hoofdstuk 3**. Deze

nieuwe antilichamen werden gebruikt om de expressie van verschillende HS epitopen in humane long te bestuderen. HS epitopen bleken op verschillende plaatsen in humaan longweefsel voor te komen. Sommige HS epitopen waren aanwezig in de basale membraan, terwijl anderen slechts op zeer specifieke plaatsen voorkwamen, in het bijzonder met betrekking tot macrofagen en bronchiolaire epitheelcellen. We hebben aangetoond dat een aantal antilichamen in staat bleek om een FGF-2-bindingsplaats op HS te blokkeren, terwijl slechts een enkel antilichaam een VEGF-bindingsplaats op heparine kon blokkeren. Antilichamen die specifieke HS epitopen herkennen, kunnen gebruikt worden als hulpmiddelen om de structurele dynamica van HS op een (sub)cellulair niveau te bestuderen. In **Hoofdstuk 4** wordt dieper ingegaan op de karakterisatie van het epitooop dat wordt herkend door antilichaam NS4F5. Door een combinatie van biosynthetische HS oligosacchariden, weefsels van muizen die deficiënt zijn in HS-biosynthetische enzymen en een panel van chemisch gemodificeerde heparines, hebben we de monosaccharidesequentie van het epitooop achterhaald. De HS sequentie is (GlcNS6S-IdoA2S)₃ en deze sequentie was, naast heparine-bevattende mestcellen, uitsluitend aanwezig in een subpopulatie van HS. Een hooggesulfateerde HS sequentie suggereert een specifieke rol in celgedrag en dit heeft ons doen besluiten om de celbiologische relevantie van dit HS-epitooop te bestuderen. Het antilichaam werd gebruikt als blokkeermiddel in gecultiveerde humane epitheelcellen en we hebben laten zien dat het HS-epitooop betrokken is bij celproliferatie en apoptose, maar niet bij

celadhesie. Het NS4F5 antilichaam is het eerste, met phage display techniek-opgewekte, antilichaam, waarvan de monosaccharidesequentie bepaald kon worden. In **Hoofdstuk 5** hebben we longweefsel bestudeerd dat afkomstig is van patiënten die de eerste verschijnselen van emfyseem vertonen als bepaald op basis van de Destructive Index (DI), de meest gevoelige parameter voor het vaststellen van emfyseem. We hebben ons gefocuseerd op vroege veranderingen binnen de ECM en laten zien dat in emfysemateus longweefsel de expressie van HSPGs (zowel zijketen als eiwitketen) is verminderd in tegenstelling tot andere matrix componenten zoals collagene en laminine. Bovendien laten we zien dat de expressie van het HS-afbrekende enzym heparanase is toegenomen. We hebben muizen met een transgene overexpressie van humaan heparanase gebruikt om te bepalen of heparanase-expressie causaal kan zijn voor de inductie van emfysemateuze lesies. In vergelijking met controles werden in longen van muizen die heparanase tot overexpressie brengen, emfysemateuze lesies aangetroffen, welke toenamen met de tijd, zoals ook in de humane situatie het geval is. Deze resultaten suggereren dat een toegenomen heparanase-expressie en het verlies aan HS in de long belangrijke gebeurtenissen zijn bij de ontwikkeling van emfyseem. Deze nieuwe bevindingen suggereren dat remmers van heparanase activiteit als potentiële middelen kunnen worden gebruikt om het proces van emfyseemvorming te vertragen. In **Hoofdstuk 6** hebben we ons gericht op een ander ECM molecuul, fibrilline-1. Fibrilline-1 is een belangrijk component van het microfibrillaire gedeelte van elastische vezels en bindt aan HS. Ook

hier hebben we longweefsel gebruikt afkomstig van patiënten waarbij op microscopisch niveau de eerste verschijnselen van emfyseem zijn waar te nemen. De hypothese dat fibrilline-1 een rol kan spelen bij het begin van emfyseem is in verschillende studies aangetoond. Gemuteerde vormen van fibrilline-1 zijn causaal voor de ontwikkeling van emfyseem in muizenmodellen, waaronder de ‘tight skin muizen’, die worden gekenmerkt door een tandem duplicatie van 30-40 kb in het gen dat codeert voor fibrilline-1, alsmede een muizenmodel dat een 6 kb deletie heeft in het fibrilline-1 gen. Wij hebben aangetoond dat in controles, fibrilline-1 in overvloed aanwezig is, in een vezelachtig patroon, terwijl bij patiënten met een hoog gehalte aan microscopisch emfyseem de lineaire vezels bijna geheel gefragmenteerd zijn. Andere ECM componenten zoals type I en IV collageen en laminine vertoonden dit verschil niet. We hebben aangetoond dat een afwijkende fibrilline-1-kleuring geassocieerd is met vroege parenchymale destructie en met het groter zijn van de alveoli. Concluderend kunnen we zeggen dat een afwijkende fibrilline-1-kleuring in longweefsel significant geassocieerd is met de drie meest belangrijke morfometrische parameters voor emfyseem: de DI (alveolaire destructie), de MLI (grotere diameter van de alveoli), en de PG (emfyseem-gerelateerde morfologische abnormaliteiten). Dit, tesamen met het gegeven dat mutaties in het fibrilline-1-gen kunnen resulteren in emfysemateuze lesies bij de mens (Marfan syndroom) en bij de muis, maakt het fibrilline-1-gen een belangrijke kandidaat bij het ontstaan van longemfyseem.

Toekomstvisie

In dit proefschrift wordt de rol van HS in humane long, inclusief emfysemateuze long beschreven. Antilichamen gericht tegen HS zijn geselecteerd en gebruikt om de distributie van specifieke HS epitopen in de normale long te bestuderen. Dit panel aan antilichamen kan nu gebruikt worden om de betrokkenheid van specifieke HS-epitopen in longpathologie te onderzoeken. Er bestaan duidelijke aanwijzingen dat HS geassocieerd is met processen die uiteindelijk resulteren in emfyseem. Daarom is het een uitdaging om de exacte structuren binnen HS te identificeren welke van belang zijn bij de ontwikkeling van emfyseem. Hiertoe zou HS geïsoleerd moeten worden uit zowel emfysemateuze als controle longen en zou de chemische samenstelling bepaald moeten worden met behulp van massaspectrometrie en HS-disacchariden analyse. Dit zou uiteindelijk kunnen leiden tot de rationele ontwikkeling van gedefinieerde, op HS-gebaseerde therapeutica. De potentiële rol van zulke op HS-gebaseerde glycomimetica bij de behandeling van emfyseem zou *in vivo* bestudeerd moeten worden in experimentele modellen voor emfyseem.

De huidige gegevens geven inzicht in de diversiteit en de functie van een aantal HS-epitopen. Het is bekend dat anti-HS-antilichamen een duidelijke voorkeur hebben voor een specifiek modificatie patroon op de HS-keten. Echter, er zou nader onderzocht moeten worden of deze HS-epitopen ook uniek zijn voor specifieke eiwitketens. Daarnaast is het een uitdaging om de exacte monosaccharidesequenties te ontrafelen van de HS epitopen die door de antilichamen herkend worden.

GAGs, waaronder HS, zouden een

belangrijke rol kunnen spelen bij de neutralisatie van oxidanten en vrije radicalen. Sigarettenrook is een belangrijke risicofactor voor het ontstaan van emfyseem en het zou interessant zijn om het effect van sigarettenrook op alveolaire proteoglycanen te bestuderen. Het ligt nu voor de hand om goed gekarakteriseerde phage display antilichamen te gebruiken om het effect van roken op longen te bestuderen en zo te achterhalen welke HS-structuren worden afgebroken.



Chapter 8

Author Information

Curriculum Vitae

List of Publications

Dankwoord

Color Figures

Nicole Christianne Smits werd geboren op 8 januari 1976 te Ulft. Van 1988 tot 1992 doorliep zij de Blumers MAVO te Silvolde en in 1994 behaalde zij haar HAVO diploma aan het Isala College te Silvolde. Vervolgens heeft zij in 1998 haar diploma Microbiologie behaald aan het Rijn-IJssel college te Arnhem, waarvoor stage werd gelopen bij de afdeling Kindergeneeskunde & Neurologie aan de Radboud Universiteit Nijmegen. In datzelfde jaar begon zij haar studie aan de Faculteit Techniek van de Hogeschool van Arnhem en Nijmegen te Nijmegen. Binnen dit studietraject werd gekozen voor het hoofdvak Biochemie, waarvoor een stage- en afstudeeropdracht werd uitgevoerd bij de afdeling Biochemie van de Radboud Universiteit Nijmegen, Nijmegen Centre for Molecular Life Sciences (NCMLS) te Nijmegen. In juni 2001 ontving zij haar ingenieursdiploma.

Van augustus 2001 tot februari 2006 was zij werkzaam als junior onderzoeker bij de afdeling Biochemie verbonden aan de Radboud Universiteit Nijmegen, NCMLS. Onder begeleiding van Dr. T. H. van Kuppevelt werd het promotieonderzoek uitgevoerd waarvan de resultaten staan beschreven in dit proefschrift.

Tijdens haar promotieonderzoek was Nicole betrokken bij diverse onderwijstaken en het begeleiden van studenten en stagiaires. Tevens heeft zij haar onderzoeksresultaten mogen presenteren op zowel nationale als internationale congressen, waaronder de Biochemical Society Meeting (Londen, december 2002), American Thoracic Society (ATS) International Conference 2004 (Orlando, mei 2004), ATS International Conference 2005 (San Diego, mei 2005), de Proteoglycans in Signaling Meeting (Stockholm, september 2005) en de Nederlandse Vereniging voor Matrix Biologie (Lunteren, mei 2006).

Sinds december 2006 is zij werkzaam als Research Associate bij het Dartmouth-Hitchcock Heart and Vascular Research Center, afdeling Medicine van de Dartmouth Medical School in Hanover, New Hampshire, USA. Hier onderzoekt zij of een speciale vorm van heparansulfaat, anticoagulant heparansulfaat, betrokken is bij het verbeteren van de gevolgen van septic shock. Dit onderzoek is gesubsidieerd door National Institutes of Health (NIH) en wordt uitgevoerd onder begeleiding van Dr. N. W. Shworak.

Nicole Christianne Smits was born on January 8, 1976 in Ulf, The Netherlands. From 1988 till 1992 she studied at the Bluemers MAVO (Silvolde, The Netherlands), and she received her HAVO certificate in 1994 at the Isala College (Silvolde, The Netherlands). In this year she started her studies Microbiology at the Rijn-IJssel College (Arnhem, the Netherlands) for which she performed scientific research at the Department of Pediatrics & Neurology at the Radboud University Nijmegen, Medical Centre, Nijmegen, The Netherlands.

She studied a B.Sc. degree at the 'Hogeschool van Arnhem en Nijmegen' (Nijmegen, the Netherlands). For her major in Biochemistry she performed scientific research at the Department of Biochemistry at the Radboud University Nijmegen, Medical Centre, Nijmegen Centre for Molecular Life Sciences (NCMLS), Nijmegen, The Netherlands. In June 2001 she received her B.Sc. degree majoring in Biochemistry.

From August 2001 till February 2006 she worked as a graduate student at the Department of Biochemistry at the Radboud University Nijmegen, Medical Centre, NCMLS, under the supervision of Dr. T. H. van Kuppevelt. During this period research was performed, which has been described in this thesis.

During her Ph.D. studies, Nicole has supervised several trainees and undergraduate students. She presented her work at a number of scientific conventions, including the Biochemical Society Meeting (London, December 2002), the American Thoracic Society (ATS) International Conference 2004 (Orlando, May 2004), the ATS International Conference 2005 (San Diego, May 2005), the Proteoglycans in Signaling Meeting (Stockholm, September 2005), and the Dutch Society for Matrix Biology (Lunteren, May 2006).

As of December 2006 she works as a Research Associate at the Dartmouth-Hitchcock Heart and Vascular Research Center, Department of Medicine at the Dartmouth Medical School in Hanover, New Hampshire, USA. Here, she investigates whether a special form of heparan sulfate, anticoagulant heparan sulfate, is involved in amelioration of septic shock. This research is funded by National Institutes of Health (NIH) and is carried out under supervision of Dr. N. W. Shworak.

List of publications

1. **Smits, N. C.**, Shworak, N. W., Dekhuijzen, P. N. R., and van Kuppevelt, T. H. Heparan sulfates in the lung: structure, diversity, and role in pulmonary emphysema (2009) *Anat Rec*, In press
2. **Smits, N. C.**, Lensen, J. F. M., Wijnhoven, T. J. M., ten Dam, G. B., Jenniskens, G. J., and van Kuppevelt, T. H. Phage display-derived human antibodies against specific glycosaminoglycan epitopes (2006) *Methods Enzymol*, **416**, 61-87
3. **Smits, N. C.**, Robbesom, A. A., Versteeg, E. M. M., van de Westerlo, E. M., Dekhuijzen, P. N. R., and van Kuppevelt, T. H. Heterogeneity of heparan sulfates in human lung (2004) *Am J Respir Cell Mol Biol*, **30**, 166-173
4. **Smits, N. C.**, Robbesom, A. A., Koenders, M. M. J. F., Versteeg, E. M. M., van der Vlag, J., Berden, J. H., Vlodaysky, I., Li, J-P., Bulten, J., Dekhuijzen, P. N. R., and van Kuppevelt, T. H. Overexpression of heparanase and loss of heparan sulfate: initiating events in pulmonary emphysema, *Submitted*
5. **Smits, N. C.**, Kurup, S., ten Dam, G. B., Hafmans, T., Turnbull, J. E., Spillmann, D., Li, J-P., Dekhuijzen, P. N. R., and van Kuppevelt, T. H. A rare, highly sulfated heparan sulfate sequence (GlcNS6S-IdoA2S)₃ has a strict topography and is involved in cell behavior, *Submitted*
6. Robbesom, A. A.*, Koenders, M. M. J. F.*, **Smits, N. C.**, Hafmans, T., Versteeg, E. M. M., Bulten, J., Veerkamp, J. H., Dekhuijzen, P. N. R., van Kuppevelt, T. H. Aberrant fibrillin-1 expression in early human emphysematous lung parenchyma: A predisposition for emphysema (2008) *Mod Pathol*, **21**(3), 297-307
7. Wijnhoven, T. J. M., van de Westerlo, E. M., **Smits, N. C.**, Lensen, J. F. M., Rops, A. L. W. M. M., van der Vlag, J., Berden, J. H., van den Heuvel, L. P. W. J., van Kuppevelt, T. H. Characterization of anticoagulant heparinoids by immunoprofiling (2008) *Glycoconj J*, **25**(2), 177-185
8. Isaev, D., Isaeva, E., Shatskih, T., Zhao, Q., **Smits, N. C.**, Shworak, N. W., Khazipov, R., and Holmes, G. L. Role of extracellular sialic acid in regulation of neuronal and network excitability in the rat hippocampus (2007) *J Neurosci*, **27**(43), 11587-11594
9. HajMohammadi, S., **Smits, N. C.**, Lawrence, R., Rhodes, J. M., Esko, J. D., Shworak, N. W. Major gD-type 3-O-sulfotransferases make anticoagulant heparan sulfate, *In preparation*

*, Authors contributed equally to the manuscript

Het is AF!

Maar is het nu ook 'klaar'? In dit boekje misschien wel, maar een promotieonderzoek is eigenlijk nooit écht klaar. Na ruim vier jaar van phage-displayen, 'peri's maken', coupes bekijken, antilichamen karakteriseren, pipetteren, op-en-neer pendelen naar Nijmegen en schrijven, zit ik hier op een ochtend in Lebanon achter mijn laptop en ben ik nog steeds niet uitgeschreven. Feit is dat bij de meeste proefschriften het dankwoord het meest gelezen en misschien ook wel het meest bediscussieerde deel (al dan niet openbaar!) is van het proefschrift. Een proefschrift schrijven doe je niet alleen en daarom wil ik iedereen bedanken die direct of indirect heeft bijgedragen aan 'mijn boekje'. Het gebeurt immers niet vaak dat je in de gelegenheid bent om de mensen te bedanken die een rol hebben gespeeld bij het bereiken van een mijlpaal, als je een proefschrift tenminste als zodanig kunt beschouwen.

Hierbij gaat mijn dank dan ook uit naar iedereen die ook maar enige bijdrage heeft geleverd of interesse heeft getoond in wat ik al die jaren tijdens mijn promotieonderzoek bij Biochemie heb gedaan, gepresenteerd en beschreven.

Voor de totstandkoming van mijn proefschrift wil ik allereerst mijn copromotor Dr. Toin van Kuppevelt bedanken. Toin, ik ben je vooral dankbaar dat je mij met mijn 'HLO achtergrond' de mogelijkheid hebt gegeven om een promotieonderzoek uit te voeren. Een carrière in de wetenschap was iets dat ik na mijn opleiding ambieerde en jij hebt me deze gelegenheid gegeven. Dat ik bovenop mijn vierjarig contract nog een half jaar verlenging heb gekregen, is zeker de moeite waard geweest voor ons 'Blue Journal manuscript'! Daar wil ik jou en natuurlijk ook promotor Professor Jan Joep De Pont hartelijk voor bedanken.

Promotor Professor Richard Dekhuijzen wil ik bedanken voor de snelle correctie van mijn manuscripten, voor de nodige adviezen wat betreft longfunctie data van patiënten in onze 'longbank' en natuurlijk voor de financiële ondersteuning voor het bezoek aan het proteoglycanen congres in Stockholm waar ik destijds mijn huidige supervisor heb ontmoet.

De afdeling Biochemie wil ik bedanken voor de fijne samenwerking en

de gezellige dagjes uit. Wat blijft zijn goede herinneringen aan mijn tijd in de Researchtoren en, niet te vergeten, lab 2.66 in het Trigon, waar het voor mij als stagiaire allemaal begon. Een aantal mensen wil ik in het bijzonder danken:

Allereerst Elly, jou wil ik bedanken voor alle hulp die je me tijdens mijn promotieonderzoek hebt gegeven. Jouw bijdrage aan mijn proefschrift is van onschatbare waarde. Van het verzamelen van longweefsel bij Dekkerswald en het Canisius-Wilhelmina ziekenhuis, het opsturen van CD's met extra foto's naar de United States (omdat de reviewers om extra data vroegen en de files te groot waren om te emailen), het doorsturen van tabellen met longfunctie gegevens, tot aan het doorspitten van de 'longbank' (omdat ik daar zelf geen toegang meer tot had) en dan heb ik het niet eens over de experimenten die je allemaal hebt uitgevoerd/herhaald. Bedankt voor al je hulp!

Guido! Als mijn voormalig stagebegeleider ben jij eigenlijk degene die mij heeft geïntroduceerd in het 'GAG-wereldje' en heb je mij de fijne kneepjes

van het pipetteren, peri's maken en cellen kweken bijgebracht. Daar kwamen nogal eens onverwachte resultaten uit, ken je deze misschien nog: RB4EA12 + C2C12 = 'ALAAFS'! Het is overbodig te melden dat onze 'ALAAFS' rond de carnaval werden ontdekt... Jouw enorme motivatie en interesse in de research werkten erg aanstekelijk! Leuk dat we na jouw MIT periode nog een tijdje als collega's hebben samengewerkt. De parachutesprong die we samen gemaakt hebben, even als de trip naar jouw stekkie in Boston zijn Eddie en ik nog niet vergeten! Als een professionele gids heb je ons destijds New York City en Boston laten verkennen en daar maken we nu zelf dankbaar gebruik van, bedankt daarvoor!

Dan Arie, mijn ex-U-genoot! De eerste jaren van mijn AIO periode heb ik samen met jou als 'King of Culture' een U-tje gedeeld. 'Chunky-time', 'C7' en 'oublie' zullen een ander weinig zeggen, maar wij hebben er toch altijd een hoop schik om gehad! Dat we met 'Peking Express the Game' niet één, maar zelfs twee keer in staat waren een reis voor twee personen naar Beijing te winnen, was natuurlijk ondenkbaar. Toch is het gelukt en onze reis naar China zit er inmiddels alweer een tijdje op. Blijft jammer dat we niet met zijn vieren tegelijk over 'The Great Wall' hebben kunnen lopen, maar de voorpret alleen was al meer dan geweldig! Ik ben blij dat ik jou aan mijn zijde heb staan, straks tegenover de corona!

Theo en Paul, het elektronen microscopie-dreamteam! Jullie hebben heel wat bijgedragen aan het NS4F5 hoofdstuk. Ik wil jullie dan ook enorm bedanken voor al die uren die jullie hebben gestoken in het immuno EM

werk dat jullie hebben uitgevoerd en dat jullie regelmatig tot in de late uurtjes van de straat wist te houden! Theo, jou wil ik natuurlijk ook bedanken voor je 'hulp op afstand' bij het maken van mijn boekje. Bedankt voor je heldere tips waardoor het werken met *InDesign* een stuk eenvoudiger werd!

Nu dan de vakbroeders, mijn mede AIO's/OIO's/junior onderzoekers; Paul, (*Wicky*), Joost, Tessa, Suzan, Mieke, Peter en niet te vergeten de 'tissue-twins': Gerwen en Martin. Het bleek dat we naast het promoveren nog een andere gezamenlijke tijdsbesteding hadden. We hebben namelijk allemaal binnen zeer korte tijd een nieuwe woning gekocht dan wel gehuurd en daar ging zo ongeveer al onze vrije tijd (en die heb je nauwelijks als junior onderzoeker...) in zitten. Zo werd er regelmatig onder het genot van een 'bakkie en een stuk biochemietaart' gekletst over de Gamma, plamuren, schuren en schilderen, Knauf (niet te veel water bij doen...), nieuwe badkamers en keukens en natuurlijk de zeer gewaardeerde en onmisbare helpende hand van pa en ma. Ik wens jullie allemaal heel veel succes bij het afronden van jullie promotie!

Uiteraard wil ik ook alle andere (ex)-collega's van Matrixbiochemie bedanken voor de plezierige samenwerking en gezelligheid zowel binnen als buiten het lab. Velen van jullie hebben je steentje bijgedragen aan mijn proefschrift. Jullie waren altijd bereid mij ergens mee te helpen: Cindy, Els, Gerdy, Herman, Kaeius, Marianne, Ronnie, Toon, Willeke. Bedankt daarvoor!

Bij het doen van experimenten, die aan de basis kunnen komen te liggen van een manuscript kun je natuurlijk alle ondersteuning gebruiken. Daarom wil ik

jullie: Bram, Maartje, Wan-Ying en ook Ellen heel erg bedanken voor jullie inzet en interesse in het onderzoek en voor het werk dat jullie hebben verzet. Dat niet elk experiment direct tot het gewenste resultaat leidt, hebben jullie zelf allemaal wel een keer ondervonden. Toch heeft jullie werk aan de basis gestaan voor een aantal mooie publicaties waarvan de resultaten in dit proefschrift staan beschreven. Ik wens jullie heel veel succes in jullie verdere loopbaan.

Dr. Johan van der Vlag en Professor Jo Berden van de afdeling Nierziekten wil ik bedanken voor het beschikbaar stellen van hun antilichamen JM72 en JM403 waarvoor een belangrijke rol is weggelegd in hoofdstuk 5.

Next, I would like to thank our collaborating colleagues. Professor Dr. Israel Vlodavsky, Dr. Eyal Zcharia and Dr. Jin-ping Li, I would like to thank you for providing the lungs from the transgenic heparanase overexpressing mice which we used in Chapter 5. Further I would like to thank our colleagues from Sweden, Dr. Dorothe Spillmann and Dr. Sindhulakshmi Kurup for all their input in our (never-ending) NS4F5 story. Dear Dorothe and Sindhu, with your expertise and help we were finally able to unravel the exact monosaccharide sequence of the NS4F5 epitope which greatly strengthened our manuscript. I greatly appreciate your help and input in this chapter. I would like to thank Professor Jeremy Turnbull for critical review of this manuscript. Last but not least, I would like to thank my current Principal Investigator, Dr. Nicholas Shworak. Dear Nick, I would like to thank you not only for your input in Chapter 1 but also for providing the funding that allows me to continue my research in the intriguing

field of heparan sulfate proteoglycans.

Sleutels... Ik weet ook niet wat dat is met die dingen, maar in mijn geval schijnt het een soort 'must' te zijn om ze vooral zo snel mogelijk te 'verliezen'. Herman, bedankt dat je altijd weer paraat stond met de reservesleutel van mijn locker 36 (*ja, die met het oranje stickertje...*).

Als je werkt in Nijmegen, maar woont in het pitoreske dorpje Zeddam dan ben je behoorlijk wat tijd kwijt met je woonwerkverkeer. Mijn berekening is de volgende: ongeveer een uurtje per dag enkele reis betekent dat je zo'n twee uur per dag onderweg bent. Twee uur × vijf dagen per week maakt tien. Tien uur × vier weken is veertig uur per maand (en dat is weer ongeveer gelijk aan een volledige werkweek). Gelukkig bestaat er zoiets als carpoolen en daarvoor wil ik jou, Jan, bedanken. Samen met Luc, Emma en later ook Roos, hebben we regelmatig het retourtje Zeddam – Nijmegen afgelegd. Deze ritten werden dan nuttig besteed met gesprekken op het gebied van onze gezamenlijke wetenschappelijke interesse en afgewisseld met gezellige gesprekken over koetjes en kalfjes, het eten van Duitse broodjes en het luisteren naar 'de leeuw' en 'pieniemenie'.

Beste familie, vrienden en vriendinnen (*ja, ook jullie van de VVRG!*). Ook jullie kan ik natuurlijk niet vergeten te betrekken in mijn dankwoord. Ik neem aan dat jullie nog steeds niet helemaal begrijpen waar ik de afgelopen jaren in Nijmegen nou precies mee bezig ben geweest... Toch wil ik jullie allemaal enorm bedanken voor de interesse en natuurlijk voor de broodnodige afleiding die jullie me in het weekend vaak, onder het genot van een drankje (*lees: wijn / Martini*), gaven. Ik ben blij dat jullie altijd wel weer een reden hadden om iets

te vieren, want geen reden is immers ook een hele goede reden.... Ik hoop dat ik jullie als deze harde kern van supporters nog lang in mijn omgeving aanwezig mag hebben, ook al zitten we nu wat verder weg. Marieke, ik vind het super dat jij mijn paranimf wilt zijn!

Jurje en Mariska, jullie runnen met z'n beiden 'ons' vijf-sterren verblijf in Zeddum. Bedankt dat we tijdens onze bezoeken aan Nederland telkens weer bij jullie terecht kunnen. Het is altijd weer fijn om thuis te komen in de Majellastraat!

Pap en mam, jullie hebben mij altijd gestimuleerd om eruit te halen wat erin zit en staan daarmee zonder twijfel aan de basis van mijn proefschrift. Ik waardeer het zeer dat jullie een onvoorwaardelijk vertrouwen in mij hebben, mij op allerlei manieren steunen en dat jullie tot op de dag van vandaag voor me klaar staan. Fijn dat jullie ons wekelijks op de hoogte houden van het reilen-en-zeilen in de Achterhoek!

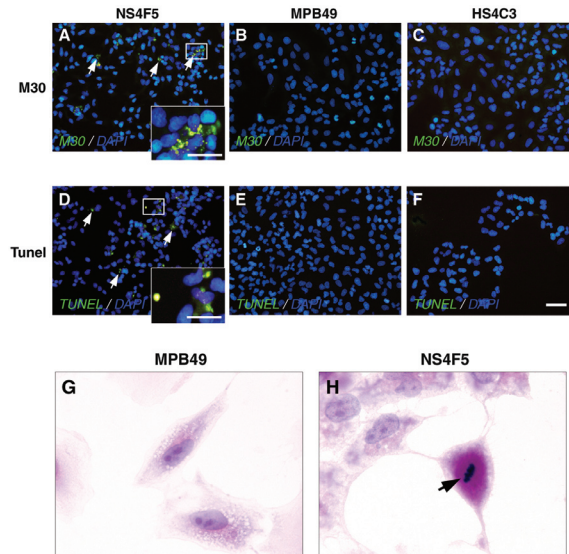
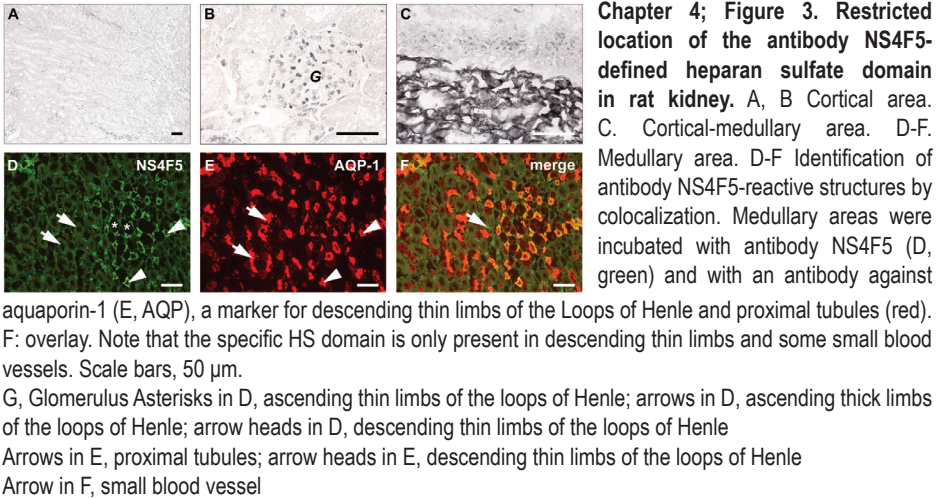
Mieneke, Wendy & Kevin, Wido, Ine & Dianthe! Ook al was hetgeen waar ik dagelijks mee bezig was niet altijd even makkelijk in begrijpelijke taal te vatten, jullie waren altijd razend enthousiast en geïnteresseerd, bedankt daarvoor!

Het allerlaatste woord blijft voor jou, Eddie. Jij hebt vaak gezegd dat ik je niet

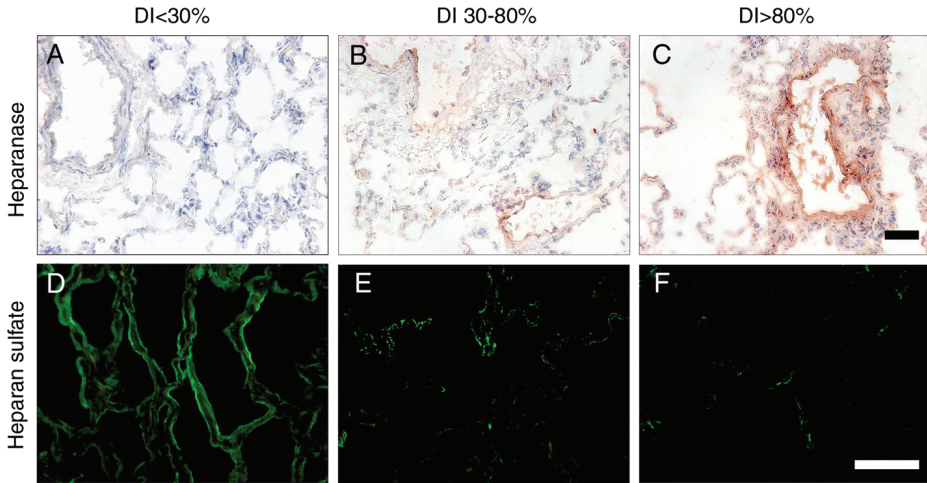
hoef te bedanken in mijn proefschrift, maar ik weet zelf heel goed dat juist jij degene bent die veel meer verdient dan alleen een geschreven 'dankjewel'. Jij hebt mij altijd vrij gelaten om mijn eigen keuzes te volgen ook al bracht die weg ons naar de andere kant van de oceaan. Mijn promotieperiode heb je van dichtbij en van begin tot eind meegemaakt en je weet dus als geen ander dat een promotie behalve *ups* ook de nodige *downs* met zich mee kan brengen. Bedankt voor al je vrolijkheid en afleiding waardoor het werk op het lab makkelijker te relativeren was. Ik ben superblij en zeker ook trots dat we de stap hebben genomen om het eens 'te gaan proberen' in the States. We wonen straks alweer drie jaar in Lebanon, New Hampshire en de verhuizing hiernaartoe bleek de beste beslissing ooit! Fijn dat we hier allebei onze draai hebben kunnen vinden en dat we er nog elke dag vol overgave van genieten. Bedankt voor dat je bij me bent!

Ni wole


augustus 2009
Lebanon, NH, USA



Human



Chapter 5; Figure 4. Overexpression of heparanase is associated with loss of heparan sulfate (HS). A-F: morphologically analyzed sections of subjects without clinically evident emphysema and with normal (DI < 30%, MLI normal A, D), slightly affected (DI 30 - 80%, MLI normal B, E), or moderately affected (DI > 80%, increased MLI C, F) lung parenchyma were incubated with antibodies against human heparanase (A-C) or HS (D-F). Heparanase expression increased with DI in alveolar basement membranes (arrows), peri-vascular areas (arrowheads), and peribronchiolar areas (not shown) whereas HS decreased. Scale bars, 50 μ m.

Printing and distribution of this thesis was financially supported by:



The Netherlands
Asthma Foundation



RU Nijmegen



AstraZeneca BV



Boehringer Ingelheim



Pfizer BV



ProfAffin
Biotechnologie AG



Stichting Astma
Bestrijding



affects over 16 million people
 since 1982². COPD is the fifth
 prevalence and mortality
 emphysema remains elusive.
 of emphysema is the
 the time of clinical diagnosis
 advanced state, precluding



Sulfation

ScFv antibody

